

A SEDIMENTOLOGICAL INVESTIGATION OF THE B-REEF AT MASIMONG 5 SHAFT

by

Michael Botes van den Heever

Dissertation submitted in fulfillment of the requirements
for the degree of

MASTERS OF SCIENCE

In the Faculty of Natural and Agricultural Science
Department of Geology
University of the Free State
Bloemfontein
Republic of South Africa

MAY 2008

Supervisor: Mr L. Nel

ABSTRACT

The ultimate objective of all exploration within the Witwatersrand Basin is to locate concentrations of gold which can be exploited economically. Gold in the B placer has high variance. The gold present in the B placer consists of small heavy detrital particles which are contained in the sedimentary host rock. In order to interpret the variable distribution of the gold within the B placer, cognisance must be taken of the sedimentological framework.

The aim of this study was to employ a different approach to acquire an insight into the nature of the B placer and to shed more light on the depositional environments that played a major role during the formation of the B placer. Pebbles of the B placer conglomerates were investigated macroscopically in order to determine localities of possible gravel bar formation within the B placer.

It was established that the B placer represented a braided river system with three different depositional environments, namely a fluvial environment, braid plain and a braid delta environment. The Upper Shale Marker at Masimong 5 Shaft played a major role in the development of these different depositional environments.

The B placer remained river dominant and neither tide nor wave-related processes had an overwhelming influence on the system. The extreme fluvial dominance of the B placer improved the sorting of the braided delta system. The degree of reworking of the gravel bars in the braid delta by waves and current action resulted in the formation of thicker and better sorted conglomerates which, in turn, led to the formation of the B1 facies. Reworking and re-sedimentation of the B1 conglomerate occurred in the subaqueous setting. The B3 facies present at Masimong 5 Shaft were deposited in a purely fluvial braided environment.

The improved perspective of the B placer made it possible to identify four potential scenarios for the development of gravel bars within the braided river system, namely channel junctions, point bars, side bars or lateral bars; mid-channel bars and barrier bars.

UITTREKSEL

Die doelstelling van enige eksplorasië program binne die Witwatersrand Kom, is om die voorkoms van gekonsentreerde goud wat ekonomies ontgin kan word, vas te stel. Goud in die B-rif kom voor as klein detritale partikels binne die sedimentêre gesteente, naamlik konglomeraat. Die sedimentologiese prosesse wat geheers het tydens die vorming van die B-rif, speel 'n belangrike rol om die sporadiese voorkoms van die goud te verstaan.

Die doel van die studie was om die B-rif uit 'n ander oogpunt te benader en sodoende 'n beter begrip te kry van die afsettingsomgewing wat 'n rol gespeel het tydens die vorming van die B-rif. Die rolstene van die B-rif konglomeraat was makroskopies ondersoek om sodoende die vorming en moontlike ligging van gruis bankette binne die B-rif vas te stel.

Tydens die studie is vasgestel dat die B-rif 'n vlegstroom afsetting met drie verskillende afsettingsomgewings verteenwoordig, naamlik 'n fluviële omgewing, 'n vlegstroom omgewing en 'n vlegstroom delta. Die Boonste Skalie Merker by Masimong 5 Skag het 'n belangrike rol gespeel tydens die vorming van die drie verskillende afsettingsomgewings.

Die B-rif het fluviëel dominant gebly en geen gety of golf prosesse het enige invloed op die afsettingsomgewing gehad nie. Die fluviële afsettingsomgewing was dus baie dominerend tydens die vorming van die B-rif en het aanleiding gegee tot beter sortering van die vlegstroom delta sisteem. Die graad van herwerking van die gruis bankette in die vlegstroom delta deur golf en gety werking het aanleiding gegee tot die ontwikkeling van dikker en beter gesorteerde konglomeraat lae van die B1 fasies. Die herwerking en hersedimentasie van die B1 fasies konglomeraat het hoofsaaklik plaasgevind in 'n onderwaterse omgewing. Die B3 fasies by Masimong 5 Skag verteenwoordig 'n eg fluviële vlegstroom afsettings gebied.

TABLE OF CONTENTS

	<i>Page</i>
1. INTRODUCTION.....	1
1.1 Surface Relief, Vegetation and Climate.....	3
1.2 Historical Review.....	3
1.3 Previous Work.....	5
2. GENERAL GEOLOGY.....	7
2.1 Witwatersrand Supergroup.....	10
2.1.1 West Rand Group.....	10
2.1.2 Central Rand Group.....	11
2.1.2.1 Johannesburg Subgroup.....	12
2.1.2.2 Turffontein Subgroup.....	15
2.2 Ventersdorp Supergroup.....	17
2.2.1 Klipriviersberg Group.....	17
2.2.2 Platberg Group.....	18
2.2.3 Pniel Sequence.....	19
3. SEDIMENTOLOGY OF THE B PLACER.....	20
3.1 General.....	20
3.2 Macroscopic description and subdivision of the B placer.....	20
3.2.1 B1 Facies.....	22
3.2.2 B2 Facies.....	22
3.2.3 B3 Facies.....	22
3.3 Underground compilation of sedimentary information.....	25
3.4 Detail description and subdivision of the B placer	26
3.4.1 Facies Gmoc/Gmpc or Gmom/Gmpm: Massive or crudely bedded gravel.....	26
3.4.2 Facies Gtom/Gtpm or Gtoc/Gtpc: Trough-crossbedded gravel.....	27

3.4.3	Facies Glo/Glp: Pebble lag.....	27
3.4.4	Facies Stq/Spq: Trough- and Planar crossbedded sand.....	28
3.4.5	Facies Smw/Shw: Massive- or Horizontally-bedded sand.....	28
3.5	The Upper Shale Marker.....	31
3.6	Underground Sections of the B-placer.....	32
3.6.1	Geological Sections A to C (B1 Facies).....	32
3.6.2	Geological Sections D and E (B3 Facies).....	34
4.	PEBBLES AND QUARTZITES OF THE B PLACER.....	36
4.1	Varieties and relative abundances.....	36
4.1.1	Durable Pebbles.....	37
4.1.2	Non-Durable Pebbles.....	39
4.2	Matrix.....	39
4.2.1	Carbon.....	40
4.3	Pebble sizes.....	41
4.4	Pebble morphology (shape and roundness).....	45
4.4.1	Shape.....	45
4.4.2	Roundness.....	50
4.5	The Sorting and Packing of the Pebbles.....	51
4.5.1	Sorting of the Pebbles.....	51
4.5.1.1.	Site 1-6: (B1 Conglomerate).....	51
4.5.1.2.	Site 7-10: (B3 Conglomerate).....	55
4.5.2	Packing.....	59
4.6	Vectorial and Scalar Data.....	59
4.6.1	Ripple-bedding.....	60
4.6.2	Megaripples and cross-bedding.....	62
4.6.3	Pebble size.....	65
4.6.4	Clast Imbrication.....	65
4.6.5	Pebbles of shale.....	65
4.7	Classification of Quartzites within the B placer.....	66

5.1	GEOMETRY OF THE B PLACER.....	68
5.1	B-placer facies plan.....	68
5.1.1	The highly channelised region.....	69
5.1.2	The braided plain.....	69
5.1.3	The braid delta.....	70
5.2	Reconstruction of the B-placer palaeo-floor.....	71
5.2.1	Section line A-B.....	71
5.2.2	Section line C-D.....	72
5.2.3	Section line E-F.....	72
5.2.4	Section line D-G.....	73
5.2.4	Section line H-I.....	73
5.3	Reconstruction of a three-dimensional B-placer palaeo- floor.....	73
5.4	Interpreted trap sites for the formation of gold bearing gravel bars.....	74
5.4.1	Channel Junction (Location 1).....	76
5.4.2	Point bars, side bars or lateral bars (Location 2).....	76
5.4.3	Mid channel bars (Location 3).....	76
5.4.4	Barrier bars (Location 4).....	77
6.	CONCLUSION.....	79
	REFERENCES.....	81
	ACKNOWLEDGEMENTS.....	87
	APPENDIX I.....	88
	APPENDIX II.....	97
	APPENDIX III.....	101

LIST OF FIGURES

	<i>Page</i>
Figure 1.1. Location of mining areas in the Free State Goldfields.....	4
Figure 2.1. Simplified map showing outcrops of the Witwatersrand Supergroup and the approximate geographic extents of the goldfields (after Myers, McCarthy and Stanistreet, 1989).....	9
Figure 2.2. Stratigraphic column of Central Rand Group in the Welkom Goldfields.....	12
Figure 3.1. Generalized stratigraphic column of the B placer at Masimong 5 shaft (Not to scale).....	21
Figure 3.2. An oligomictic, matrix supported B1 conglomerate located at site number 2.....	23
Figure 3.3. A hand sample of B1 conglomerate from 1750 E14 Drive S3.....	24
Figure 3.4. A polymictic B3 conglomerate with khaki coloured shale, with an argillaceous fine to medium grained matrix.....	24
Figure 3.5. A single layer of pebbles (pebble lag) with carbon.....	28
Figure 3.6. Photograph showing a siliceous quartzites with cross-bedding.....	29
Figure 3.7. Black Upper Shale Marker located in the eastern region of Masimong 5 Shaft.....	31
Figure 3.8. Khaki Upper Shale Marker located in the western region of Masimong 5 Shaft.....	31
Figure 3.9. Quartz vein located between the Upper Shale Marker and the Bottom B1 facies.....	33
Figure 3.10. B3 conglomerate indicating the upward fining cycle observed at geological section D.....	34

Figure 4.1.	Photograph showing the in situ secondary alteration of milky quartz to smoky quartz. Note how the alteration started at the edge of the milky quartz.....	38
Figure 4.2.	Photograph showing an agate intersected in one of the underground bore holes.....	38
Figure 4.3.	A carbon seam with a thickness of 10 cm at location 1810 W1 W5 A.....	41
Figure 4.4.	Decrease in pebbles sizes in an eastern direction.....	44
Figure 4.5.	Outlines the six roundness classes of particles having high and low sphericity, after Powers, 1953.....	50
Figure 4.6.	Histogram of the particle distribution at Site 1.....	52
Figure 4.7.	Histogram of the particle distribution at Site 2.....	52
Figure 4.8.	Histogram of the particle distribution at Site 3.....	53
Figure 4.9.	Histogram of the particle distribution at Site 4.....	53
Figure 4.10.	Histogram of the particle distribution at Site 5.....	54
Figure 4.11.	Histogram of the particle distribution at Site 6.....	54
Figure 4.12.	Histogram of the particle distribution at Site 7.....	56
Figure 4.13.	Histogram of the particle distribution at Site 8.....	56
Figure 4.14.	Histogram of the particle distribution at Site 9.....	57
Figure 4.15.	Histogram of the particle distribution at Site 10.....	57
Figure 4.16.	Histogram of the particle distribution of all the B1 conglomerates.....	58
Figure 4.17.	Histogram of the particle distribution of all the B3 conglomerates.....	58
Figure 4.18.	Ripple marks encountered in the hanging wall at site 2.....	61
Figure 4.19.	Ripple marks observed on the hanging wall at site 7.....	61
Figure 4.20.	A closer view of the ripples, encountered underground.....	62
Figure 4.21.	Megaripples observed in the hanging wall at site 1810 1W5A.....	63

Figure 4.22. Illustrating the presence of cross-bedding within the mega-ripples.....	64
Figure 4.23. Flow chart for the classification of Witwatersrand Supergroup quartzites after Law <i>et al.</i>, 1990.....	67
Figure 5.1. Three-dimensional reconstruction of the B-placer palaeo floor. Red arrow indicate inwash direction and the yellow dotted line indicates the outer limits of the B-placer.....	75
Figure 5.2. Illustrating potential scenarios for the development of pebble supported conglomerates.....	78

LIST OF TABLES

	<i>Page</i>
Table 3.1. Lateral depositional facies description and interpretation of the B placer, after Knowles (1968).....	30
Table 4.1. Wentworth Particle Grade-Size Scale (Friedman and Sanders, 1978).....	43
Table 4.2. Geological Section A – Pebble Size Distribution B1 Conglomerate (Cockeran, 2006).....	46
Table 4.3. Geological Section B – Pebble size Distribution B1 Conglomerate (Cockeran, 2006).....	47
Table 4.4. Geological Section C – Pebble size Distribution B1 Conglomerate (Cockeran, 2006).....	47
Table 4.5. Geological Section D – Pebble size Distribution B3 Conglomerate (Cockeran, 2006).....	48
Table 4.6. Geological Section E – Pebble size Distribution B3 Conglomerate (Cockeran, 2006).....	49

1. INTRODUCTION

Almost 50 000 tonnes or 40% of the gold ever mined has originated from the Witwatersrand Basin, which still contains over a third of the world's unmined reserves (Jolley *et al.*, 2004).

The Witwatersrand basin is located in the Kaapvaal craton of southern Africa and is the biggest known gold province in the world. Three models have been used to explain the source of the gold contained in the basin (Kirk, *et al.*, 2001).

1. A placer model, which postulates that gold is detritus from an older granite-greenstone source area and has been mechanically transported into the basin and concentrated by fluvial/deltaic processes.
2. A modified placer model, which has the same assumptions as the placer model, but emphasizes the hydrothermal modification of much of the gold. In this model, detrital gold may be mobilized by hydrothermal or metamorphic fluids and be re-precipitated locally with other associated phases.
3. A metamorphic/hydrothermal model, which proposes that gold was transported in solution from outside the basin by metamorphic or hydrothermal fluids between 2.7 and 2 Ga, after basin sedimentation ceased.

The unique and evolving nature of the Precambrian geological environment in many ways was responsible for significant differences between Precambrian clastic sedimentary deposits and their Phanerozoic equivalents.

Omitting possible factors such as shorter days, enhanced tidal forces, different atmospheric composition and the absence of vascular plants which

are likely to have stamped their influence in any depositional environment, further complicate the interpretation of pre-Devonian depositional environments. Three major influences are to be considered in a vegetation-free environment (Fuller, 1985).

1. Chemical weathering would be less aggressive.
2. Once liberated from the host rocks, particles would immediately enter the transport phase of the sedimentary cycle.
3. Bank stability of active channels would have been greatly reduced, especially in bedload-dominated streams.

Pre-Devonian conditions would have favoured development of braided, bedload-dominated, fluvial systems and theoretical analysis of braided-river forms suggests that the channels would have been wide and shallow (Fuller, 1985).

The fluvial conglomeratic B placer occurs at the base of the Turffontein Subgroup of the Welkom goldfield and is considered to be confined to “discrete, interconnected channel ways which are entrenched into the shale/silt of the Dagbreek Formation” (Minter et al., 1986).

Economically, the B placer is of secondary importance compared to the Basal placer. Although the B placer is distributed over an area of 400 km², it is confined to shallow channels, which covers less than 35% of the paleosurface (Minter, 1978).

The B placer at Masimong 5 Shaft mine is typically between 1-2 m thick and contains coarse conglomerates and quartzite interbeds. The B placer can be subdivided into three facies, each representing a different deposition environment, referred to as the B1 facies, which represent a series of oligomitic conglomerates, a quartzitic layer representing the B2 facies and a polymictic conglomerate layer, the B3 facies.

1.1 Surface Relief, Vegetation and Climate

Masimong 5 Shaft is located approximately 15 km east of Welkom and is situated in the western segment of the Orange Free State Goldfields (Figure 1.1). The study area is situated on the plateau region known as the Highveld, with an average elevation of about 1370 m above mean sea level. Most of the area consists of grass-covered veld that has a gentle undulating surface, while dense thorn bushes cover the alluvial flat along the Sand River and certain ground presumably underlain by Karoo dolerite. The hillocks in the vicinity are formed by remnants of Karoo dolerite sheets on Lower Beaufort sandstone. The Sand River which flows through the area meanders in an alluvial flat, for its entire course through the terrain (Coetzee, 1960).

The climate is characterised by long hours of sunshine, moderate extremes of temperature, and a fair rainfall. Most of the precipitation falls as summer rains between October and March, often in the form of local thunderstorms and showers. Numerous dust storms are a feature especially after a dry summer. The fine dust, raised by the storms, rises as thick clouds, blotting out the landscape and penetrating everywhere (Coetzee, 1960).

1.2 Historical Review

During the years 1933 to 1949, a successful exploration campaign for gold in the Orange Free State, yielded a tremendous amount of stratigraphical data. Geological data from the boreholes disclosed a sequence of sedimentary rocks below the Ventersdorp System which has been correlated with the Witwatersrand System.

The historical borehole, W.E. 1, which was drilled in 1933 on the farm Aandenk, near Loraine, proved the presence of gold-bearing conglomerates of the Witwatersrand System below the overlying rocks of the Ventersdorp and Karoo Systems (Coetzee, 1960).

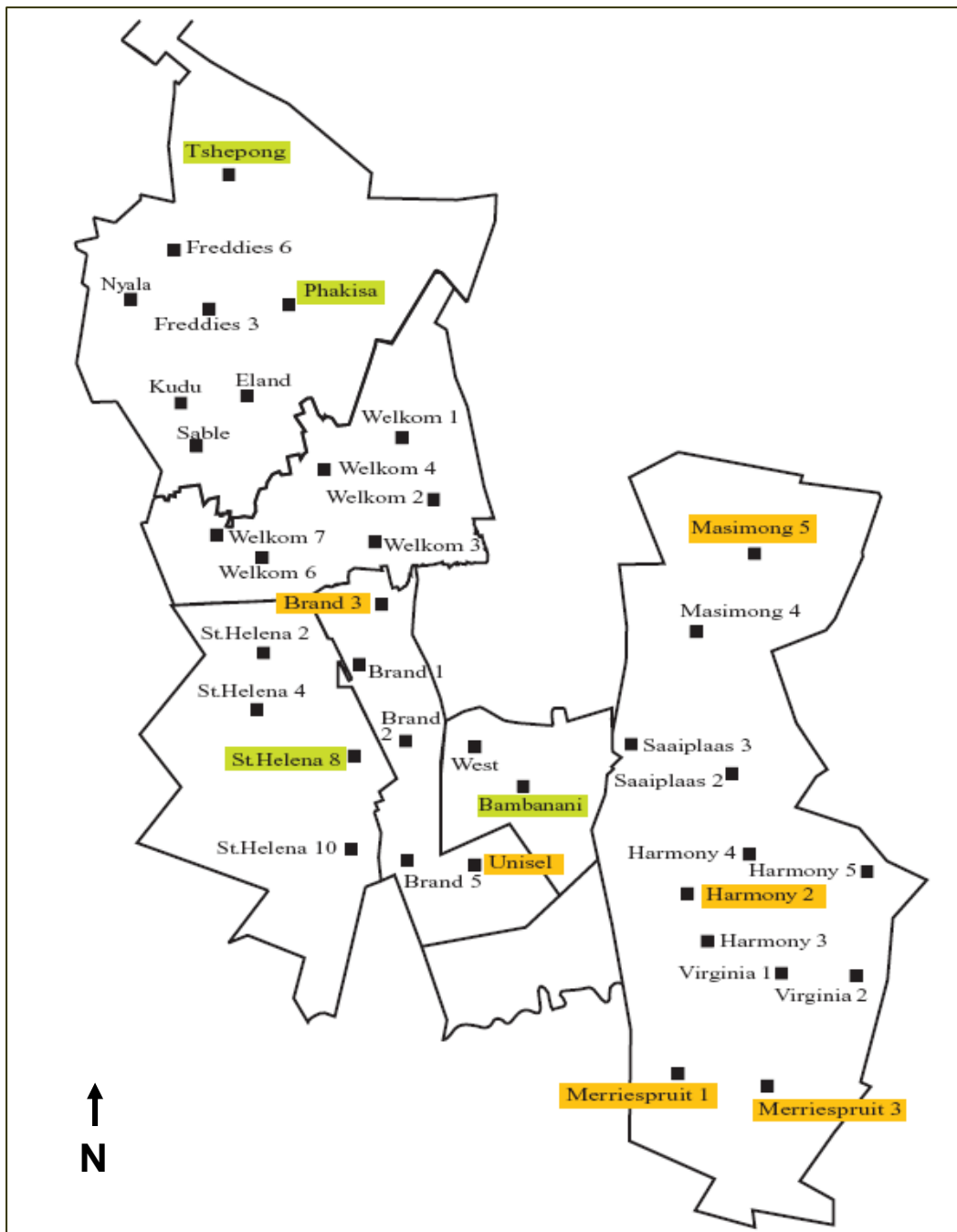


Figure 1.1. Location of mining areas in the Free State Goldfields.

The terms “A” placer and “B” placer originated during the last quarter of 1944 when two conglomerate bands returned payable values in borehole KK 1 on Kalkkuil 153. At that time both the “A” and “B” horizons were intersected in other boreholes, but this did not indicate that the gold values within these placers persisted laterally. A considerable period elapsed before the terms “A” and “B” placer became accepted as being indicative of potential economic deposits. In October 1945, after a payable intersection was obtained in borehole KK 2 (Kalkkuil 153), the conglomerates which intersected were referred to as the “A” and “B” placers (Coetzee, 1960).

1.3 Previous Work

Knowles (1968) studied the B placer in the northern part of the Orange Free State Goldfields. This area included the Freddie's Consolidated Mines, Loraine Gold Mines and the mining lease area of the Jeanette Gold Mines. The study was performed on 20 surface boreholes and 7 underground boreholes, which were all concentrated in the western half of the study area. Underground observations have only been exposed at Freddie's Number 3 Shaft.

Knowles subdivided the B placer conglomerates into the Basal, Middle and Top Conglomerates. The Basal conglomerate unconformably overlies the Upper Shale Marker and represents a polymictic conglomerate with pebbles of white and smoky vein quartz, chert, shale and quartzite. The pebbles are fairly well packed, but very poorly sorted and range in size from 4 -75 mm. The Middle conglomerate is separated from the Basal conglomerate by a yellow medium-grained quartzite. The Middle conglomerate represents a robust, poorly sorted, large pebble polymictic conglomerate, which has a similar pebble composition to the Basal conglomerate. The Top conglomerate consists of a polymictic smaller pebble conglomerate, which is fairly well packed and sorted.

Knowles (1968) also mentioned the presence of a “grey facies” which consist of a well-packed and very well-sorted vein quartz, chert, quartzite and black shale pebbles in a light grey, fine-grained matrix. This conglomerate degenerated rapidly to the east into a light grey quartzite. The only shales observed within the grey facies were dark grey to black.

Minter (1973) described the external geometry of the B placer as various lithological units with lenticular shapes that are interlayered to form a heterogeneous zone and therefore the pebbly layers cannot be correlated over considerable distances. Minter et al. (1986) stated that the B-placer is confined to discrete, interconnected channel-ways, which are entranced into the Upper Shale Marker and that “the channel banks are steep in places, due to the cohesive nature of the footwall”. The formation of the discrete channels, separated by islands onto which no placer sediment was deposited, is due to the cohesive nature of the light coloured khaki shale of the Upper Shale Marker that served as the palaeo-surface.

3. GENERAL GEOLOGY

The Witwatersrand Basin is located in the north central part of South Africa and is underlain by a basement of granitoids and greenstone (3.1 Ga and older) belts belonging to the Middle Archaean Kaapvaal Craton (Catuneanu, 2001).

An early Kaapvaal cratonic nucleus (south-southeastern of the present day craton) was created by an active plate tectonic regime by the Neoproterozoic, when the Witwatersrand Basin formed, with early thin-skin thrusting in oceanic and arc settings (from c. 3.6-3.4 Ga), followed (from c. 3.3-3.2 Ga) by amalgamation of the displaced oceanic and arc terrains, together with extensive granitoid magmatism. Additional development of the Kaapvaal Craton followed from c. 3.0-2.7 Ga, probably involving Cordilleran-type accretion of composite terrains along the western and northern borders of the initial nucleus. The c. 3.1-2.7 Ga Witwatersrand basin formed during this second period of craton development and has an origin comprising an older "Swazian" granitoid crust >3.1 Ga and a younger "Randian" granitoid crust <3.1 Ga (Erikson *et al.*, 2005).

The Witwatersrand Basin is a typical foreland basin, yoked to an active, fold-thrust belt in its hinterland. A foredeep, adjacent to the thrust front and late syntectonic sediments, tapered distally to a foreland-basinal facies. The foredeep and associated features were orthogonal to the compressional orogenic forces acting upon the sectors of the active basin margin, with contemporary warping dominantly parallel to the foredeep (Winter, 1987).

The Witwatersrand Basin formed over a period between 3074-2714 Ma. Pulses of sedimentation within the sequence and its precursors were episodic, occurring between 3086-3074 Ma (Dominion Group), 2970-2914 Ma (West Rand Group) and 2894-2714 Ma (Central Rand Group) (Robb and Meyer, 1995).

The sediments of the Upper Witwatersrand Group occupy an oval-shaped basin, which covers an area of 9750 km². The long axis of the basin extends north-eastwards through Welkom and Johannesburg for 160 km, while the shorter north-western axis is 80 km wide.

The deposits that represent Proterozoic placers in the Witwatersrand Basin are situated in three goldfields, which are located near the towns of Welkom, Klerksdorp and Cartletonville respectively. These placers, referred to in mining terms as reefs, are known as the Basal Reef (Welkom Goldfield), the B Reef (Welkom Goldfield), the Vaal Reef (Klerksdorp Goldfield) and the Ventersdorp Contact Reef (Cartonville Goldfield) (Figure 2.1).

The B placer deposit at the base of the Spes Bona Formation is economically of secondary importance compared to the Basal and Steyn placers. The B placer deposit is confined to shallow channel-ways with a very short paleoslope that covers less than 35% of the deposition area of 400 km² (Minter, 1978).

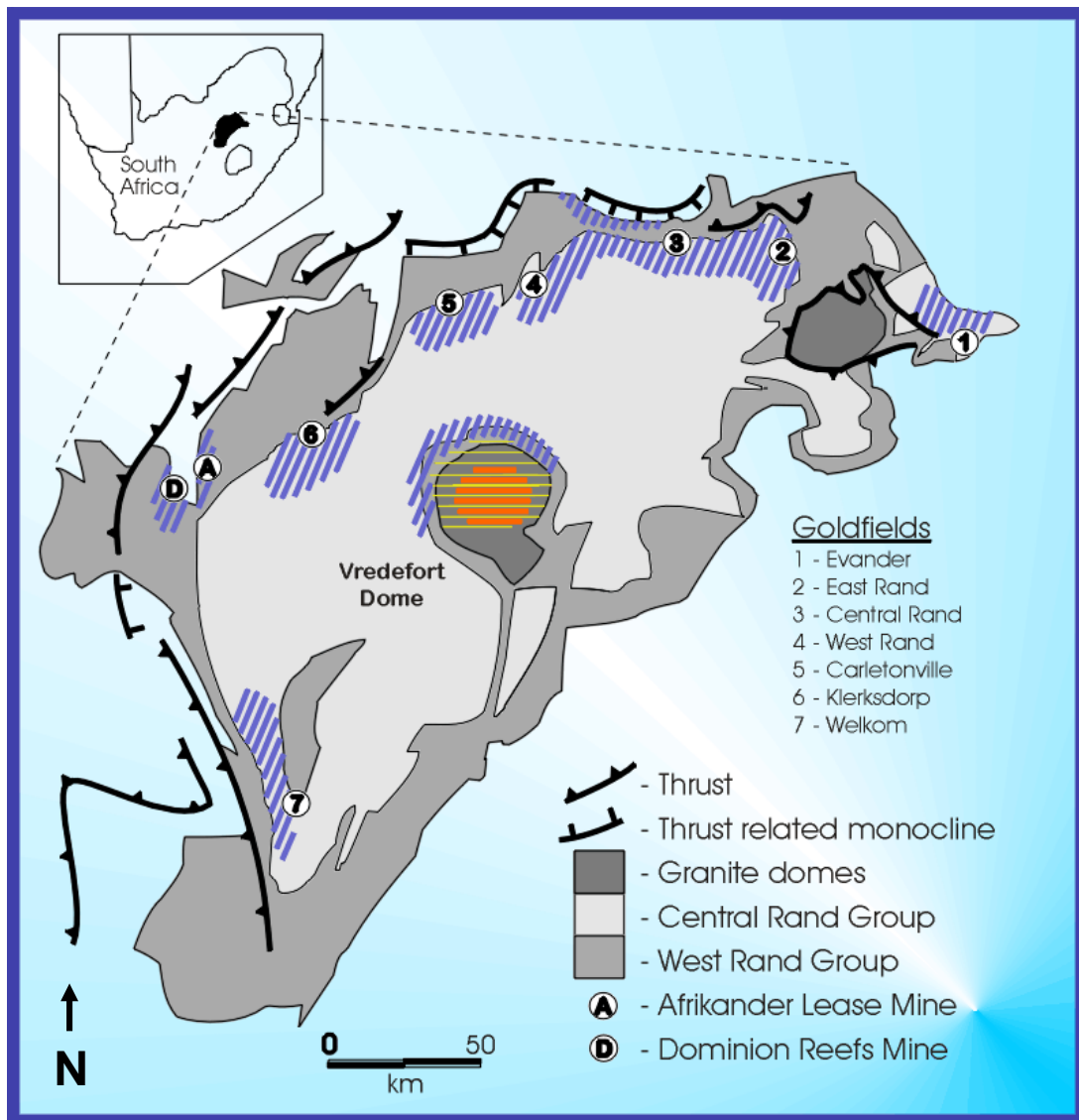


Figure 2.1. Simplified map showing outcrops of the Witwatersrand Supergroup and the approximate geographic extents of the goldfields (after Myers, McCarthy and Stanistreet, 1989).

2.1 Witwatersrand Supergroup

Deposition of sediments within the Witwatersrand Basin took place in a shallow-water lake or inland sea. The north-western side of the Basin was continuously rising at regular intervals, causing the basin-edge to advance increasingly further towards the depositional axis. At the end, the concluding depository was much smaller than the original, and as a consequence, sediments were deposited in a shrinking basin. Conditions were transgressive during the deposition of the West Rand Group and regressive for the Central Rand Group (Pretorius, 1979). Shales and texturally mature sandstones dominate the West Rand Group, whereas the Central Rand Group comprises predominantly sandstones and conglomerates, some of which contain gold in economically viable concentrations (Karpeta and Els, 1999).

2.1.1 West Rand Group

The West Rand Group rock types are represented by approximately equal proportions of sandstone and shale (Robb and Robb, 1998). The West Rand Group is subdivided, based on the different sandstone/shale ratios and basin-wide unconformities, into the Hospital Hill, Government and Jeppestown Subgroups (with shale dominating in the Hospital Hill and Jeppestown Subgroups) (Frimmel and Minter, 2002).

Law *et al.* (1990) lithologically described the sandstones as quartz arenites, subfeldspathic arenites and quartz-feldspar wackes. Feldspathic arenites and wackes are more prevalent in the Government and Jeppestown successions, whereas laterally persistent quartz arenites are more typical in the Hospital Hill Subgroup. Small pebble conglomerates occur within the Government and Jeppestown Subgroups, whereas a great many of these are laterally persistent and associated with unconformities. Shales in the West Rand Group typically contain quartz, chlorite and white mica and are dark green to grey in colour, weathering red in outcrop (Robb and Robb, 1998).

Deposition of the West Rand Group sediments took place in a large shallow marine environment, with the Hospital Hill Subgroup sands being described as subtidal. Cycles in sedimentation, reflecting fluctuations between fluvial and marine shelf environments in the West Rand Group were caused by eustatic sea level changes (Frimmel and Minter, 2002).

2.1.2 Central Rand Group

The Central Rand Group unconformably overlies the West Rand Group and attains a thickness of as much as 2 880 m near the centre of the Witwatersrand Basin (Frimmel and Minter, 2002). The lithologies of the Central Rand Group are characterised by sandstone and conglomerate that dominate over shale (sandstone/shale ratio 12:1, compared to 1:1 for the West Rand Group).

The sandstones of the Central Rand Group are typical quartz arenites and quartz wackes, with little feldspar. The conglomerates of the Central Rand Groups contain a diversity of pebble types, vein quartz being the principal clast type, with chert, quartzite, argillite and porphyry in lesser abundance. Shale beds present in the Central Rand Group vary in colour between dark grey and green, and comprise quartz, chlorite, chloritoid, pyrophyllite, muscovite and rutile (Robb and Robb, 1998).

The Central Rand Group is subdivided into the Johannesburg and Turffontein Subgroups (Figure 2.2) and similarly as the West Rand Group, a series of distinguishable cycles, each comprised of fluvial dominated coarse siliciclastic rocks above an erosion surface (Frimmel and Minter, 2002). At least ten basin-wide unconformities are recognized, each one overlain by conglomerate beds, and these are used to further subdivide the two subgroups into formations (Robb and Robb, 1998).

2.1.2.1 Johannesburg Subgroup

Environmental and structural changes that took place within the Witwatersrand Basin are reflected in the sediments of the Johannesburg Subgroup. Fluvial conditions prevailed over previous, extensive lacustrine or marine-shelf environments. The Palaeocurrent and palaeostrike of unconformities within the subgroup indicate that there was a closure and that fluvial sediments entered the depository at a number of points around its periphery. Around the margin of the basin, regression took place as a result of structural warping.

The Johannesburg Subgroup is approximately 1 525 m thick and can be subdivided into five formations, which represent genetically individual packages that are separated by unconformities composed predominantly of coarse-grained, argillaceous quartzite. Conglomerate beds (comprising placer deposits in many places) in the stratigraphic proximity of unconformities represent only 0,7 percent of the total sequence.

		Formation	Members, beds and markers		Placers	
Central Rand Group	Turffontein Subgroup	Eldorado	Uitkyk Member	●●●●	VS5 Placer	
			Van den Heeverrust	●●●●		EA
			Rosedale Member	●●●●		
		Aandenk	Earls Court Memb. Big Pebble Marker	●●●●	A	
		Spes Bona		●●●●	B	
	Johannesburg Subgroup	Dagbreek	Upper Shale Marker Leader Reef Zone	——— ●●●●	Leader	
		Harmony	Waxy Quartzite, Saaiplaas Quartzite, Khaki shale	●●●●	Basal/Steyn	
		Welkom	Uitsig Member	●●●●	Intermediate	
		St. Helena		●●●●		
		Virginia		●●●● ●●●●	Commonage Ada May	

Figure 2.2. Stratigraphic column of Central Rand Group in the Welkom Goldfields.

The **Virginia Formation** at the base of the Johannesburg Subgroup is up to 800 m thick and is composed almost entirely of quartzites (Figure 2). The quartzites are divided into three to six informal units on the basis of their colour and composition. Collectively, these units are referred to as the Lower Footwall (LF 1-6) and are numbered 1 to 6, from the top downwards.

The **St Helena Formation** is predominantly quartzitic and is up to 320 m thick (Figure 2.2). The formation can be subdivided into four informal members on the basis of persistent beds of super mature quartzite and successions of pebbly layers that are used as markers. They are known as the Middle Footwall (MF 1-4), and are numbered 1 to 4 from the top downwards.

The **Welkom Formation** is approximately 240 m thick and thins out from the western to the eastern side of the goldfield, with some of the upper beds thinning and disappearing from 300 m to 200 m, in a sedimentary wedge, down the eastward palaeodip (Figure 2.2). The strata are comprised of argillaceous quartzites and quartzites, with grits and small-pebble conglomerates in places throughout the sequence. The clast assemblage is distinctly different from the underlying formations and comprises of polymictic green, yellow and black lithologies, in addition to vein quartz. This assemblage resembles the Eldorado Formation, at the top of the Central Rand Group. The Welkom Formation can be divided into four informal members, known as the Upper Footwall (UF 1-4), which are numbered 1 to 4 from the top downwards.

The yellow clasts in the formation represent silicified shale, sometimes intraclasts, while the green clasts are composed of siliceous quartzite and green talcose material. The black clasts are mainly chert, with minor amounts of chloritic schist and cream coloured quartz porphyry. The sediments are coarser along the western, more proximal part of the Welkom Formation fan.

The **Harmony Formation** has a thickness of 32 m and can be subdivided into three members on the basis of lithology. They are the basal, Khaki Shale Member, a Waxy Quartzite Member, and a Siliceous Quartzite Member (Figure 2.2).

The Khaki Shale Member disconformably overlies the Welkom Formation. The contact is sharp and can be observed as muddy sediments percolated about a centimetre into the matrix of the underlying sand. The remainder of the Harmony Formation consists predominantly of argillaceous quartzites that have a diamictite texture and indistinct bedding. The Waxy Quartzite Member averages 18 m in thickness and unconformably overlays the top of the Khaki Shale Member, while the Siliceous Quartzite Member occurs as lenticular, channel-like bodies of light-grey, siliceous quartzite at a number of stratigraphic positions within the waxy quartzite sequence.

The **Dagbreek Formation** is a clastic, wedge-shaped, upward fining deposit and is subdivided into three members, which are known as the Leader Reef Zone, the Dagbreek Quartzite, and the Upper Shale Marker (Minter *et al.*, 1986) (Figure 2.2).

The basal conglomerates and arenites of the Dagbreek Formation unconformably overlie the Harmony Formation and are subdivided into the oligomictic Alma facies (Leader Reef) and the overlying polymictic Bedelia facies (Leader Reef Zone) (Bailey, 1991).

The Leader Reef marks the base of the Leader Reef Zone and is a composite placer, with older oligomictic conglomerates and younger polymictic conglomerates. The remainder of the Leader Reef Zone is composed of interbedded, siliceous quartzites, argillaceous quartzites, and lithic argillaceous quartzites, with scattered thin pebble beds (Minter *et al.*, 1986).

The Dagbreek Quartzite that overlies the Leader Reef Zone is a yellow-grey lithic- to sublithic quartzite, with irregular scattered, polymictic granules to medium-pebble conglomerates (Bailey, 1991). The contact between the

Dagbreek Quartzite and the Upper Shale Marker is sharp and distinctive, from a quartzite to silty shale (Minter *et al.*, 1986).

The Upper Shale Marker, also known as the Booyens Shale, is considered as the most persistent and reliable marker of the Central Rand Group and can be traced over virtually the entire preserved Central Rand Basin (Engelbrecht *et al.*, 1986). The Upper Shale Marker consists of two or three upward coarsening sequences, 4 to 11 m thick, composed of black, laminated shale, ripple- and plane-laminated silty shale, and argillaceous quartzite. Slumped bedding and load casts are also common (Minter *et al.*, 1986). The characteristic sedimentary structures and the absence of desiccation cracks are consistent with a distal, muddy marine shelf. The basal gradational transition from the sandstones of the Johannesburg Subgroup to the laminated slate suggests a gradually diminishing input of coarse clastic sediment into the basin, allowing the settling of mud from suspension to become dominant (Karpeta and Els, 1999).

2.1.2.2 Turffontein Subgroup

The **Spes Bona Formation** lies unconformably on the Upper Shale Marker and is approximately 80 m thick (Figure 2.2). The Spes Bona Formation is composed of numerous polymictic conglomerates, interbedded with khaki-yellow, coarse- to very coarse-grained, argillaceous quartzites. Coarse grains of black chert and silicified, yellow, lithic fragments are conspicuous in the argillaceous quartzites. The polymictic conglomerates are composed of quartz (white and smoky), chert (grey, black, and layered), black shale fragments, and yellow quartz porphyry. Individual beds of quartzite are very lenticular, and trough cross-bedding is conspicuous.

The B placer at the base of the Spes Bona Formation is confined to discrete interconnected channels and transverse and longitudinal bars of gravel grew down the channels and spread laterally (Minter, 1978). The channel profiles are seldom symmetrical and range in width from 1 to 200 m and are up to 2 m deep. The channels were not filled sideways, as by pointbar migration, but

symmetrically. The B placer is generally a well-packed conglomerate, with poorly- to well-sorted quartz, chert, minor shale, and jasper pebbles, set in a siliceous to slightly argillaceous matrix (Minter *et al.*, 1986). The most prominent facies of the B placer are scour surfaces overlain by pebble lags, low relief pebble bars, pebble filled depressions, and tabular planar crossbedded quartzites. Facies changes down the paleoslope of the B placer are rapid and the mean quartz-pebble size decreases from -3.7Φ to -2.5Φ over a distance of 4 km. A similar change in pebble size in the Steyn placer occurred over approximately 15 km. Pyrite nodules in the B placer display the same change in grain size over 4 km as the nodules in the Steyn placer do over 20 km (Minter, 1978).

The **Aandenk Formation** lies unconformably above the Spes Bona Formation (Figure 2.2). The sediments of the Aandenk Formation are composed of black shales, sandy diamictites, and cobble conglomerates. Aandenk placers occur within the sequence of argillaceous quartzites, at positions from 10 to 40 m above the base. The placers are thought to represent degradation events on the Aandenk fan, possibly as a result of autocyclic channel processes.

The **Eldorado Formation** lies unconformably on the Aandenk Formation, forming a wedge-shaped coarsening-upward sequence, composed primarily of lithic, argillaceous quartzites, with siliceous quartzites (Minter *et al.*, 1986) (Figure 2.2). The Eldorado Formation is subdivided into four members namely the ED zone (Rosedale Member), the EC-EB zone (Van den Heeversrust Member), the 'EA' zone (Welkom facies) and the Uitkyk Member (Figure). The Eldorado formation thickens from west to east from 200 m to 600 m over a distance of 5 km (Kingsley, 1987).

The *Rosedale Member* consists of the Rosedale Placer, a polymictic conglomerate, at the base, succeeded by an alternation of litharenites and quartzarenites (Kingsley, 1987). The immature, polymictic conglomerate consists of a variety of pebbles, namely vein quartz, black chert, banded chert, and black siliceous shale, set in a dark-grey, gritty, argillaceous matrix.

The overlying quartzites are medium-grained, immature dark-grey quartzites, containing yellow shale fragments (Minter *et al.*, 1986).

The *Van den Heeversrust Member* is a very gritty litharenite and subgreywacke in the lower part with increasing minor quartzarenite beds jutting upwards.

The *EA zone* is characterized by subgreywacke and polymictic conglomerates alternating with minor quartzarenites and oligomictic conglomerates (Kingsley, 1987).

The *Uitkyk Member* is a coarsening-upward sequence that grades from a large-pebble conglomerate, near the base, to a cobble and a boulder conglomerate higher up in the succession. The conglomerates are composed of a variety of pebbles, consisting of greenstones, black, yellow and green silicified shales, altered porphyritic lava, cherts, quartzites and quartz.

2.2 Ventersdorp Supergroup

The Ventersdorp Supergroup represents a volcano-sedimentary sequence of late Archaean age that overlies the Witwatersrand Supergroup and basement granite-gneiss (Meintjes *et al.*, 1989). The development of the Ventersdorp Supergroup on the Kaapvaal Craton was initiated by the outflow of lava of komatiitic resemblance during a period of crustal extension. The Ventersdorp sequence consist of three groups, namely the Klipriviersberg Group at the base, followed by the Platberg Group and Pniel Sequence (Van der Westhuizen *et al.*, 1991).

2.2.1 Klipriviersberg Group

The Klipriviersberg Group attains a maximum thickness of between 1 500 m - 2000 m and represents the lowermost deposit of the Ventersdorp Supergroup

(Myers *et al.*, 1990). The Klipriviersberg Group consists of amygdaloidal and non-amygdaloidal, andesitic lavas, tuffs, and agglomerates. The lack of glass shards in the volcanic breccia and interbedded tuffs signifies that the style of Klipriviersberg volcanism was low-energy eruptions rather than explosive volcanic action (Meintjes *et al.*, 1989).

Winter (1976), in his analysis, subdivided the Klipriviersberg Group (Edenville, Loraine, Jeannette, Orkney, Alberton and Westonaria formations) according to variations in colour, presence of amygdaloids, agglomerates, tuffs, and the degree of metamorphism of the lavas. The individual lava flows range between 10 m and 50 m thickness and lavas are highly altered and coloured at the top 30 m of the succession, due to weathering (Meintjes *et al.*, 1989).

2.2.2 Platberg Group

The Platberg Group represents the succeeding phase of sedimentation and volcanism in response to the tectonic activity (Minter *et al.*, 1986). Winter (1976) divided Platberg Group into three separate formations: the New Kameeldoorns, the Makwassie Quartz Porphyry, and the Rietgat formations.

In the Welkom Goldfield, the Platberg Group is represented by a thick sequence of sediments and andesitic volcanics, the Klippan Formation, which is stratigraphically equivalent to the Kameeldoorns and Rietgat formations. The Makwassie Formation is not developed in the Welkom Goldfield region. The Klippan Formation is stratigraphy divided into the Video and Dirksburg members.

The intense tectonic activity in the region resulted in the formation of the De Bron Horst, a large, centrally situated horst block, surrounded by grabens and smaller horsts, forming a typical horst-and-graben topography. Three sedimentary basins have been recognized and are referred to as the Arrarat, Virginia, and Dankbaarheid basins (Minter *et al.*, 1986).

The sedimentary rocks in the Virginia and Dankbaarheid basins are subdivided into five lithofacies units: the Hakkies-, Welgelegen-, Doornrivier-, Bloemhoek- and the Sandrivier Units. The lower four units correspond with the Video Member in the Arrarat basin, whereas the upper unit is the equivalent of the Dirksburg Member in the same basin (Meintjes *et al.*, 1989).

The sediments consist of clastic debris, derived from degradation of the horst blocks, and comprising fragments of lava from the Klipriviersberg Group and of quartzites from the Witwatersrand Supergroup, together with their weathering products. Erosion of high ground was more severe at selected localities, resulting in the incision and entrenchment of valleys into the rocks of the Klipriviersberg Group and the Witwatersrand Supergroup, for instance, the Homestead Valley.

2.2.3 Pniel Sequence

The Pniel Sequence, which forms the uppermost parts of the Ventersdorp Supergroup, and is subdivided into the Bothaville and Allanridge formations. Both formations are correlated on a regional scale and represent a change from the locally derived and locally deposited sedimentary environments of the Platberg Group to environments of regional extent (Minter *et al.*, 1986).

The **Bothaville Formation** consists of a thick sequence of clastic sediments, following conformably upon those of the Klippan Formation. The Bothaville Formation has been subdivided into the Zomerveld, La Riviera, and Gelukspan members (Minter *et al.*, 1986).

The **Allanridge Formation** is composed of amygdaloidal and non-amygdaloidal, augite andesite lavas and lies conformably upon the Bothaville Formation. These lavas have been truncated, due to post-Ventersdorp erosion, but thicknesses of 580 m have been recorded (Minter *et al.*, 1986).

3. SEDIMENTOLOGY OF THE B PLACER

3.1 General

The B placer in the Welkom Goldfield was deposited in a braided fluvial environment. Braided streams are characterized by a series of rapidly shifting channels and mid-channel bars, high width/depth ratios (possibly exceeding 300), steep slopes and generally, low sinuosities. The deposits of braided streams are coarser than those of other river-type deposits and are dominated by sand or gravel (Miall, 1977).

Braided rivers show very large fluctuations in discharge. The main conditions for these variations in discharge are (Doeglas, 1962):

- Climatic conditions: Arid or semi-arid, with heavy cloudbursts and long dry periods; or arctic, with long periods of snowfall and rapid thawing.
- Impermeable subsoil in the catchment area and along the course of the river; no water is lost by penetration into the subsoil, and therefore no sources in the form of an aquifer can provide a continuous supply of water.
- Little vegetation, causing a strong superficial runoff and less evaporation.
- A steep gradient.

3.2 Macroscopic description and subdivision of the B placer

The B placer can be subdivided into three facies, according to the maturity of the conglomeratic layers, sedimentary structures and the pebble lithology present in each of the conglomeritic layers. The facies, each representing a different deposition environment, referred to as the B1 facies, which represent a series of oligomitic conglomerates, a quartzitic bed representing the B2

facies and a polymictic conglomerate bed as the B3 facies. The generalized stratigraphic column of the B placer can be observed in Figure 3.1.

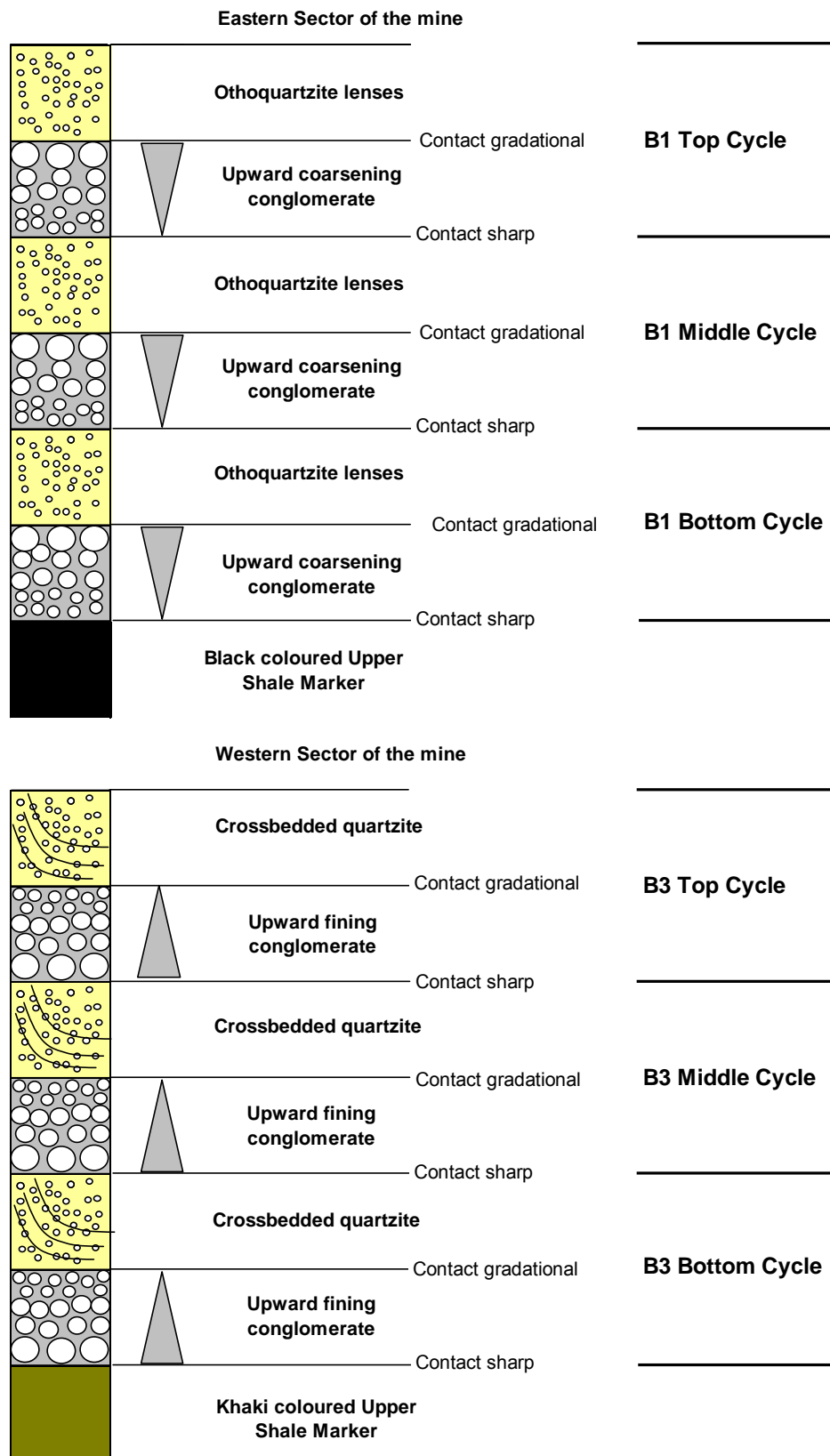


Figure 3.1. Generalized stratigraphic column of the B placer at Masimong 5 shaft (Not to scale).

3.2.1 B1 Facies

The B1 facies at Masimong 5 Shaft consist of oligomictic, clast supported massive to horizontal bedded gravel beds (Gm). The beds unconformably overlie the Upper Shale Marker. Occasionally the B1 facies comprise only a thin pebble lag deposit varying in thickness from 2 cm to 5 cm. The B1 facies consist of up to five cycles, varying in thickness between 5 cm to 1.5 m.

The B1 facies demonstrated typical upward coarsening cycle. The pebbles in the B1 facies are fairly well packed and moderately sorted. Intercalated orthoquartzite lenses, containing nodular carbon and buckshot pyrite on the foresets, occur in the B1 facies. The quartzite varies in thickness from 15 cm to 2 m and contains numerous scattered small pebbles comprising dark grey to black Upper Shale Marker clasts.

The B1 facies conglomerates are moderately to well sorted, with subrounded to rounded clasts (Figure 3.2 and 3.3). Where shale clasts are present, they occur as angular to sub-angular black and khaki-coloured clasts derived from the underlying Upper Shale Marker. The nature of the upper contact between the B1 and B3 facies could not be determined, due to inadequate exposures at the stopes and drives underground.

3.2.2 B2 Facies

The B2 facies consist of an argillaceous, medium to coarse-grained quartzite. In places a thin pebble lag is developed which thickens to form a matrix-supported conglomerate of up to 5 cm in thickness. Small angular chert and smoky quartz pebbles are scattered throughout the B2 facies. The upper contact of these facies is marked by the bottom scour surface of the B3 facies.

3.2.3 B3 Facies

The B3 facies consist of a poorly-sorted, clast supported, polymictic, small to medium pebble conglomerate, with sub-rounded clasts in an argillaceous

matrix (Figure 3.4). The B3 facies grade into a matrix-supported, small-pebble conglomerate indicative of an upward fining cycle. Primary sedimentary structures occur within the facies as cross-bedding. The presence of opalescent blue quartz clasts and khaki coloured shales is distinctive to this facies. The upper contact of the facies is defined by the bottom scour of the Spes Bona channels.

A significant feature of these facies is the presence of massive, columnar carbon, often associated with free gold. The carbon is found along the unconformity between the B3 facies conglomerate and the Upper Shale Marker and occasionally on the contact between upper cycles within the B3 conglomerate.



Figure 3.2. An oligomictic, matrix-supported B1 facies conglomerate located at site number 2.



Figure 3.3. A hand sample of B1 facies conglomerate form 1750 E14 Drive S3.



Figure 3.4. A polymictic B3 facies conglomerate with khaki coloured shale clasts matrix.

3.3 Underground compilation of sedimentary information

Site selection for underground mapping was planned prior to underground visits, typically only the areas close to zones of active mining were accessible to direct observation and sample collection. Despite the practical difficulties experienced in face-mapping, in challenging underground conditions, 5 sections at a total sum of 300 m were map, depicting all the sedimentary facies and primary sedimentary structures within the B placer.

Upon arrival at the site the nearest survey peg was located and the number of the survey peg was recorded. The general setting of the exposure, for instance, the part of a channel or gravel bar, together with a short description of the conglomerate, was noted.

Mapping of the sites underground was done by the traverse mapping method. A base tape drawn out along the selected mapping site was used to obtain a spatial indication of the different facies present in section. An incline ruler was used to measure the sidewalls and the relevant thickness of the different facies encountered. The data were recorded on laminated sheets with a permanent marker. All the data collected were then used to draw sections upon arriving on surface.

Samples were obtained at the same time the sites were mapped. A geological hammer was used to collect representative samples, where practically possible, of the different facies and clast types occurring at a specific exposure. The samples were separated from the sidewalls and placed into sample bags. The sample bags were then marked accordingly. Colour photographs were taken, depicting the general appearance of the conglomerate and its general spatial relation.

3.4 Detail description and subdivision of the B placer

A systematic, logical facies code, developed from Miall's (1977) system for braided river deposits and modified by Knowles (1968), was applied for the facies description and interpretation of the B placer (Table 3.1). The code is represented by three or four letters, each signifying a different parameter. The first letter of the code refers to the grain size of the sediment and is represented by a capital letter. The other parameters are represented by lower-case letters. The second letter refers to the sedimentary structure observed in the facies. The third letter refers to the composition of the conglomerates associated with the facies and the fourth letter refers to whether the conglomerate type is clast or matrix supported. Fine-grained facies have not been significantly changed from Miall's system as they only constitute a minor portion of the stratigraphy.

3.4.1 Units Gmoc/Gmpc or Gmom/Gmpm: Massive or crudely bedded conglomerates

These units represent massive or crudely horizontal bedded conglomerates with minor quartzite lenses. The conglomerate varies in thickness from 10 cm to over 1.5 m. Detrital carbon is present in the matrix or on the basal contact, but columnar carbon is rare. The polymictic nature is highlighted by a large number of yellow shale clasts. These facies commonly exhibit upward-fining, graded bedding and pebble imbrication. Crossbedding is common, with detrital carbon on the foresets.

These units represent longitudinal gravel bars within the braided channel system. The longitudinal bars are diamond- or lozenge-shaped in plan, and are elongated parallel to the flow direction. The longitudinal bars are formed as follows:

In an originally single or undivided channel, the coarsest load is carried along the deepest portion of the channel where the energy is the greatest. A large amount of the pebbles will accumulate as a lag in scour pools. Waning flow

caused a reduction in flow energy, where the channel widens. The result is that the deposition of part of the coarsest bedload appears as a short, submerged central bar. Finer particles are trapped in the interstices of the initial deposit, and more bedload is deposited downstream, in the lee of the bar, so that growth continues. The flow diversion caused by the bar will divide the channel resulting in the erosion of the channel banks and general channel widening is the result. The initial bar relief may be no greater than the size of the largest pebble but as growth continues it may increase to as much as a metre. Bar length may reach several tens of metres. The coarsest material is concentrated along the central bar axis and generally grain size diminishes upwards and downstream. The internal structure of the bars is massive or crude horizontally bedded (Miall, 1977).

3.4.2 Units Gtom/Gtpm or Gtoc/Gtpc: Trough-crossbedded gravel

This unit was only seldom found within the B3 and B2 facies. The B placer varies between a pebbly quartzite and a compact conglomerate. The pebbles may be seen avalanching down the foresets. Carbon may be developed on the basal contact, or on the foresets, indicating a temporary termination in sedimentation.

The polymictic unit did not have time to mature, while the oligomictic unit represents a prolonged erosion and winnowing cycle. The degree of packing is also indicative of the degree of reworking.

3.4.3 Units Glo/Glp: Pebble lag

Facies Glo or Glp represent a single layer of pebbles, or layers of conglomerate 5 cm thick (Figure 3.5). Imbrication is evident if the pebbles are elongated. Carbon is occasionally present. These facies are interpreted as a pebble wash or gravel sheet.



Figure 3.5. A single layer of pebbles (pebble lag) with carbon.

3.4.4 Units Stq/Spq: Trough- and planar crossbedded quartzite

This unit is usually found in association with *Gtom/Gtpm* and *Gtoc/Gtpc* deposits in channels. These facies are interpreted as sand dunes deposited under lower flow regimes conditions in open channels. The planar crossbedded quartzites accreted laterally across the channel, while the troughs prograded down the channel (Figure 3.6).

3.4.5 Units Smw/Shw: Massive- or horizontally-bedded quartzite

This is the most common quartzite unit in the B placer stratigraphy, which is associated with most conglomeratic facies and occurs as lenses within the placer. The quartzite is coarse grained and often contains scattered pebbles and grit-size inclusions.

These facies represent sheet deposition during waning flood stages, and represent the major sediment influx facies.



Figure 3.6. Photograph showing siliceous quartzites with cross-bedding.

Table 3.1 Lateral depositional facies description and interpretation of the B placer, after Knowles (1968).

GRAIN SIZE	STRUCTURE	COMPOSITION	CONGLOMERATE TYPE	FACIES CODE	INTERPRETATION	GOLD PLACER POTENTIAL
GRAVEL (G)	MASSIVE (m)	OLIGOMICTIC (o) POLYMICTIC (p)	CLAST (c) MATRIX (m)	Gmoc, Gmpc Gmom, Gmpm	Longitudinal bars Longitudinal bars of debris flows	VERY HIGH HIGH-LOW
	TROUGH CROSS-BEDS (t)	OLIGOMICTIC (o) POLYMICTIC (p)	CLAST (c) MATRIX (m) LAG (l)	Gtoc, Gtpc Gtom, Gtpm Gtol, Gtpl	Channel fill lags of various maturities Single layer of pebble lag	HIGH-MODERATE
	PLANAR CROSS-BEDS (p)			Gpoc, Gppc Gpom, Gppm Gpol, Gppl	Laterally accreted channel-fill lags, generally or distal facies	HIGH-LOW
	LAG (l)		NONE	Glo, Glp	Deflated pebble washes, thin gravel sheets or high velocity channels	LOW-MODERATE
SAND (S)	HORIZONTAL (h)	QUARTZITE (q) QUARTZWACKE (w)		Shq Shw	Low flow regime or transitional plane beds	LOW-NIL
	TROUGH CROSS-BED (t)			Stq Stw	Transverse bars (dunes) with sinuous crests. Fluvial or perhaps eolian during low flow stages	HIGH-LOW
	PLANAR CROSS-BED (p)			Spq	Straight-crested dunes. Alluvial (or eolian?), more common in distal environments	MODERATE-LOW
	RIPPLED (r)			Srq	Low flow regime current ripples	LOW-NIL
FINE (F)	LAMINATED (l)			Fl	Termination of fluvial cycle	NIL
NON-DEPOSITIONAL FACIES	SCOUR SURFACE COLUMNAR CARBON DETRITAL CARBON			Ss Cc Cd	Scoured bedrock. Erosive surface Fossil algal growth in-situ Detrital algal growth	NIL-LOW HIGH LOW

3.5 The Upper Shale Marker (USM)

The Upper Shale Marker at Masimong 5 shaft consists of a black shale present in the eastern region of the mine and a more sandy, light khaki coloured shale in the western region of the mine (Figures 3.7 and 3.8). The role of the Upper Shale Marker on the depositional environments will be discussed in chapter 5.



Figure 3.7. Black Upper Shale Marker located in the eastern region of Masimong 5 Shaft.



Figure 3.8. Khaki Upper Shale Marker located in the western region of Masimong 5 Shaft.

3.6 Underground Sections of the B placer

Geological sections A to C were mapped in the eastern sector at Masimong 5 Shaft and consist of the oligomictic B1 facies. Sections D and E were mapped in the western sector of the mine and consist of the polymictic B3 conglomerate.

3.6.1 Geological Sections A to C (B1 Facies)

The strike of geological section A is from east to west, parallel to the flow direction of the B placer. Geological sections B and C are perpendicular to the flow direction, striking north-south. These sections consist mainly of upward coarsening, oligomictic conglomerate sheets with interbedded massive or trough-crossbedded quartzite lenses.

Geological sections A and C consist of various lithological units with lenticular shapes that are interbedded to form a heterogeneous zone and therefore the pebbly layers cannot be correlated over considerable distances.

Geological section A consists mainly of 30cm to 1m thick massive conglomerates, with interbedded quartzite lenses. Depressions present in the USM at sites 1 to 3 served as trap sites for the deposition of conglomerates. The conglomerate layers encountered consist of the oligomictic B1 conglomerate within an upward coarsening cycle. The quartzite lenses displayed both massive and trough crossbedding. The presence of a quartz vein with striations was also noted on the contact between the USM and the Bottom B1 conglomerate (Figure 3.9). The influence of this quartz vein on the geometry of the B placer is not fully understood and further work is required.



Figure 3.9. Quartz vein located between the Upper Shale Marker and the Bottom B1 facies.

Geological section B consists mainly of a 1.2 m thick, ologimitic, upward coarsening conglomerate, with a massive quartzite lens. The average pebble size of this section is considerably larger compared to the other two sections as seen in Tables 4.2 to 4.4 and represents a substantial conglomerate bar. The contact between the B1 conglomerate and the USM is sharp, whereas the points of contact of the conglomerate and the quartzite lenses are gradational. The quartz vein observed in geological sections A and C was not developed in geological section B.

Geological section C consists of thin pebble lag deposits in the east, which gradually increase in thickness to the west as the main channel is approached. The facies comprise massive upward coarsening conglomerates, massive quartzites and trough-crossbedded quartzites. The quartz vein observed in section A was also present in geological section C.

The considerable vertical and lateral variance of the conglomerate units in geological sections A and B relate to an upper flow regime. The sharp contacts between the lithological units observed are the result of highly irregular and often

catastrophic discharges that resulted from high variable stream energy and sediment discharge which occurred during the formation of the B placer.

3.6.2 Geological Sections D and E (B3 Facies)

The lithological units of geological sections D and E indicated the development of sheet-like conglomerates over the length and width of the depositional environment. The strike of geological section D is from east to west, parallel to the flow direction of the B placer, whereas geological section E is perpendicular to the flow direction, striking north-south.

The mean thickness of the conglomerates varies between 5cm and 40cm. The predominant facies present in these sections are massive, upward fining polymictic conglomerates (Figure 3.10) with massive and trough-crossbedded quartzites.

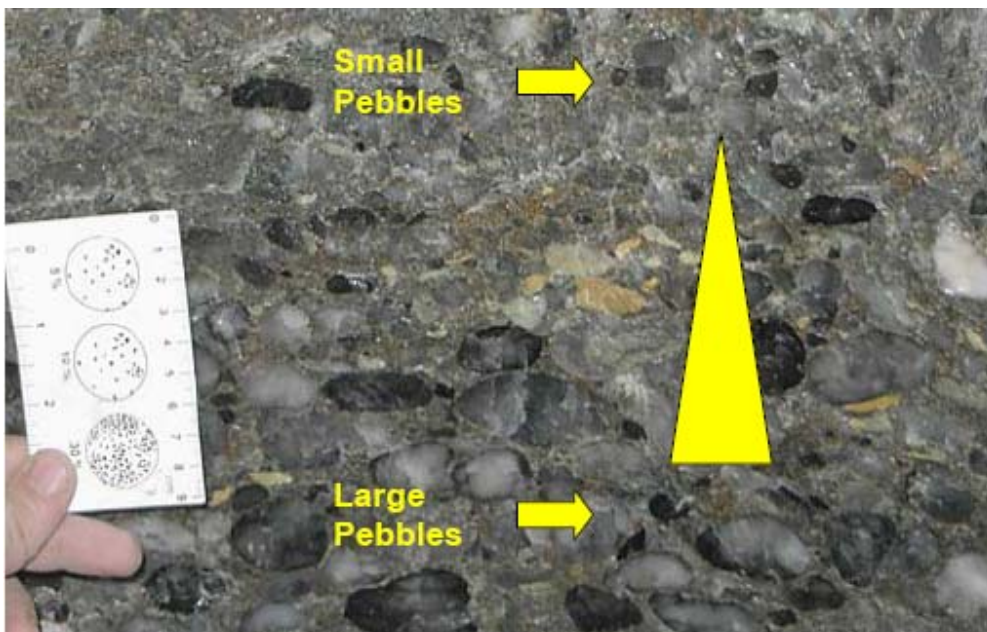


Figure 3.10. B3 conglomerate indicating the upward fining cycle observed at geological section D.

Minter et al. (1986) stated that the B placer is confined to discrete, interconnected channel-ways, which are entrenched into the Upper Shale Marker and that “the channel banks are steep in places, due to the cohesive nature of the footwall” Minter et al. (1986). The formation of the discrete channels, separated by islands onto which no placer sediment was deposited, is due to the cohesive nature of the light coloured khaki shale of the Upper Shale Marker that served as the palaeo-surface.

The discrete channel resulted in the highly channelised fluvial deposits of the B3 facies, and represents deeper and more sustained flow. As a result more abundant cross-stratification in the form of sand waves is present in this lithological unit (section 4.6.2).

The quartz vein between the contact of the B placer and the USM can be observed in the eastern part of geological section D. Once again, the influence of this quartz vein on the geometry of the B placer is not fully understood and further work is required.

4. THE B PLACER LITHOLOGY

Investigation, pertaining to pebble composition, pebble size, sorting and sedimentary structure, associated with the pebbles of a conglomerate, can reveal information regarding to the origin of the conglomerate, the transport mechanism as well as the sedimentary depositional environments.

Parameters, related to the pebbles, associated with the conglomerates that were investigated, include:

1. Varieties and relative abundances
2. Pebble sizes
3. Pebble morphology (shape and roundness)
4. The sorting and packing of the pebbles

4.1 Varieties and relative abundances

A wide range of pebble types constitute the pebble assemblage of the B placer conglomerates, which can be divided into durable and non-durable types. Pebbles were classified by means of their lithology type (eg. quartz, chert, etc.), colour, texture and hardness. Hardness was determined by scratching the pebbles with a knife blade (+- 5.5 on Mohs scale). This test served to distinguish between cherts from similar looking, but softer, non-durables.

The varieties and relative abundances of the different pebbles were determined by constructing a counting frame for grid counting. An eight-centimetre Perspex frame was constructed, with inside dimensions of 220 mm x 220 mm. Small holes 20 mm apart were drilled into the sides and then strung with bright yellow fishing line. This result was 100 intersection points. The varieties and relative abundances were then determined by holding the frame against a clean,

reasonably flat exposure. The clast type and matrix at each intersection point within the counting frame was then recorded on laminated sheets with a permanent marker. The outline of each frame was marked with a wax crayon on the sidewall to prevent overlapping of areas that had already been counted. Two frames were counted at each exposure, resulting in a total of 200 counts per exposure.

The *a*, *b* and *c* axes of the pebbles were measured to calculate the sizes, shape and sorting of the pebbles.

4.1.1 Durable Pebbles

4.1.1.1 Quartz pebbles. The quartz pebbles in the layers of conglomerate mainly consist of white and dark quartz. The white quartz pebbles vary from clear, almost transparent quartz, to milky white quartz. The milky white quartz is the most abundant and only a very few opalescent blue quartz pebbles were encountered. The dark quartz pebbles vary from dark smoky quartz to a translucent smoky quartz. The smoky quartz is due to in situ secondary alteration in various stages of progress, converting white quartz to smoky or dark quartz. This process normally starts in fractures and along the outer rim of the clear and white milky quartz pebbles and is due to the radiation of uranium particles present in the host rock. Fractures in the quartz pebbles are common and are mostly filled by other material, due to secondary action after deposition of the pebbles. The edges of the pebbles of milky quartz can sometimes be very irregular and can easily be mistaken for angularity, but careful investigation reveals that solution of the quartz pebbles took place after their deposition, causing their edges to show this phenomenon.

4.1.1.2 Chert pebbles. Black and brown colours are the most common in chert pebbles in the B placer conglomerates, but banded chert is also

found with alternating colours of black, brown and grey. Fractures in the chert pebbles are not as abundant as in the quartz pebbles. Fractures that do occur are normally filled by secondary chert.



Figure 4.1. Photograph showing the in situ secondary alteration of milky quartz 2 cm in diameter to smoky quartz. Note how the alteration started at the edge of the milky quartz.

4.1.1.3 *Agate pebbles.* Agate pebbles are only rarely encountered. They have complex patterns of alternating black, brown, grey or white bands (Figure 4.2).



Figure 4.2. Photograph showing an agate 1.5 cm in diameter intersected in one of the underground bore holes.

4.1.2 Non-Durable Pebbles

An important factor, which is seldom taken into account, is the nature and quality of light available underground. The yellow light from a cap lamp enhances the yellowish colours underground. Due to this, pebbles that appeared yellow underground might in fact be of a much paler colour. The colour descriptions of the pebbles were therefore done in natural light on wet samples.

4.1.2.1 *Quartzite Pebbles.* Pebbles of blackish-grey, brownish-grey, white and green quartzites are present in the B placer conglomerates. Fractures in the pebbles are rare and it appears that the quartzite pebbles withstand stress and strain better than the quartz pebbles.

4.1.2.2 *Silicified Shale Pebbles.* The pebbles of shale are the most common type amongst the non-durable pebbles in the B placer and vary from yellow to black. The shale is always present in the layers of the conglomerates and varies in quantity from moderate to abundant. The pebbles have angular to subrounded edges or flattened shapes. Pettijohn (1957) proposed that the pebbles of shale were deposited as soft clay within the conglomerate layers and were flattened during diagenesis.

4.2 Matrix

The matrix consists predominantly of sand size quartz, with varying amounts of pyrite and detrital or flyspeck carbon. Pyrite is the next most common constituent of the matrix. Compact rounded or buckshot pyrite is the most common type in the conglomerates and usually has a grain diameter of less than 2mm. The buckshot pyrite is a detrital mineral, presumably derived from deposits of vein-quartz. The detrital pyrite generally occurs in the form of a layer or series of layers in the conglomerates. These layers may sometimes be at an angle to the

quartzite bedding, showing clearly that the pebble portion and matrix portion of the conglomerates were transported and deposited in succession, in currents of diminishing strengths.

4.2.1 Carbon

Two terms, kerogen and bitumen, are used to describe Precambrian carbonaceous matter. Kerogen refers to the insoluble particulate-macromolecular organic matter dispersed in consolidated sediments and has been virtually immobile since deposition. Precambrian kerogen was probably similar to type-I and/or type-II kerogen. Type-I kerogen is derived from lacustrine algae and type-II from phytoplankton. Type-III kerogen is absent and is derived from terrestrial vascular plant debris. Bitumen refers to a random macromolecular organic substance, which is mobile as a viscous fluid, once as a fluid, but has subsequently solidified by poly-merization to an immobile solid phase (Spangenberg and Frimmel, 2001).

The carbon present in the B-reef occurs as granules (flyspeck) of about 2 mm in diameter or less, and as seams that are composed of slender carbon columns arranged perpendicularly to the contact of the seams. The carbon seams may vary from 5 mm to 10 cm in thickness and occur along the unconformity between the Upper Shale Marker and the lower B reef facies, or occasionally between the Bottom and Middle cycles of the facies (Figure 4.3).

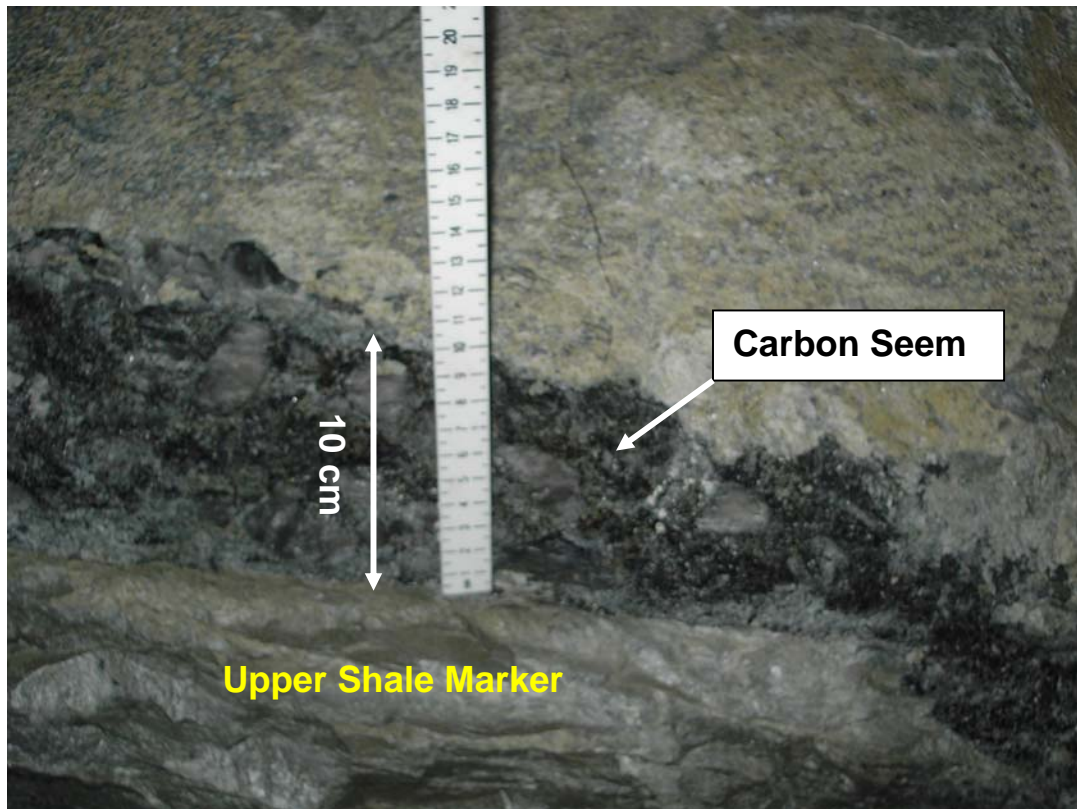


Figure 4.3. A carbon seam with a thickness of 10 cm at location 1810 W1 W5 A.

4.3 Pebble sizes

Pebble size variation assists one to determine the in-wash direction of the fluvial system. Regardless of the fact that the size of pebbles vary considerably within channels in both a vertical and lateral sense, some useful generalized conclusions can be drawn from this data. The size of pebbles in a stream is mainly a function of three factors:

1. The size of clasts derived from the source.
2. The decline in size due to abrasion.
3. The competence of a stream at any given point.

The B placer conglomerate is a very well-cemented conglomerate, making it impossible to remove the pebbles from the matrix for size measurement. This is a considerable disadvantage and complicates the measurements of pebble sizes

to a certain extent. Pebble size measurements were therefore carried out on two-dimensional surfaces, with the pebbles still being part of the conglomerate.

According to Hodgson (1967), the angle of observation, in respect to the conglomerate, must always be the same. Hodgson measured pebbles at a view from the bottom, looking at a plane parallel to the bedding, and secondly from the side. Hodgson found that all the pebbles viewed from the bottom are larger than the same pebbles viewed from the side, suggesting that the pebbles are orientated with their longest and intermediate axes horizontally and that the shortest axis is orientated at right angles to the bedding. Another feature that must be considered is the possible preferred orientation of the pebbles. This will have the effect that the pebbles viewed in section, along the inwash direction, will have a different mean diameter than that for the same pebbles viewed at right angles to this direction.

It is therefore obvious that pebble measurements should always be made in one selected direction relative to the bedding plane. Pebbles were therefore only measured on east-west striking faces, which represent the major in-wash direction. This resulted in only the c-axis and b-axis being measured.

Steyn (1963) measured the 10 largest pebbles within a square foot. The mean diameters of the different kinds of pebbles in the B placer conglomerates were attained by measuring the 10 largest pebbles, each pebble type represented as non-durable pebbles, durable pebbles and the 10 largest pebbles, in a two-metre exposure.

The actual size of a pebble was calculated by obtaining the square root of the product of the two pebble diameters (a and c axis). This procedure was followed in order that the author could classify his observations according to a commonly used grade scale, the Wentworth scale (Table 4.1), for size subdivisions (Wentworth, 1922).

Particle Size Range (in mm)	phi unit	Sediment grade Name	Rock Name (Visually Discernible)	
4096	-12	Very large boulders	Conglomerate (if the fragments are round in shape)	
2048	-11	Very large boulders		
1024	-10	Medium boulders		
512	-9	Small boulders		
256	-8	Very large cobbles		
128	-7	Very large cobbles		Or
64	-6	Very Coarse pebble		
32	-5	Coarse pebbles		Breccia (if the fragments are angular)
16	-4	Medium pebbles		
8	-3	Fine pebbles		
4	-2	Very fine pebbles		
2	-1	Very coarse sand	Sandstone	
1	0	Coarse sand		
1/2	1	Medium sand		
1/4	2	Fine sand		
1/8	3	Very fine sand		

Table 4.1. Wentworth Particle Grade-Size Scale (Friedman and Sanders, 1978).

Ten locations were selected to determine the pebble size distribution for the overall 10 largest pebbles, the 10 largest durable pebbles and the 10 largest non-durable pebbles within the B1 and B3 conglomerates. From this data, the in-wash direction of the B-reef material could be determined. Map 1 indicates the location of the ten sites and the measurement of the pebble sizes can be observed in Appendix II.

The data of the pebble sizes were plotted on a graph indicating the decrease in pebble sizes in an eastern direction (Figure 4.4). The western sector of the mine is characterized by larger pebble sizes, which decrease gradually up to site number 1, from where the pebble sizes tend to level out. The pebble sizes at site 6 showed an increase due to a trap site, resulting in the formation of a gravel bar.

An overall decrease in pebble size was experienced from west to east in the 10 largest pebbles, 10 largest durable pebbles and the 10 largest non-durable pebbles. The 10 largest pebbles measured in the B3 conglomerate, North-western sector, decreased from 44 mm to 32 mm in the B1 conglomerate in the south-eastern sector of the mine. The 10 largest durable pebbles decreased from 40 mm in the B3 conglomerate to 29 mm in the B1 conglomerate, and the 10 largest non-durable pebbles decreased from 40 mm in the B3 conglomerate to 28 mm in the B1 conglomerate.

The decrease in the pebble sizes clearly indicates that the in-wash direction of the B placer was from the west, flowing in an eastern direction.

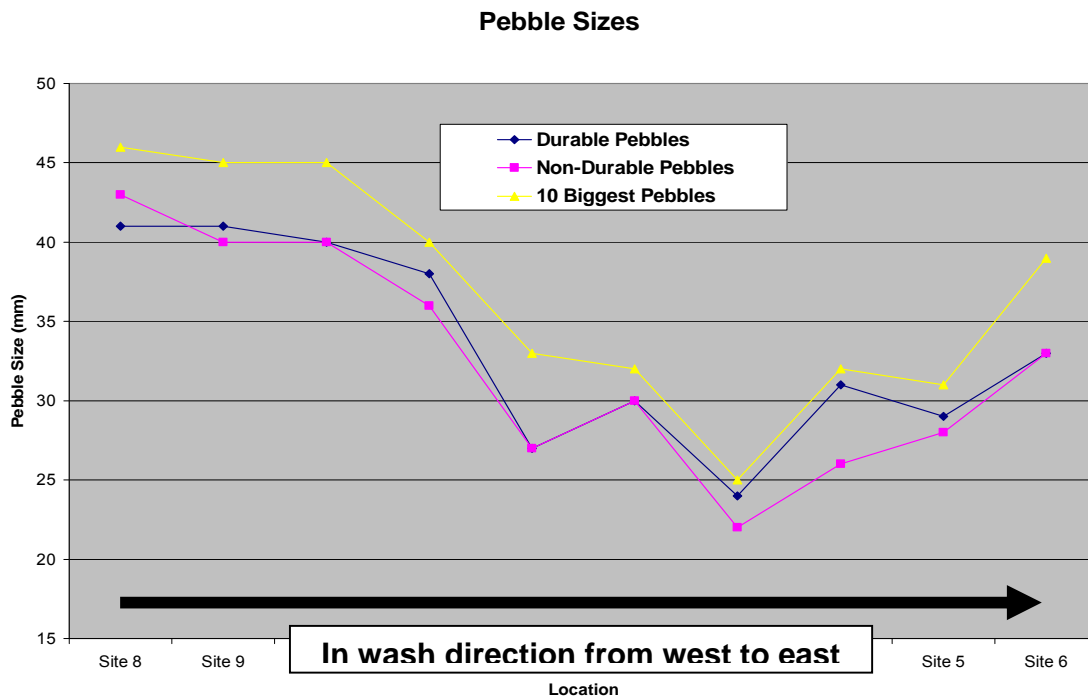


Figure 4.4. Decrease in pebble sizes in an eastern direction.

Tables 4.2 to 4.6 reveal the different cycles present in the B placer. The upward fining cycles of the B3 conglomerates and the upward coarsening cycles of the B1 conglomerates can be clearly observed. The upward fining cycle of the B3 conglomerate is typical of fluvial deposits, while the upward coarsening cycles of the B1 were formed by the progradation of a fluvial braided system into a standing body of water.

4.4 Pebble morphology (shape and roundness)

The morphology of the pebbles has two aspects: *shape*, determined by various ratios of the long, intermediate and short axes and *roundness*, concerned with the curvature of the corners of the pebbles.

4.4.1 Shape

The shape of the pebbles can be classified into definite shape classes according to the ratios of the longest, intermediate and shortest axes. This makes it possible to classify the pebbles into four classes, namely, disk, spheroid, blade or rod shaped.

As mentioned before, the B-reef conglomerates are very well cemented and as a result the pebbles could only be viewed in two-dimensions. It was however possible to obtain some loose pebbles at the mining face, underground. The durable pebbles present in the B-reef varied between rod to spherical in shape indicating a predominantly fluvial depositional environment, while the shales present in the layers of the conglomerates varied between rod to blade (flattened) in shape. The reason for the flattened shapes of the shale has already been discussed in section 4.1.2.2.

Table 4.2: Geological Section A – Pebble Size Distribution B1 Conglomerate (Cockeran, 2006)

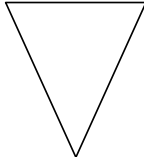
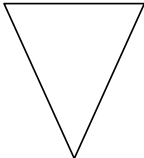
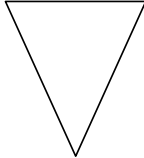
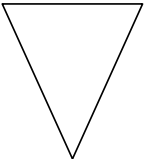
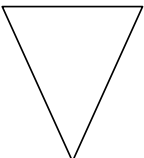
Locality of the pebble count on section line	Pebble size	Feature
14 m Top Cycle	62	Upward Coarsening 
	50	
	46	
	43	
	42	
	38	
	37	
	37	
	34	
	32	
Average Size	42	
14 m Bottom Cycle	38	Upward Coarsening 
	36	
	35	
	35	
	32	
	32	
	27	
	25	
	25	
	22	
Average Size	31	
28 m Top Cycle	38	Upward Coarsening 
	36	
	35	
	35	
	32	
	32	
	27	
	25	
	25	
	22	
Average Size	31	
28 m Middle Cycle	45	Upward Coarsening 
	35	
	27	
	27	
	25	
	25	
	25	
	22	
	22	
	20	
Average Size	27	
28 m Bottom Cycle	45	Upward Coarsening 
	35	
	28	
	27	
	25	
	25	
	25	
	22	
	22	
	20	
Average Size	27	

Table 4.3: Geological Section B – Pebble size Distribution B1 Conglomerate (Cockeran, 2006)

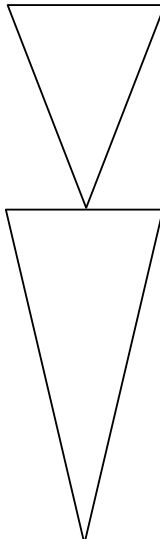
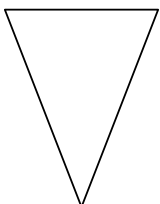
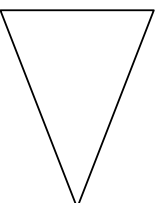
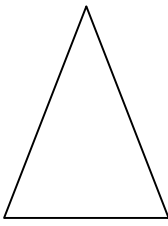
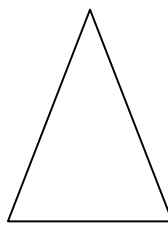
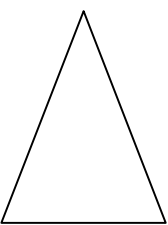
Locality of the pebble count on section line	Pebble size	Feature
22m	57	Upward Coarsening 
	42	
	47	
	47	
	59	
	38	
	41	
	32	
	65	
	47	
	68	
	39	
	53	
	45	
	51	
	46	
	58	
	36	
56		
48		
Average Size	49	

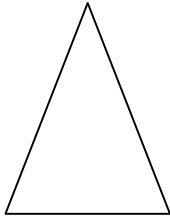
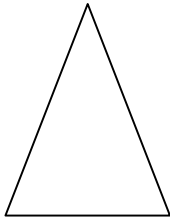
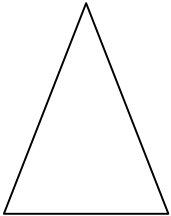
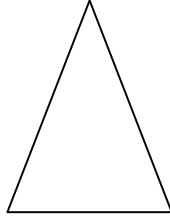
Table 4.4: Geological Section C – Pebble size Distribution B1 Conglomerate (Cockeran, 2006)

Locality of the pebble count on section line	Pebble size	Feature
29 m Top Cycle	62	Upward Coarsening 
	50	
	46	
	43	
	42	
	38	
	37	
	37	
	34	
	32	
Average Size	42	
29 m Bottom Cycle	34	Upward Coarsening 
	34	
	34	
	32	
	32	
	30	
	29	
	29	
	28	
	28	
Average Size	31	

**Table 4.5: Geological Section D – Pebble size Distribution B3 Conglomerate
(Cockeran, 2006)**

Locality of the pebble count on section line	Pebble size	Feature
1 m Top Cycle	20	Upward Fining 
	22	
	22	
	22	
	26	
	32	
	35	
	37	
	45	
	45	
Average Size	31	
11 m Top Cycle	10	Upward Fining 
	21	
	23	
	24	
	26	
	32	
	33	
	35	
	36	
	42	
Average Size	28	
11 m Bottom Cycle	32	Upward Fining 
	42	
	48	
	48	
	52	
	53	
	56	
	61	
	62	
75		
Average Size	53	

**Table 4.6: Geological Section E – Pebble size Distribution B3 Conglomerate
(Cockeran, 2006)**

Locality of the pebble count on section line	Pebble size	Feature
2 m Top Cycle	14	Upward Fining 
	15	
	17	
	18	
	20	
	20	
	20	
	20	
	25	
	26	
Average Size	20	
2 m Bottom Cycle	15	Upward Fining 
	15	
	17	
	20	
	20	
	23	
	23	
	24	
	25	
	30	
Average Size	21	
16 m Top Cycle	5	Upward Fining 
	8	
	8	
	8	
	11	
	12	
	12	
	13	
	16	
	18	
Average Size	11	
16 m Bottom Cycle	15	Upward Fining 
	16	
	17	
	18	
	18	
	20	
	23	
	25	
	28	
	31	
Average Size	21	

4.4.2 Roundness

The roundness of a pebble is related to the sharpness of curvature of the edges and corners of the pebbles, and reflects, in part, the abrasional history of the pebbles (distance of transportation), as well as indicates the number of cycles through which the pebbles have passed. Large angular pebbles tend to round more rapidly than smaller pebbles. The rate of roundness also depends on the hardness of the pebbles.

The roundness of the pebbles was determined by matching the outlines of the individual pebbles with diagrams of two sets, each set having different sphericity (Figure 4.5). The roundness of the pebbles can then be placed into categories that range from very angular to well-rounded.

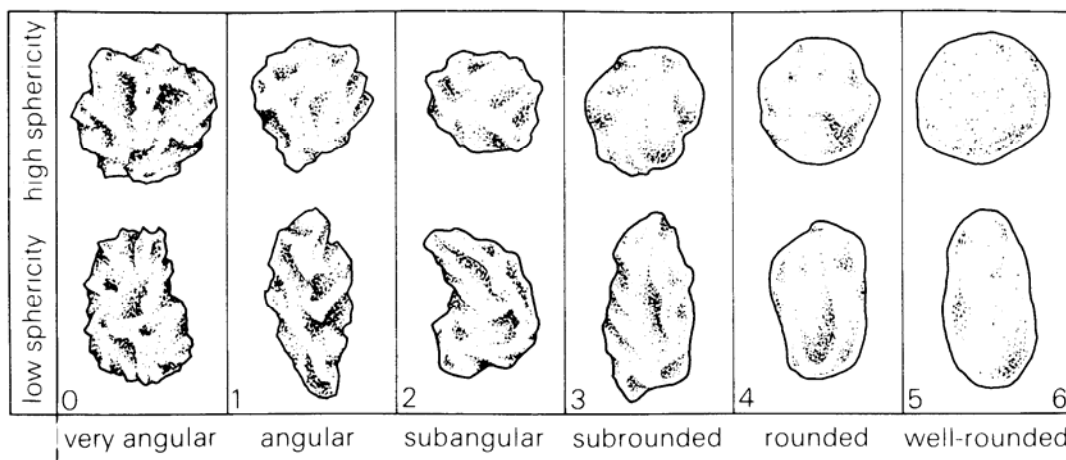


Figure 4.5. Outlines the six roundness classes of particles having high and low sphericity, after Powers, 1953.

The durable pebbles of both the B3 and B1 conglomerate varied between rounded and well rounded, which indicated that this material has been subject to much reworking and/or was transported over a vast distance. The non-durable pebbles, consisting of shales, derived from the underlying paleofloor (Upper Shale Marker), varied from sub-angular to round. The shales are relatively well

rounded for the distance travelled - this is due to the shales being less competent than the durable pebbles.

4.5 The Sorting and Packing of the Pebbles

4.5.1 Sorting of the Pebbles

The term “sorting” of sediment refers to the spread of its particle sizes and can be of great assistance in solving various problems regarding the depositional process and the level of reworking of the sediment.

The level of sorting of the conglomerate was determined by measuring the average diameters of the pebbles (see section 3.3.4). Measuring started at any random pebble, working outwards, until a hundred pebbles had been measured. The information obtained from the measurements is represented graphically in the form of histograms. The pebble measurements used to create the histograms, are attached as Appendix III.

4.5.1.1. Site 1-6: (B1 Conglomerate)

The sorting of the pebbles in Figure 4.6 is very poor and consists of 29% very fine pebbles, 31% fine pebbles and 30% medium pebbles. The coarse pebbles present at this site only contributed 2%, while the remaining 8% of the pebbles fell outside the pebble size range for conglomerates as defined by Wentworth. The poor sorting of the conglomerate at site 1 was the result of the lack of reworking of the original material (B3 conglomerate) due to the standing body of water.

The pebble sorting in Figure 4.7 (site 2) shows a higher level of sorting, compared to site 1, which is roughly 100 m further upstream of site 2. The site

consist of 2% very fine pebbles, 37% fine pebbles, 57% medium pebbles and 4% coarse pebbles.

The level of sorting from site 2 to site 6 (Figure 4.7 to 4.11) continues to improve in an eastern direction, with an additional shift of the modus from fine pebbles to medium pebbles. The higher level of sorting at sites 2 to 6 is an indication of the level of reworking that took place in the standing body of water in which the B3 conglomerate was deposited to develop into the more mature B1 conglomerate.

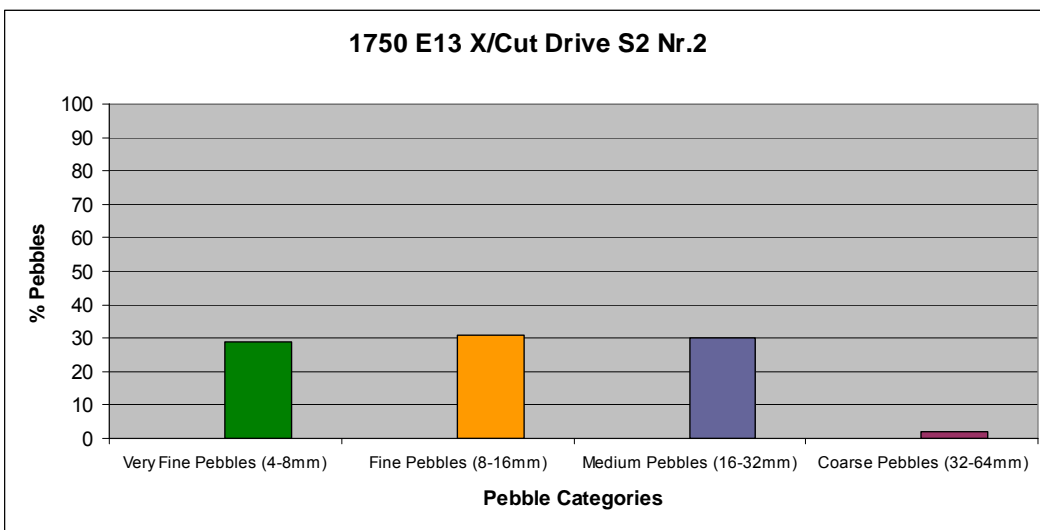


Figure 4.6. Histogram of the particle distribution at Site 1.

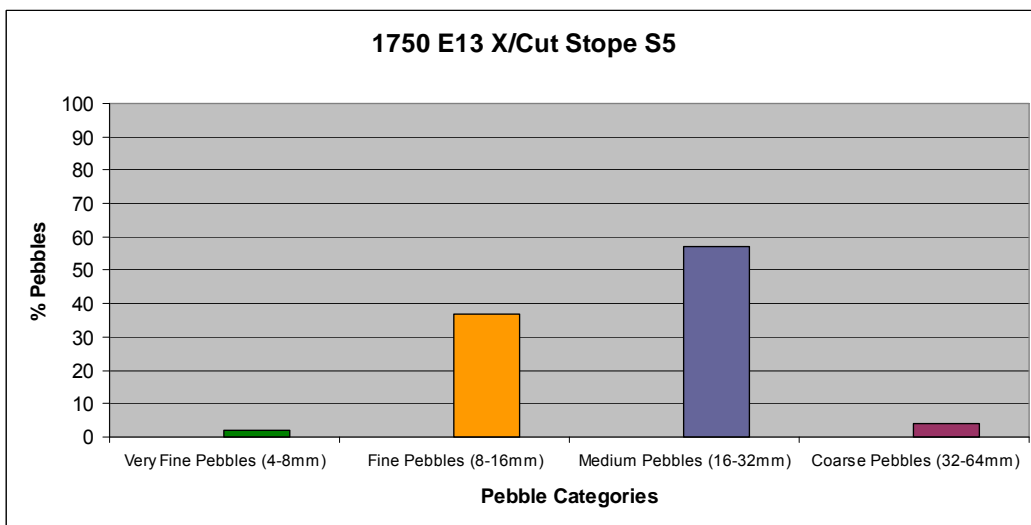


Figure 4.7. Histogram of the particle distribution at Site 2.

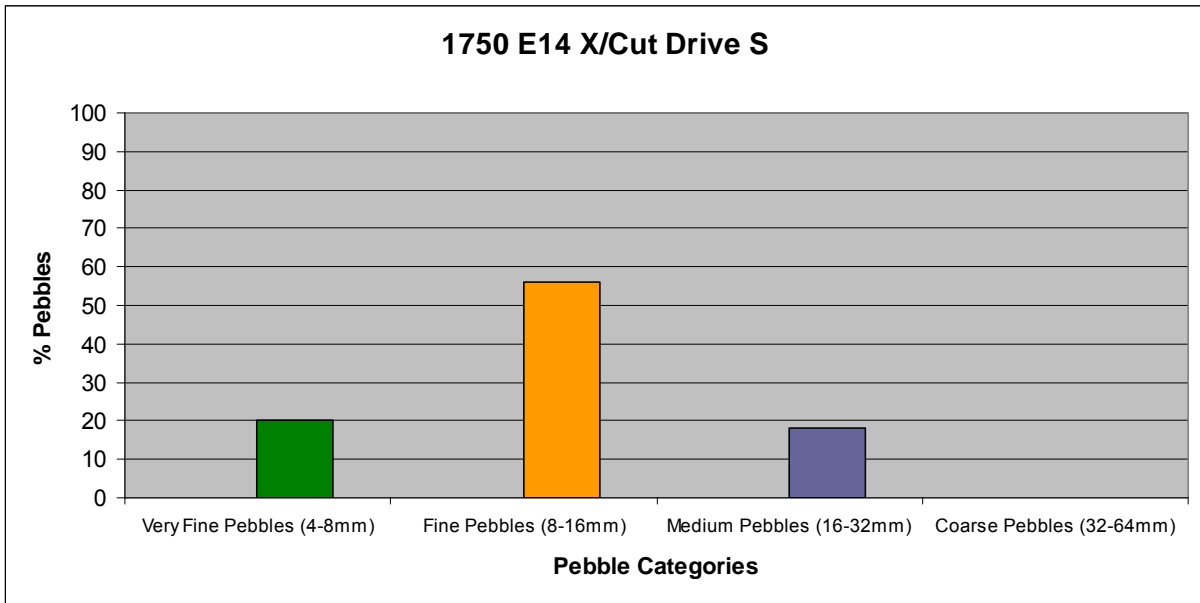


Figure 4.8. Histogram of the particle distribution at Site 3.

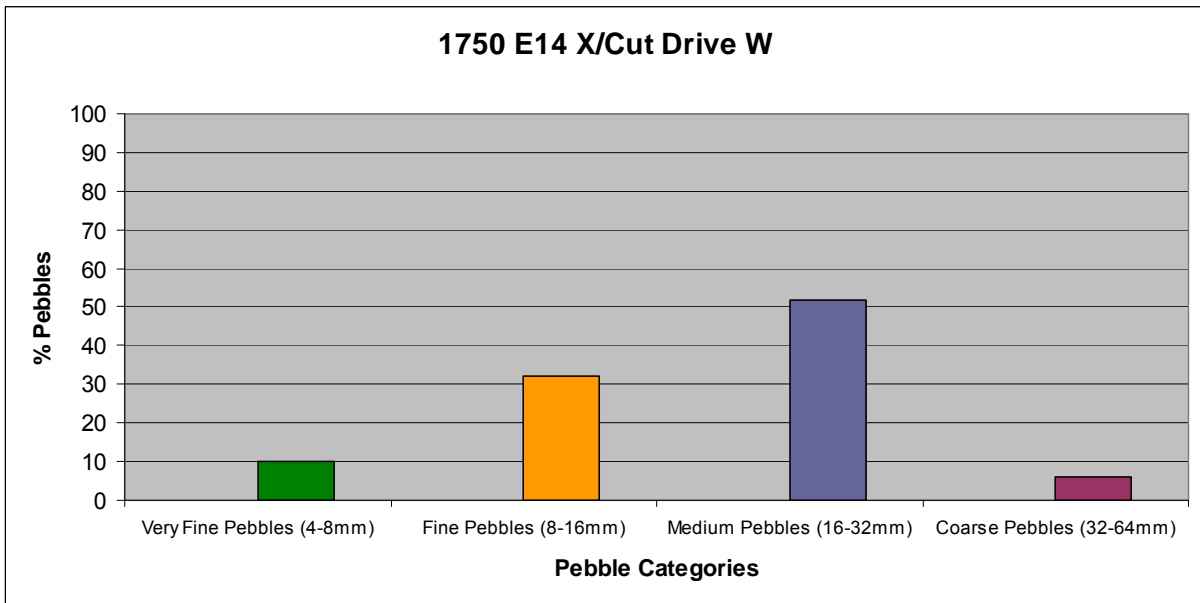


Figure 4.9. Histogram of the particle distribution at Site 4.

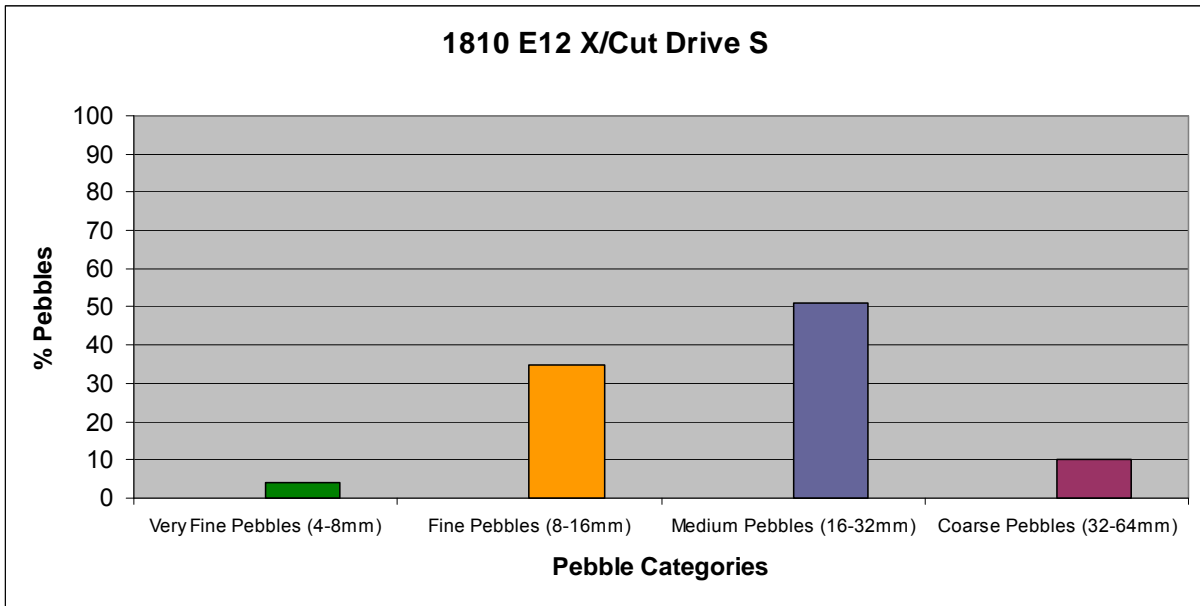


Figure 4.10. Histogram of the particle distribution at Site 5.

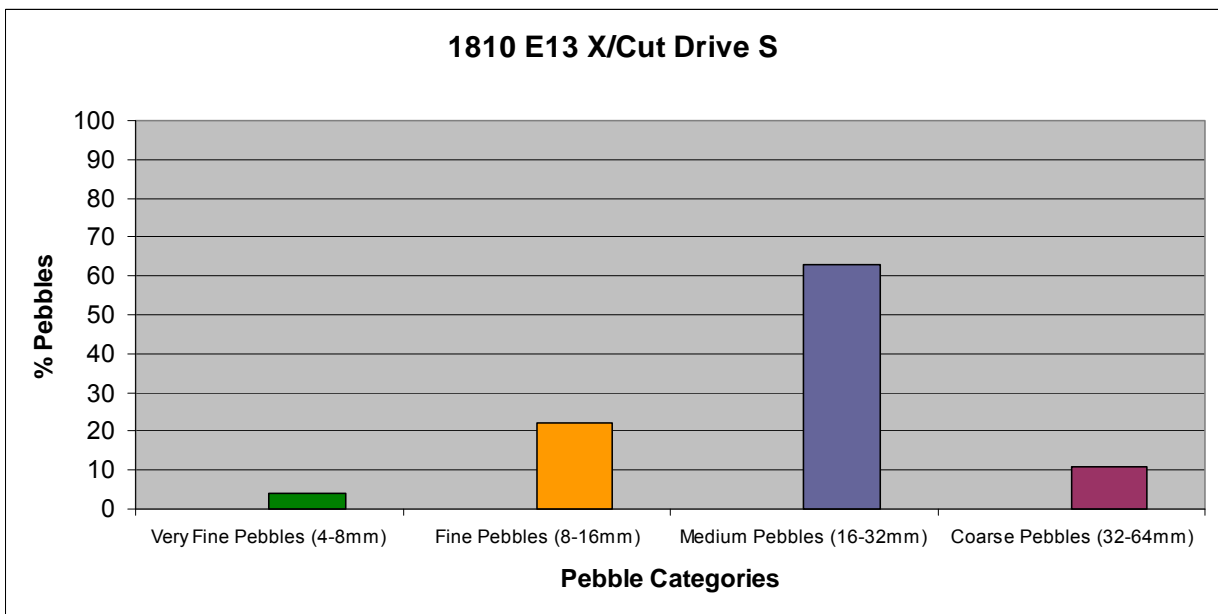


Figure 4.11. Histogram of the particle distribution at Site 6.

4.5.1.2. Site 7-10: (B3 Conglomerate)

The level of sorting at sites 7, 9 and 10 is high, with the modus representing the medium pebble size, ranging from 55% to 70%. The high level of sorting in the B3 conglomerate was not expected. A possible explanation for the high level of sorting is the location of the sites. All the above-mentioned sites are located in the same narrow channel. The narrow channel intensified the flow energy, with the result of a better level of sorting due to the fact that all the pebbles smaller than 16 mm had been washed away, and deposited further downstream.

Site 8, located in a broader channel, shows a lower level of sorting, with a higher percentage of fines present compared to sites 7 and 9.

Comparisons between the particle distribution of the B1 conglomerates and the B3 conglomerates show a great deal of similarity, as seen in Figures 4.16 and 4.17. The similarity between the B1 and B3 conglomerates indicates that the braided river was more dominant than the tide and/or wave action of the standing body of water in which it was propagating. Data, obtained from Amazon placers, indicate that typical Witwatersrand river systems maintained its braided character throughout its entire course, even within the tidal zone. The braided tidal systems are envisaged to have been similar to pure fluvial braided streams (Els, 1998).

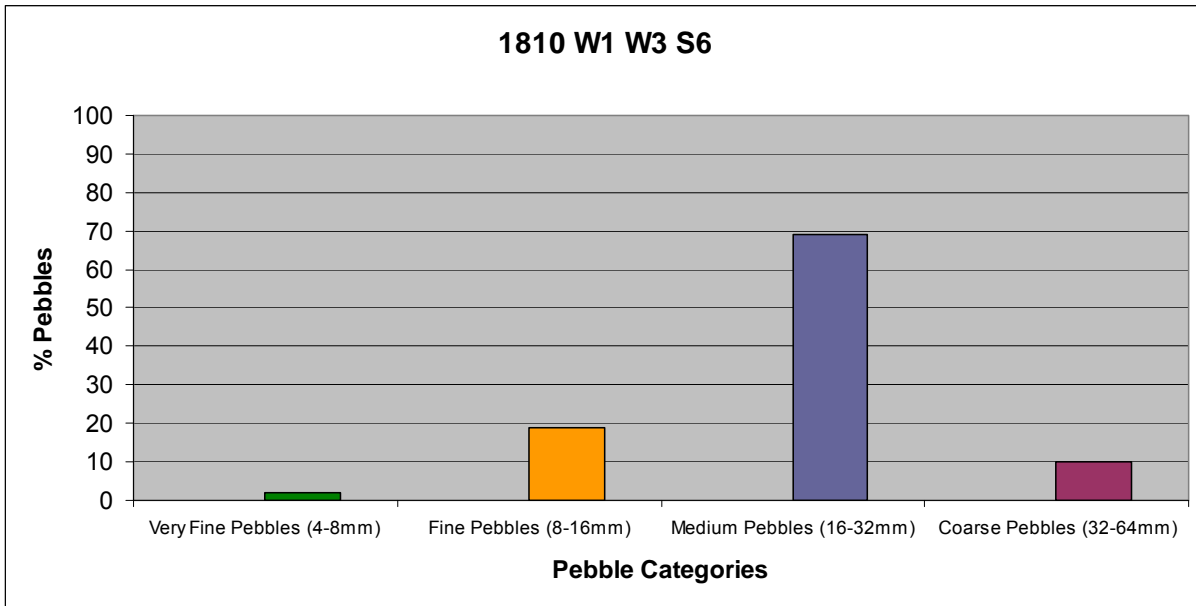


Figure 4.12. Histogram of the particle distribution at Site 7.

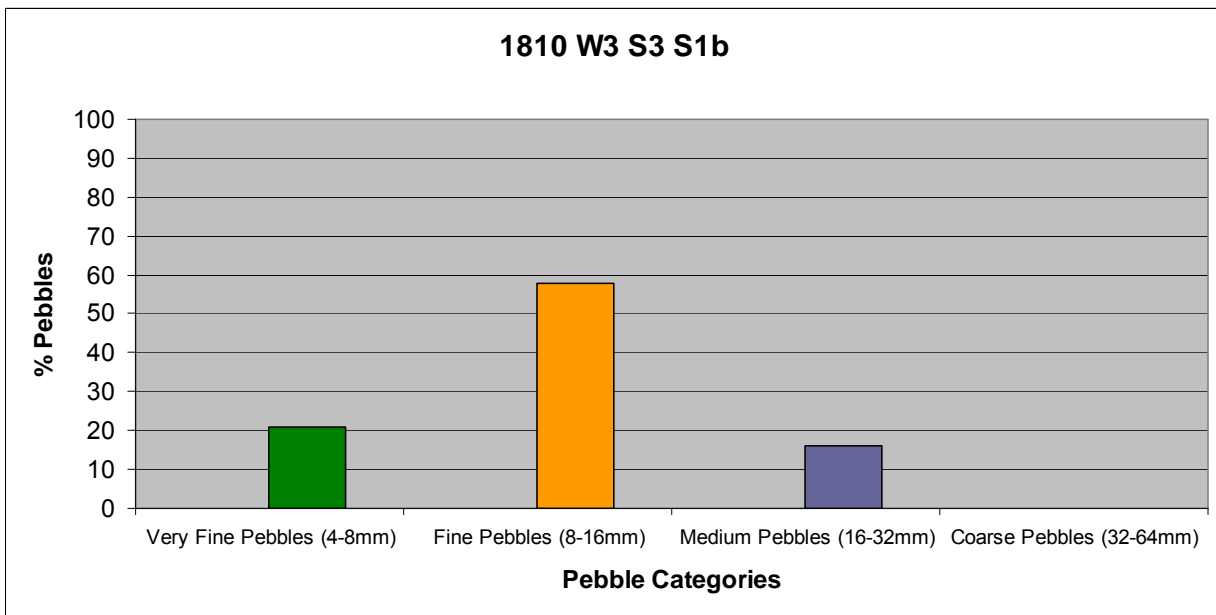


Figure 4.13. Histogram of the particle distribution at Site 8.

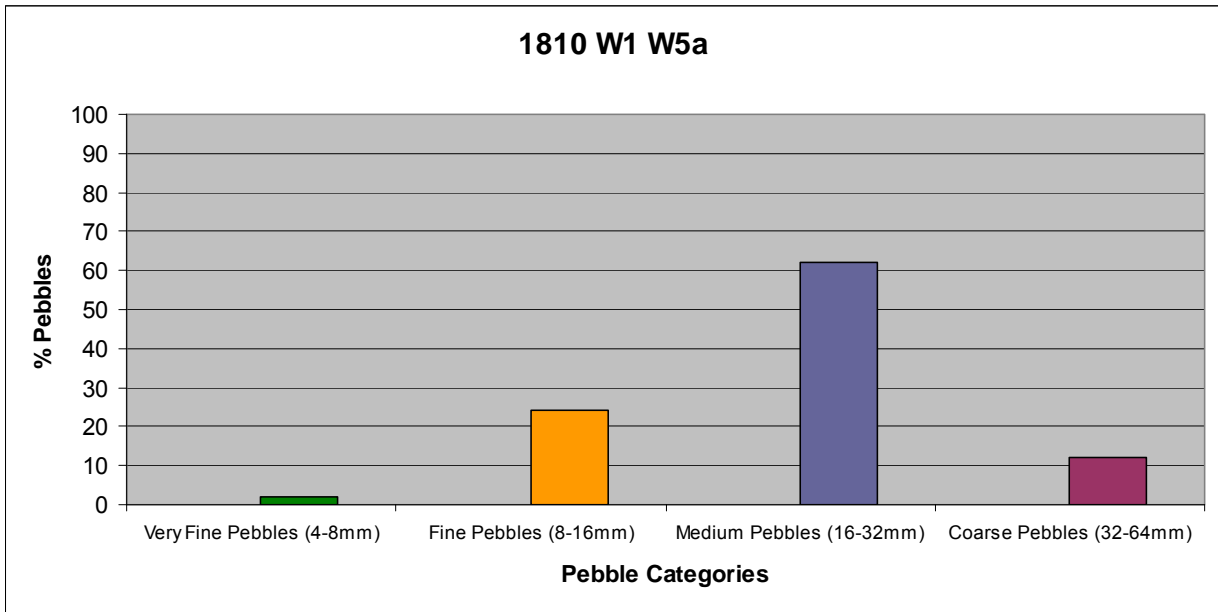


Figure 4.14. Histogram of the particle distribution at Site 9.

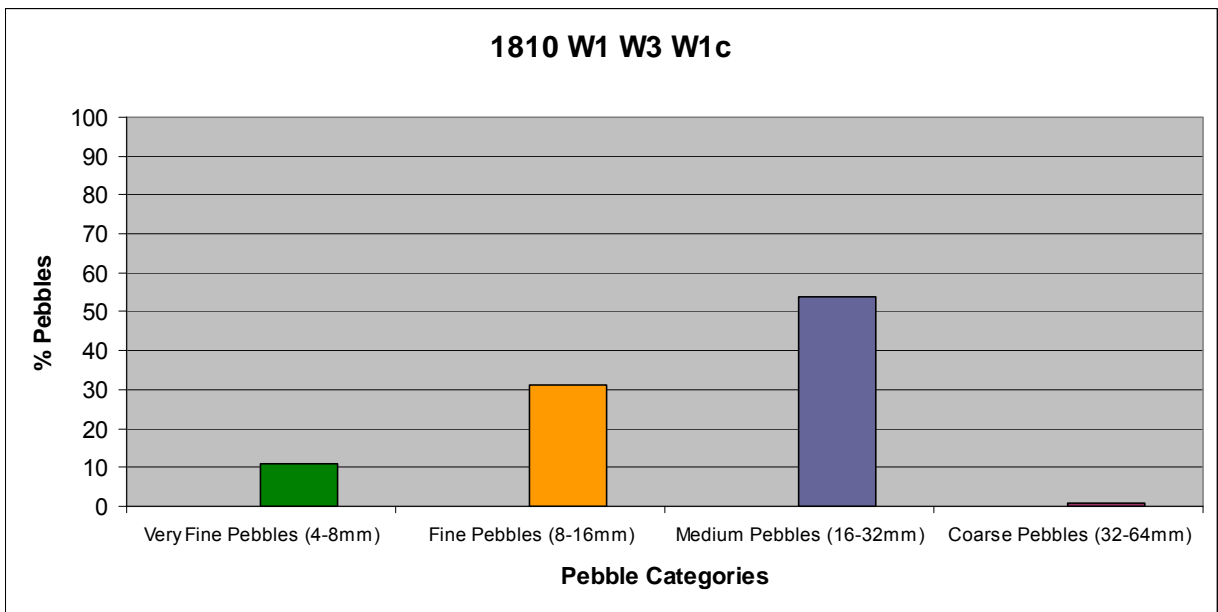


Figure 4.15. Histogram of the particle distribution at Site 10.

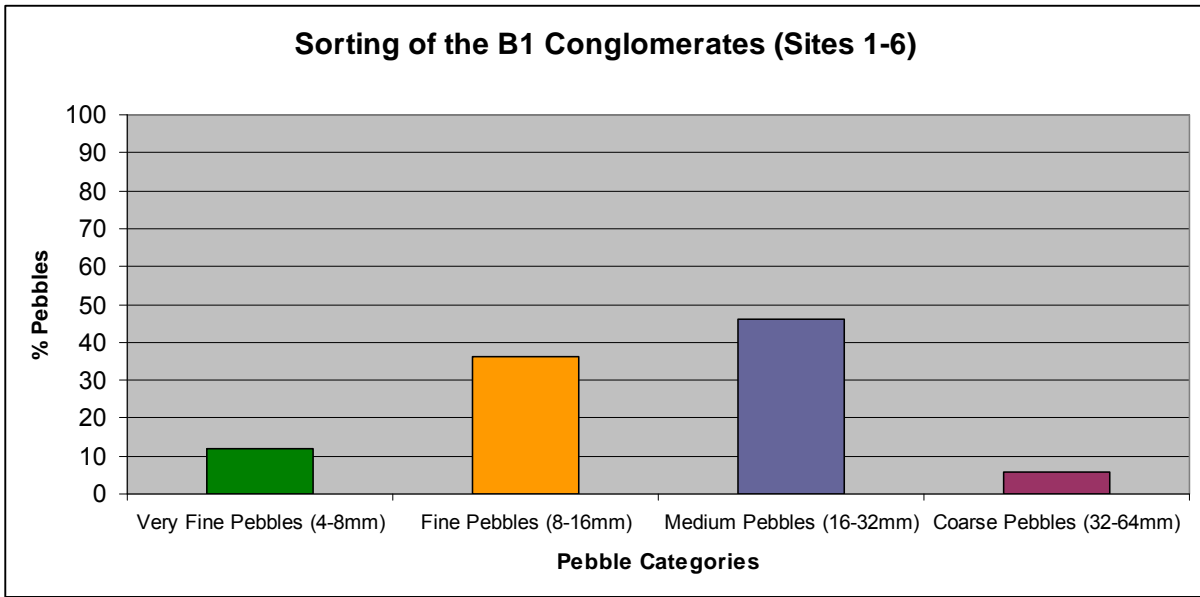


Figure 4.16. Histogram of the particle distribution of all the B1 conglomerates.

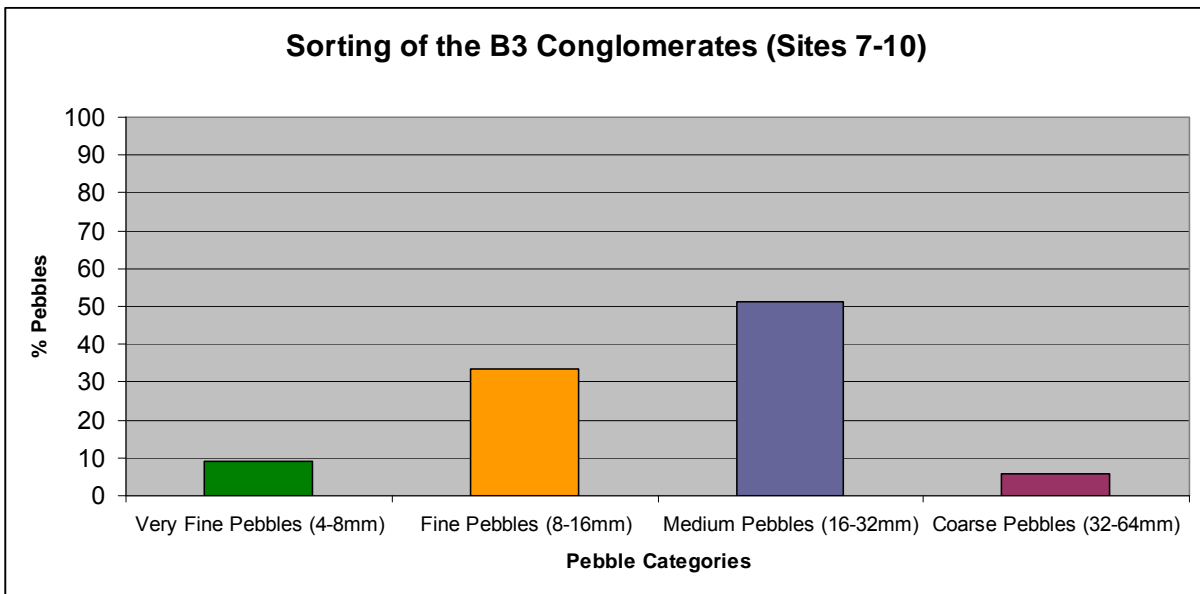


Figure 4.17. Histogram of the particle distribution of all the B3 conglomerates.

4.5.2 Packing

The term “pebble packing” refers to the percentage pebbles in a conglomerate and can be indicative of various important features like the kind of inwash, the level of rewashing after deposition, as well as the possible mixing of pebbles from another source.

The packing of the conglomerates was obtained by estimating the percentage of the pebbles in the conglomerates by using the percentages of the 200 intersected points obtained from the grid counting on the sidewall (Appendix I). The pebble percentages were then classified into three different classes, compact (more than 30% pebbles), medium packed (between 15% and 30% pebbles) and loosely packed (less than 15% pebbles).

The packing of the B1 and B3 conglomerates shows no major difference, as seen with the sorting of the conglomerates. Both the B1 and B3 conglomerates fall into the compact category. The B1 conglomerate’s packing varies from 30% to 52%, at an average of 40% pebbles present in the conglomerate, while the B3 conglomerate varies from 39% to 50%, with an average of 44% pebbles.

The bottom cycles of the B1 conglomerate at an average of 43% tends to be more compact than the upper cycles at an average of 38%.

4.6 Vectorial and Scalar Data

Many properties of sediments can be applied to determine the palaeocurrent of the deposit. Vector properties refer to primary structures that formed during sediment movement, and define the direction of the movement. Scalar properties such as grain size, sorting and unit thickness can also be used to determine the direction of sediment transport.

The scalar and vector properties can be ranked. The greater the scale of the scalar or vector property used to infer the transport direction, the lower its directional variance (Minter and Loen, 1991).

The scalar and vector properties can be ranked as follow:

Rank 1 - Pebble size, ripple-marks

Rank 2 - Braidbelts

Rank 3 - Separate channels

Rank 4 - Cross-bedding

4.6.1 Ripple-bedding

Original ripples have been observed on the roofs of drives and stopes, where the rock had broken along the bedding planes (Figures 4.18 to 4.20). Ripple bedding is common in Witwatersrand rocks, but on balance they are unreliable indicators of palaeocurrents. This is because ripple bedding represent relative low energy structures. All the ripples observed underground only consist of one set of ripples, indicating flow directions varying form 46° to 172°. These flow directions may either be due to strong prevailing winds and/or low energy currents.



Figure 4.18 Ripple marks encountered in the hanging wall at Site 2, with a wave length of 6cm.



Figure 4.19. Ripple marks observed on the hanging wall at site 7, with a wave length of 3cm.

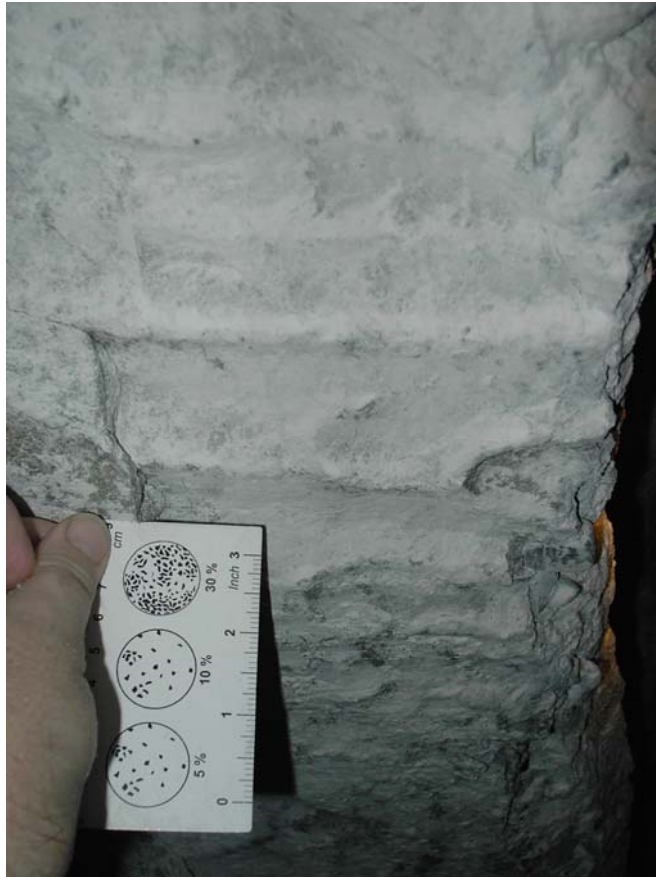


Figure 4.20. A closer view of the ripples, encountered underground.

4.6.2 Megaripples and cross-bedding

In the roofs of many stopes, much larger ripple structures (megaripples) have been observed as illustrated in Figures 4.21 and 4.22. The megaripples consist of a series of roughly parallel smoothly rounded symmetrical ridges or rolls. The megaripples have amplitudes of up to 5 cm and a wave length of up to 60 cm. A section through one of these megaripples (Figure 4.21 and 4.22) revealed primary sedimentary structures in the form of cross-bedding. The megaripples were only encountered overlying the B3 conglomerates.

Mostly planar cross-bedding was observed underground with occasional trough cross-bedding. According to High and Picard (1974), in many cases the dip azimuths of the foresets of planar cross-bedding units are transverse to the

original in-wash direction, and are therefore an unreliable palaeocurrent indicator. Unfortunately no three-dimensional observations of the trough cross-bedding were possible and therefore no reliable data with regards to the in-wash direction of the B reef could be deduced from the cross-bedding observed underground.

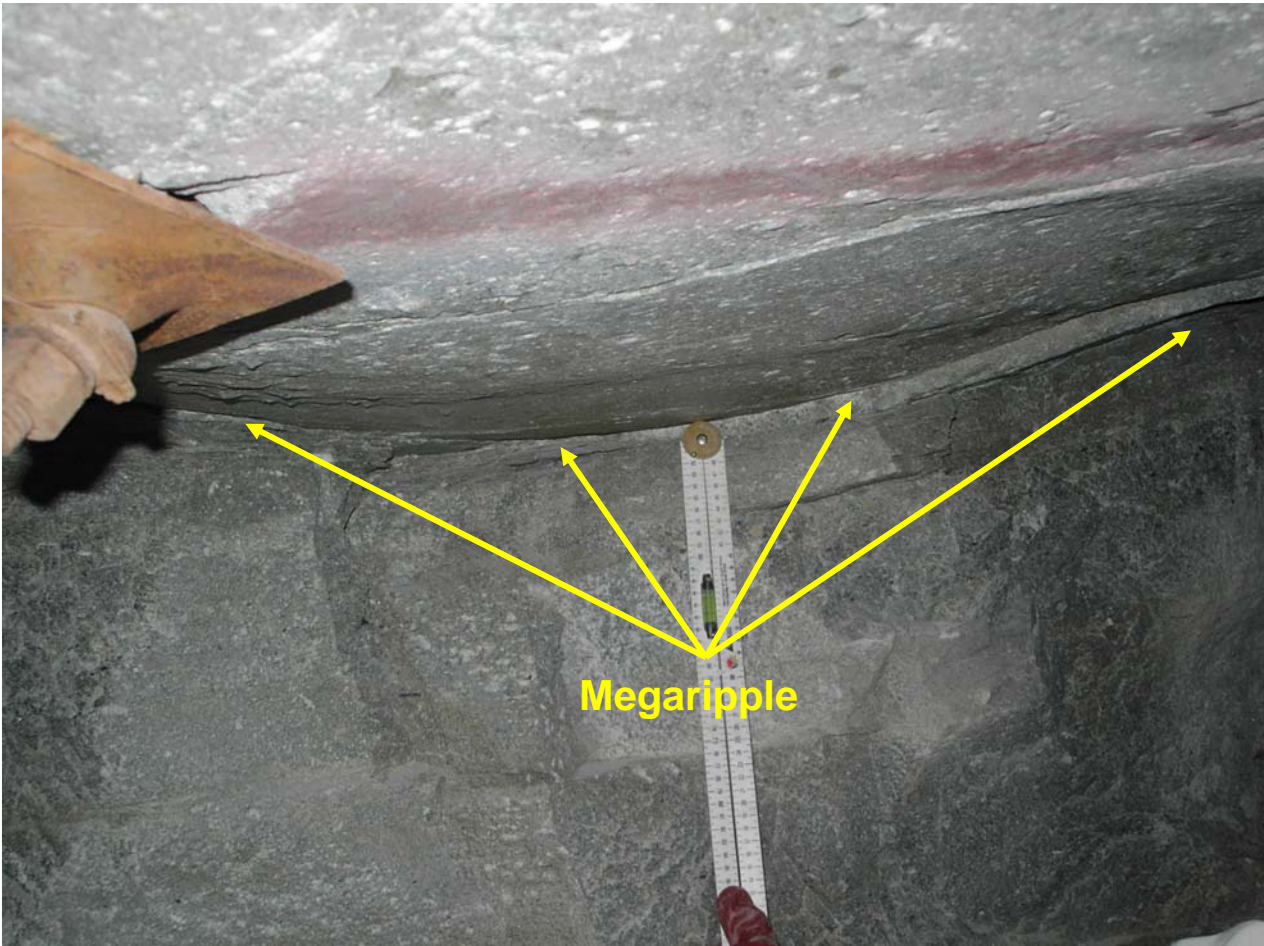


Figure 4.21. Megaripples observed in the hanging wall at site 1810 W1W5a.

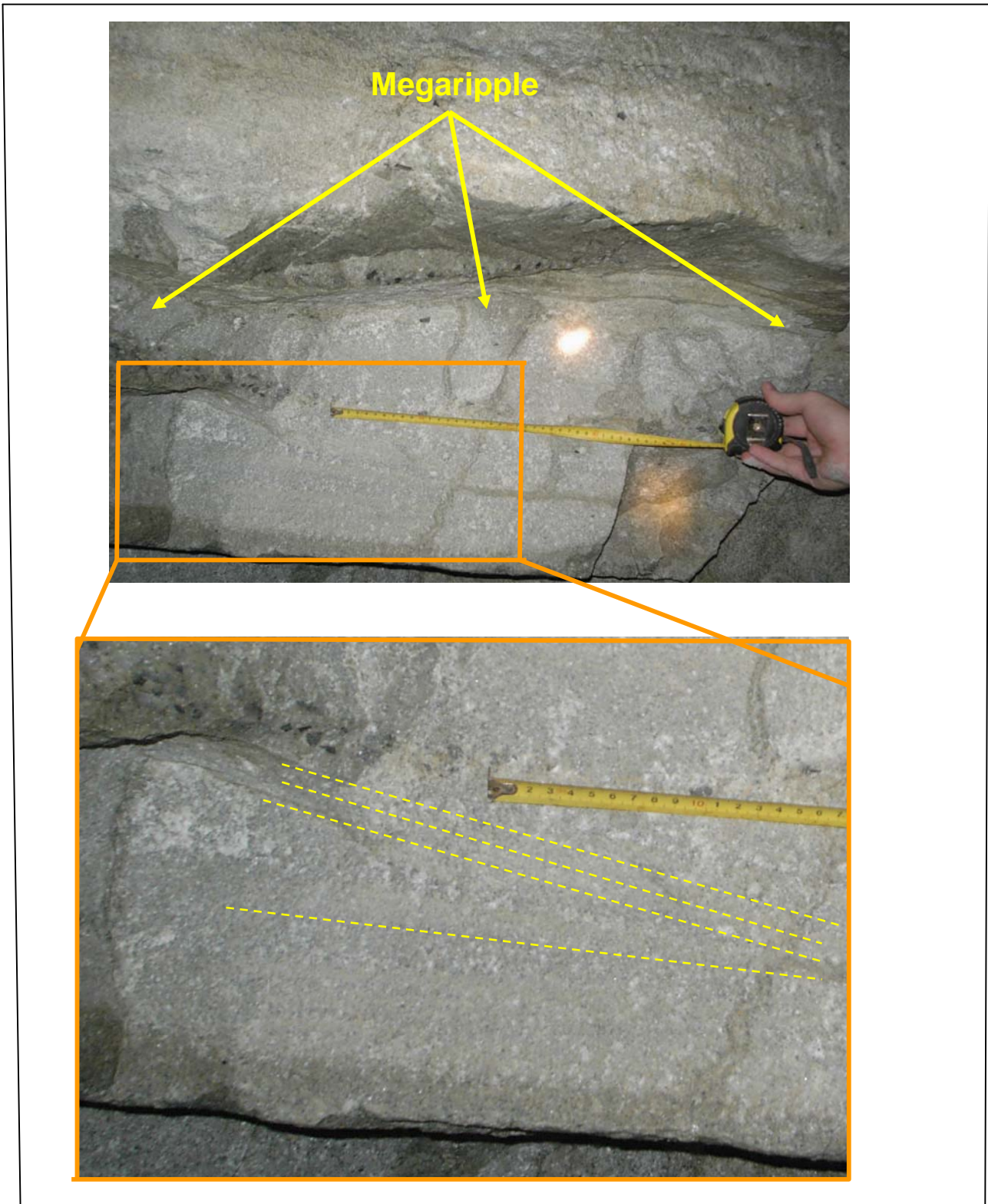


Figure 4.22. Photograph of a megaripple (at top) and an enlargement of a section of the megaripple (bottom) to reveal cross-bedding in the megaripple.

4.6.3 Pebble size

Pebble sizes variation indicated an in-wash direction from the west to the east as discussed in section 4.2.

4.6.4 Clast Imbrication

Pebbles are often imbricated in conglomerates, and in certain instances,, considered as one of the most accurate indicators of palaeocurrent direction (Minter and Loen, 1991). Pebbles in both the B1 and B3 conglomerate displayed poor imbrication due to the near spherical shape of the pebbles present in the conglomerates, and therefore no deductions with regard to in-wash direction could be determined from the pebble imbrication of the B reef.

4.6.5 Pebbles of shale

The Upper Shale Marker at Masimong 5 shaft consists of very fine grained, dark black shale present in the eastern region of the mine and a sandier, light khaki coloured shale in the western region of the mine (Map 2). Grid counting on the B3 and the B1 conglomerates indicated that the B3 conglomerate consists of up to 6% khaki shale, with only site number 8 with a mere 1% dark shale, whereas the B1 conglomerates located in the eastern region of the mine consist of up to 4% black shale and as much as 6% khaki shale. The presence of the khaki shale in the B1 conglomerate and the absence of the black shale in B3 conglomerate clearly indicate an in-wash direction from the west to the east.

4.7 Classification of Quartzites within the B placer

The classification scheme of Witwatersrand quartzites, generated by Law, *et al.* (1990), was used to classify quartzites within the B placer. The categorization implemented by this classification scheme has been modified on the basis of Pettijohn *et al.* (1972) and Dott (1964), and the modified scheme allows for the post-depositional modification of the original detrital assemblages.

The classification scheme thus has relevance to both the genetic depositional environment of the sediment and the post-depositional processes that have affected its present state.

The following modifications to the terminology of Pettijohn *et al.* have been introduced:

1. The term “arkosic” is replaced by feldspathic to avoid the quantitative estimation of feldspar content required for arkose classification. It also allows for the term “arenite” to be retained for all cross-stratified and/or well-sorted sandstones.
2. The term “greywacke” is replaced by “wacke” to avoid the genetic connotation. The term “wacke” is used as a general class of poorly sorted, argillaceous and generally massive sandstones.
3. The term “labile” is introduced to include all unstable fragments that are no longer distinguishable as either feldspathic or lithic fragments.

A flow chart (Figure 4.23) for the classification of the Witwatersrand quartzites was used to identify the quartzites within the B placer. Sediments with an excess of 95% quartz are classified as quartz arenites (orthoquartzites). Arenites and wackes are distinguished on the basis of stratification and the sorting of the quartzite, with the presence of stratification and moderately to well-sorted quartzites favouring arenites, while wackes require at least 15% matrix material.

The wacke and arenite fields are subdivided on the basis of their quartz content. Within the arenite field, quartzites with an excess of 75% quartz are referred to as sub-labile arenites and quartzite, with less than 75% quartz as labile. The labile field is further subdivided into feldspathic or lithic arenites on the basis of their dominant labile components. Within the wacke field, wacke with less than 85% quartz and less than 5% feldspathic and/or lithic fragments are termed quartz wackes. The labile wackes are subdivided into feldspathic and lithic according to the dominant labile component.

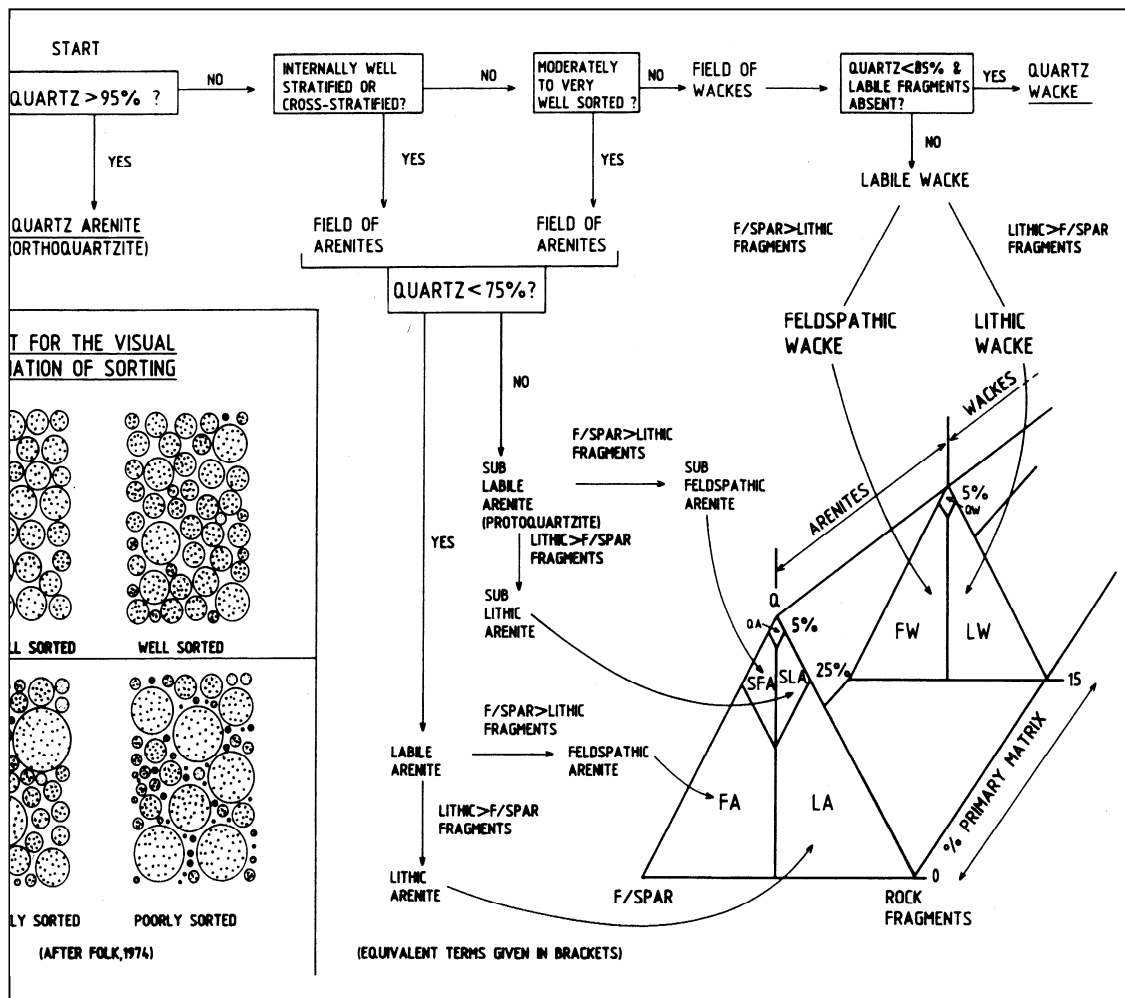


Figure 4.23. Flow chart for the classification of Witwatersrand Supergroup quartzites after Law et al., 1990.

5. GEOMETRY OF THE B PLACER

Mine plans represent a huge source of data that contain the detailed mappings collected by mine geologists and underground samplers on advancing stope faces during the history of the mine. Data gathered from these worked out areas of the mine, supplemented by the author's underground observations, were used to build a sedimentological model of the B placer.

Minter (1978) found that the B placer was at the base of the Spes Bona Formation as confined to discrete interconnected channels and transverse and longitudinal bars of gravel.

5.1 B placer facies plan

A total of 64 underground sampling maps of stope advances and all the underground borehole data were used to create a facies map of the B placer (Map 2). The precision of the sedimentological model was tested with underground bore holes and underground observations.

The difficulty to identify or discriminate between different channels within the B placer, when exposures are limited or inadequate, made the construction of the B placer facies plan a crucial part in understanding the depositional environments involved during the formation of the B placer. The facies model made it possible to attain an overall view of the geometry of the B placer at a macroscopic level, thus providing the author with the opportunity to select several sites from which to collect data and to test the sedimentological model with underground visits.

The construction of the facies plan made it possible to distinguish between three different depositional environments, namely a highly channelised region, a braid plain and a braid delta (Map 2).

5.1.1 The highly channelised region

The highly channelised region is located in the western region of the mine as seen on Map 2. Minter et al. (1986) stated that the B placer is confined to discrete, interconnected channel-ways, which are entrenched into the Upper Shale Marker; and that “the channel banks are steep in places, due to the cohesive nature of the footwall” (Minter et al. 1986). The formation of the discrete channels separated by islands onto which no placer sediment was deposited is due to the cohesive nature of the light coloured khaki shale of the Upper Shale Marker that served as the palaeo-surface.

The B3 facies represent the fluvial facies that were deposited in this highly channelised region. The confined channel-ways resulted in much higher velocities due to the much lower rate of energy dissipation downstream, as well as the much lower number of channel branches. This resulted in the formation of the fluvial polymictic, upward fining B3 facies with interbedded sand-waves as discussed in section 4.5.2.

5.1.2 The braided plain

The author could not visit this region of the mine due to inadequate underground sites available, but it is believed that this section of the mine is typical of a braid plain. The author therefore had to rely on all the old sampling maps of stope advances and underground borehole data. The data obtained from the maps indicated that the highly channelised region suddenly widened up into a braid plain. The widening up of the channels is theorized to have been caused by the transition of the competent khaki coloured shale to the darker shale present in the Upper Shale Marker. The darker shale, which was less competent, and the lack of vegetation, resulted in the formation of much wider channels and the formation of a braid plain.

Gravel bars, formed at the transition from the highly channelised region to the braid plain as a result of heavily laden streams flowing swiftly through the confined channels, expanded when it reached the braid plain and the velocity of the stream suddenly decreased. The sudden decrease in velocity ensured that much of the sediment load was deposited and gravel bars were formed (Figure 5.1).

The braid plain is postulate to consist of only B3 facies conglomerates. At the transition from the braid plain into the braid delta the B3 facies may overlay or have eroded the original B1 facies, thus giving the impression that the B1 facies were the original facies overlain by the seemingly younger B3 facies.

5.1.3 The braid delta

The braid delta is located in the eastern region of the mine as seen on Map 2. A braid delta is a coarse-grained delta formed by the progradation of a purely fluvial, braided plain into a standing body of water (Nemec and Steel, 1988). Els and Mayer (1992) stated that the presence of a palaeo-sea in the present southeastern parts of the Central Rand Group times is likely, and according to Pretorius (1987), the shales of the Witwatersrand Supergroup were deposited in deep, quiet water, well into the ocean. In addition Karpeta et al. (1991) also reported indicators of tidal and shallow marine deposition in the Central Rand Group. The implication of these findings is the distinct probability of a southeastern palaeo-sea during Central Rand times. Karpeta et al. (1991) implied that this palaeo-sea may have been an epeiric sea, probably with a poor defined coastline.

Fuller (1985) suggested that if a river system were to remain dominant, neither tide- or wave-related processes shall have an overwhelming influence on the system. Reworking and resedimentation are vital in the subaqueous setting. Extreme fluvial dominance and improved sorting of the braided delta system, due

to the degree of reworking of the gravel bars in the braid delta by waves and current action, generated the thicker and better sorted gravels and sands of the B1 facies. The absence of any mud-rich interbeds in the B1 conglomerates is caused by river dominance, and therefore the finer material present in the system was moved farther through the system and deposited deeper in the standing body of water.

The wider channels in the braid plain and the braid delta also resulted in shallower braided channels, and for this reason, large-scale migrating bedforms and their resultant cross-bedding (sand-waves) stratification are not abundant facies. The abundant lithological units present in the braid delta are unstratified (massive), clast supported beds represented by the upward-coarsening B1 conglomerate.

The B1 facies assemblage at Masimong 5 Shaft consequently represents a braid delta and was formed by the progradation of the purely fluvial B3 facies into a standing body of water.

5.2 Reconstruction of the B-placer palaeo-floor

A reconstruction of the B-placer palaeo-floor was created using more than 4000 surveying pegs and over 200 underground boreholes data. Computer software called Arcview was used to construct a contoured model of the B placer palaeo-floor (Map 3). Using the contours, three north-south striking sections perpendicular to the in-wash direction and two east-west sections longitudinal to the in-wash direction were constructed. The location of the section lines is indicated on Map 3 and 4.

5.2.1 Section line A-B

Section line A-B is longitudinal to the in-wash direction cutting, for the larger part of the section, through the braid plain. The slope of this section is 0.012 and compares well with modern-day equivalents such as the Steele Creek (0.013)

and the Donjek (0.006) (Rust, 1972). Two sites of interest are marked on the section as sites 1 and 2 and are also indicated on Map 4. Both these sites consist of a sudden downwards step in the palaeo-floor, accompanied by the formation of gravel bars (Map 4). These sites acted as trap sites providing favourable conditions for the formation of gold-bearing gravel bars.

5.2.2 Section line C-D

Section line C-D is perpendicular to the in-wash direction cutting through the highly channelised region of the B placer. Two distinctive valleys can be observed in this section. The valley to the far north of the section represents an isolated channel with B4 facies (Map 4). This channel, however, could not be confirmed, since no underground sites were available to visit. The presence of a predominant palaeo-high further to the north is noticeable.

The bigger valley on the section represents the highly channelised region. This valley confined the highly channelised region resulting in a much lower rate of downstream energy dissipation and a much lower number of channel branches. As an effect, the velocities in these channels are amplified making the deposition of the fluvial B3 facies possible.

The presence of a plateau can be observed in the southernmost end of the section. The plateau resulted in the formation of wider channels as observed on Map 4.

Several distinct topographic levels may be recognised in many braided rivers, ranging from the area of the deepest and most active channels, to elevated abandoned areas. These levels represent stages of progressive downcutting by the river and are recognisable in braided streams within valleys surrounded and fed by areas of strong relief, where degradation is active (Mial, 1977).

5.2.3 Section line E-F

Section line E-F is perpendicular to the in-wash direction cutting through the braid delta. This cross section is significantly different from section C-D. Section E-F demonstrates none of the valleys seen in section C-D and represents a much gentler north-dipping palaeo-slope.

5.2.4 Section line D-G

Section line D-G is longitudinal to the in-wash direction, parallel to section A-B, but located further to the south. This section starts in the braid plain crossing over to a non-depositional island and ending up in the braid delta. From this section, it is clear that the non-depositional islands are represented by palaeo-highs.

5.2.4 Section line H-I

Section line H-I is perpendicular to the in-wash direction cutting through the braid plain of the B-placer. In this section, both the predominant palaeo-high and the valley to the far north, observed in section C-D, is present. Underground sampling maps indicated the presence of the B4 facies in this valley.

In the south of this section, the big valley discussed in section C-D, flattened out to form part of the braid plain.

5.3 Reconstruction of a three-dimensional B placer palaeo-floor

A three-dimensional reconstruction of the palaeo-floor was generated using the software DataMine (Figure 5.1). From figure 5.1, it is clear that the highly channelised region arrives from a highland in the far west regions of the mine. The highly channelised region then propagated onto a flatter braid-plain, ending

up in a standing body of water, forming the braid delta to the far east of the mine. In-wash direction, as indicated by a red arrow on Figure 5.1, is from west to east; therefore from highland to the braid delta.

The predominant paleo-high to the far north of the mine, mentioned in sections 5.2.2 and 5.2.4, can also be observed in figure 5.1.

5.4 Interpreted trap sites for the formation of gold bearing gravel bars

During the formation of the Witwatersrand gold deposits, the accumulation and the preservation of gold were undoubtedly the consequence of many factors. The gold deposits of the Witwatersrand can be subdivided into two groups, namely the Banket type and the Carbon-Seam type. The Banket type consists of a conglomerate that contains detrital gold in the matrix, which have been entrapped mechanically. A Banket is characteristically a pebble supported conglomerate defined by a high pebble-packing density. Matrix-supported conglomerates or pebbly quartzites, defined by low pebble packing densities, were not pebble-supported, open-framework gravels and could not have functioned as mechanical traps (Minter and Toens, 1970). It is therefore of the utmost importance to identify the possible locations for the development of trap sites, which will favour the formation of pebble-supported conglomerates (gravel bars).

The mechanism of bar formation involves any changes that result in a decrease in bed-shear stress, leading to the deposition of the coarsest portion of the bedload. In other words, bar formation occurs wherever there is a local reduction in sediment transport capacity. Figure 5.2 illustrates potential trap sites for the formation of pebble supported conglomerates.

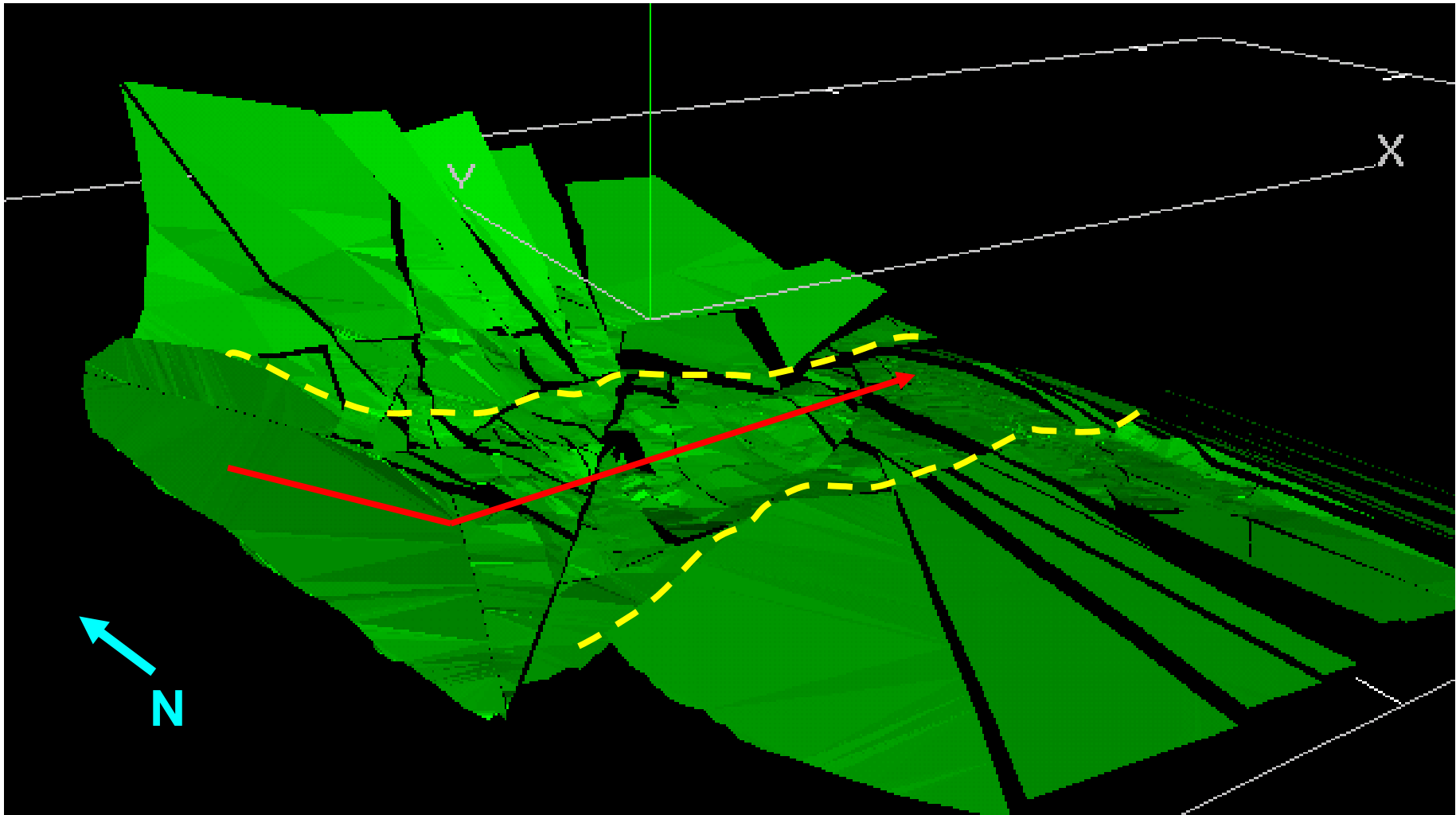


Figure 5.1. Three-dimensional reconstruction of the B-placer palaeo-floor. The red arrow indicates in-wash direction and the yellow dotted line indicates the outer limits of the B-placer.

5.4.1 Channel Junction (Location 1, Figure 5.2)

Channel junctions form where two or more well-defined streams, carrying similar discharges, join. The cross-profile of this trap site is symmetrical and shows maximum depths of up to five times that of the contributing channels. The long profile, as seen on Figure 5.2, shows a steep headwall and elongated basin from within a gentler reverse bed slope downstream of the scour centre (Ashmore, 1982). Gravel bar formation for the B-placer at channel junctions can be observed at sites 1 and 2 on Map 4.

5.4.2 Point bars, side bars or lateral bars (Location 2, Figure 5.2)

Genetically, these bars are all the same. The bars form in areas of relatively low fluvial energy, such as the inside of a meander where the main current strength is diverted against the outer bank. Point bars tend to be thought to be characteristic of meandering streams, but they also occur in braided environments, such as in the Kicking Horse River and some Scottish rivers (Mial, 1977). Minter (1978) states that “in some instances gravel accumulations appear to hug one side of the channel”. Possible examples of point bars located in the B-placer are marked as sites 3 to 7 (Map 4).

5.4.3 Mid-channel bars (Location 3, Figure 5.2)

In single or undivided channels, the coarsest load is carried along the deepest portion of the channel where competency is greatest. Waning flow of whatever cause, or a reduction in competency where the channel widens or deepens, will result in the deposition of part of the coarsest bedload, forming a mid-channel bar (Mial, 1977). Likely examples of mid channel bar formations in the B-placer are represented by sites 1, 2, 8, 9 and 10.

During flooding, possible formation of bars in depressions on the flood plains could occur.

5.4.4 Barrier bars (Location 4, Figure 5.2)

Barrier bars form almost in an identical process to the formation of point bars. The bars form in areas of relatively low fluvial energy, where a barrier diverts a channel. An example of such a deposition in the B-placer can be observed at sites 11 to 13.

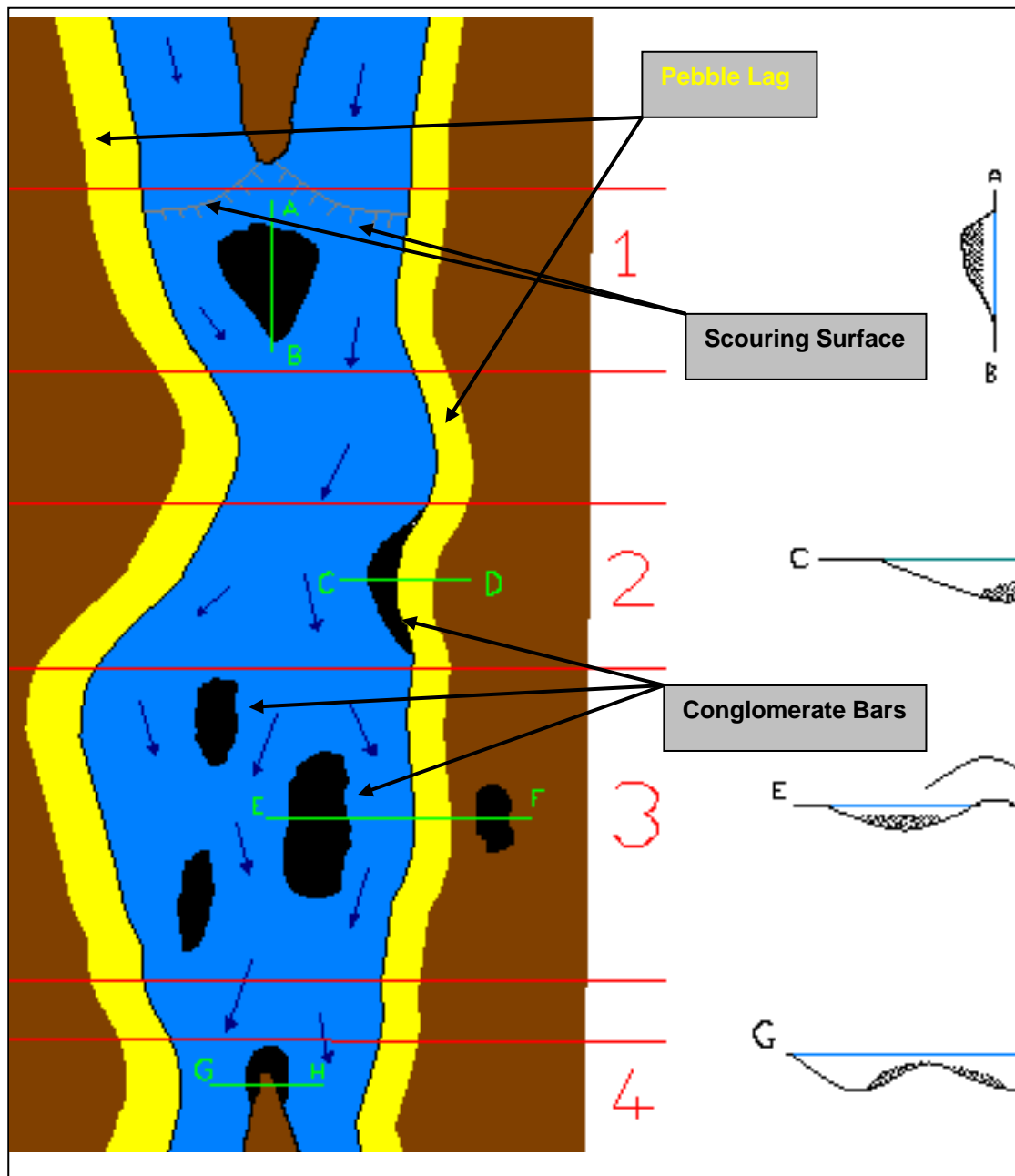


Figure 5.2. Illustrating potential scenarios for the development of pebble supported conglomerates.

6. CONCLUSION

The fluvial, upward fining, polyimictic B3 facies, with abundant sedimentary structures, are the result of the highly channelised environment in which these facies were deposited.

Reconstruction of the B-placer palaeo-floor indicated predominant palaeo-highs in the western and northern regions of the mine. A big valley located in the western region of the mine confined the B3 channels. The formation of the confined channel-ways was amplified by the cohesive nature of the light khaki coloured shale of the Upper Shale Marker that served as the palaeo-floor. As an effect, the velocities of the B3 channels were amplified making the deposition of the fluvial B3 facies possible.

The highly channelised region is followed by a braidplain. The widening up of the channels is believed to have been caused by the transition of the competent khaki coloured shale to the darker black shale present at Masimong 5 Shaft. The darker shale, being less competent, and the lack of vegetation, resulted in the formation of much wider channels and the formation of the braid-plain.

The braid delta located in the eastern region of the mine was formed by the progradation of the purely fluvial, braid plain into a standing body of water. Extreme fluvial dominance and improved sorting of the braid delta, due to the degree of reworking of the gravel bars by waves and current action, generated the thicker and better sorted gravels and sands. This resulted in the formation of the upwards coarsening, oligomictic B1 facies assemblage at Masimong 5 Shaft.

An overall decrease in pebble size was found from west to east in the 10 largest pebbles, 10 largest durable pebbles and the 10 largest non-durable pebbles. The decrease in the pebble sizes clearly indicates that the in-wash direction of the B placer was from the west, flowing in an eastern direction.

The presence of the khaki shale in the B1 conglomerate and the absence of the black shale in B3 conglomerate clearly indicate an in-wash direction from the west to the east. The geometry of the B placer channels and channel bars indicated an east-west transport direction.

The most important concepts that emerged from this investigation are:

1. The B placer at Masimong 5 Shaft represents three depositional environments, namely a highly channelised fluvial environment, a braid-plain and a braid delta.
2. The transport direction of the B placer was from west to east.
3. Four potential trap sites in favour of gold-bearing gravel bars formation were identified, namely channel junctions, side bars, mid-channel bars and barrier bars.

Altogether it can be said that this investigation serves as a basis for further investigations, and if this work is continued, valuable contributions to the knowledge of the gold distribution and the sedimentology of the B placer will be obtained.

REFERENCES

- Ashmore, P.E. (1982). Laboratory Modelling of Gravel Braided Stream Morphology. *Earth Surface Processes and Landforms*, **7**, 201-225.
- Bailey, A.C. (1991). The Stratigraphy and Sedimentology of the Upper Johannesburg and Turffontein Subgroups in the Southwestern Portion of the Welkom Goldfield. Unpub. M.Sc. Thesis, University of the Witwatersrand, 185.
- Catuneanu, O. (2001). Flexural partitioning of the Late Archaean Witwatersrand foreland system, South Africa. *Sedimentary Geology*, **141**, 95-112.
- Cockeran, N. (2006). Pebble distribution and the Geometry of the channels of the B1 and B3 conglomerates. Unpub. B.Sc Hons. Thesis, University of the Free State, 70.
- Coetzee, C.B. (1960). The Geology of the Orange Free State Gold-Field. *Geological Survey, Memoir*, **49**, 1-198.
- Doeglas, D.J. (1962). The Structure of Sedimentary Deposits of Braided Rivers. *Sedimentology*, **1**, 167-190.
- Dott, R.H. (1964). Wacke, greywacke and matrix-what approach to immature sandstone classification? *Journal of Sedimentary Petrology*, **34**, 625-632.
- Els, B.G. (1998). The auriferous late Archaean sedimentation systems of South Africa: unique palaeo-environment conditions. *Sedimentary Geology*, **120**, 205-224.

- Els, B.G and Mayer, J.J. (1992). Transgressive and progradational beach and nearshore facies in the Late Archaean Turffontein Subgroup of the Witwatersrand Supergroup, Vredefort Area, South Africa. *South African Journal of Geology*, **95**, 60-73.
- Engelbrecht, C.J., Baumbach, G.W.S., Matthysen, J.L., Fletcher, P. (1986). The West Wits Line. **In:** Anhaeusser, C.R., Maske, S. (Eds.). *Mineral Deposits of Southern Africa* Vol. 1. Geological Society of South Africa, Johannesburg, 599-684.
- Erikson, P.G., Catuneanu, O., Els, B.G., Bumby, A.J., Van Rooy, J.L. and Popa, M. (2005). Kaapvaal craton: Changing first- and second-order controls on sea level from c. 3.0 Ga to 2.0 Ga. *Sedimentary Geology*, **176**, 121-148.
- Friedman, G.M. and Sanders, J.E. (1978). Principles of sedimentology. New York, NY, John Wiley and Sons, 792 p.
- Frimmel, H.E. and Minter, W.E.L. (2002). Recent Developments Concerning the Geological History and Genesis of the Witwatersrand Gold Deposits, South Africa. *Society of Economic Geologists* (2002). Special Publication 9, 17-45.
- Fuller, A.O. (1985). A contribution to the conceptual modelling of pre-Devonian fluvial systems. *Transactions of the Geological Society of South Africa*, **88**, 189-194.
- High, L.R. and Picard, M.D. (1974). Reliability of cross-stratification types as palaeocurrent indicators in fluvial rocks. *Journal of Sedimentary Petrology*, **44**, 158-168.
- Hodgson, F.D.I. (1967). The Relationship Between the Sedimentology and the Gold Distribution of the Basal Reef Zone, Harmony Gold Mine. Unpub. M.Sc. Thesis, Univ. of the Orange Free State, 97pp.

- Jolley, S.J., Freeman, S.R., Barnicoat, A.C., Phillips, G.M., Knipe, R.J., Pather, A., Fox, N.P.C., Strydom, D., Birch, M.T.G., Henderson, I.H.C. and Rowland, T.W. (2004). Structural controls on Witwatersrand gold mineralisation. *Journal of Structural Geology* **26**, 1067-1086.
- Karpeta, W.P., Gendall, I.R. and King, J.A. (1991). Evidence for marine marginal and submarine canyon sedimentation in the Central Rand Group: implications for the geometry of the Witwatersrand basin. **In:** Abstract. Conference of Precambrian Sedimentary Basins of South Africa, 16-17.
- Karpeta, W.P. and Els, B.G. (1999). The auriferous Late Archaean Central Rand Group of South Africa: Sea-level control of sedimentation? *Precambrian Research*, **97**, 191-214.
- Kingsley, C.S. (1987). Facies changes from fluvial conglomerate to braided sandstone of the early Proterozoic Eldorado Formation, Welkom Goldfield, South Africa. **In:** *The Society of Economic Paleontologists and Mineralogists* (1987), 359-370.
- Kirk, J., Ruiz, J., Chesley, J., Titley, S., and Walshe, J. (2001). A detrital model for the origin of gold and sulfides in the Witwatersrand basin based on Re-OS isotopes. *Geochimica et Cosmochimica Acta*, **65** (13), 2149-2159.
- Knowles, A.C. (1968). A Sedimentological Investigation of the B Reef in the Northern Part of the Orange Free State Goldfields. Unpublished Confidential Report, Anglo American Corporation Limited, 37pp.
- Law, J.D.M., Bailey, A.C., Cadle, A.B., Phillips, G.N. and Stanistreet, I.G. (1990). Reconstructive approach to the classification of Witwatersrand 'quartzites'. *South African Journal of Geology*, **93**, 2191-2200.

- Meintjes, P.G., Visser, J.N.J. and Grobler, N.J. (1989). Evolution of the late Archaean volcano-sedimentary basins of the Platberg Group near Welkom, Orange Free State. *South African Journal of Geology*, **92** (3), 235-249.
- Miall, A.D. (1977). A Review of the Braided-River Depositional Environment. *Earth-Science Reviews*, **13**, 1-62.
- Miall, A.D. (1978). Lithofacies Types and Vertical Profile Models in Braided River Deposits: A Summary. **In:** A.D. Miall, ed, *Fluvial Sedimentology*. *Can. Soc. Petrol. Geologist*, **5**, 597-604.
- Minter, W.E.L. (1973). The Sedimentology and Evaluation of the B Reef at Freddie's Consolidated Mines, with Economic Implications to the O.F.S Goldfields, 50pp.
- Minter, W.E.L. (1978). A Sedimentological Synthesis of Placer Gold, Uranium and Pyrite Concentrations in Proterozoic Witwatersrand Sediments. **In:** Miall, A.D. (Ed.) (1978). *Fluvial Sedimentology* (1978), 122-134.
- Minter, W.E.L., Hill, W.C.N., Kidger, R.J., Kingsley, C.S. and Snowden, P.A. (1986). The Welkom Goldfield. **In:** Anhaeusser, C.R., and Maske, S. (Eds.) (1986). *Mineral Deposits of Southern Africa* Vol. 1, Geological Society of South Africa, Johannesburg, 497-539.
- Minter, W.E.L. and Loen, J.S. (1991). Palaeocurrent dispersal patterns of Witwatersrand gold placers. *South African Journal of Geology*, **91** (1), 70-85.
- Minter, W.E.L. and Toens, P.D. (1970). Experimental simulation of gold deposition in gravel beds. *Transactions of the Geological Society of South Africa*, **13**, 89-98.

- Myers, R.E., McCarthy, T.S., Bunyard, M., Cawthorn, R.G., Falatsa, T.M., Hewitte, T., Linton, P., Myers, J.M., Palmer, K.J. and Spencer, R. (1990). Geochemical stratigraphy of the Klipriviersberg volcanic rocks. *South African Journal of Geology*, **93** (1), 224-238.
- Myers, R.E., McCarthy, T.S. and Stanistreet, I.G. (1989). A Tectono-Sedimentary reconstruction of the development and evolution of the Witwatersrand Basin, with particular emphasis on the Central Rand Group. *South African Journal of Geology*, **93** (1), 180-201.
- Nemec, W. and Steel, R.J. (1988). What is a fan delta and how do we recognize it? **In:** Nemec, W. and Steel, R.J. (Eds.) (1988). *Fan Deltas. Sedimentology and Tectonic Settings*. (1988), 5-13.
- Pettijohn, F.J. (1957). *Sedimentary Rocks*. Harper and Brothers, New York, 718 p.
- Pettijohn, F.J. (1972). *Sand and Sandstone*. Springer-Verlag, New York, 818p.
- Powers, M.C. (1953). A new roundness scale for sedimentary particles. *Journal of Sedimentary Petrology*, **23**, 117-119.
- Pretorius, D.A. (1979). The Depositional Environment of the Witwatersrand Goldfields: A Chronological Review of Speculations and Observations. **In:** Anderson, M. and Van Biljon, W.J. (1979). *Some Sedimentary Basins and Associated Ore Deposits of South Africa*. *Geocongress 77: Geological Society of South Africa*, **6**, 33-55.
- Pretorius, D.A. (1987). The depositional environment of the Witwatersrand goldfields: a chronological review of the speculations and observations. **In:** Boyle, R.W. (Ed.), *Gold History and Genesis of Deposits*. Van Reinhold, New York, 409-438.

- Robb, L.J. and Meyer, F.M. (1995). The Witwatersrand Basin, South Africa: Geological framework and mineralization processes. *Ore Geology Reviews*, **10**, 67-94.
- Robb, L.J. and Robb, V.M. (1998). Gold in the Witwatersrand Basin. **In:** Wilson, M.G.C. and Anhaeusser, C.R. (Eds.) (1998). *The Mineral Resources of South Africa*, Sixth Edition (1998), 294-349.
- Rust, B.R. (1972). Structure and process in a braided river. *Sedimentology*, **18**, 221-245.
- Spangenberg, J.E. and Frimmel, H.E. (2001). Basin-internal derivation of hydrocarbons in the Witwatersrand Basin, South-Africa: evidence from bulk and molecular $\delta^{13}\text{C}$ data. *Chemical Geology*, **173**, 339-355.
- Steyn, L.S. (1963). The Sedimentology and the Gold Distribution of the Livingstone Reefs on the West Rand. Unpublished M.Sc. Thesis, University of the Witwatersrand.
- Van der Westhuizen, W.A., De Bruijn, H. and Meintjes, P.G. (1991). The Ventersdorp Supergroup: an overview. *Journal of African Earth Sciences*, **13** (1), 83-105.
- Wentworth, C.K. (1922). A scale of grade and class terms for clastic sediments. *Journal of Geology*, **30**, 377-392.
- Winter, H. de la Rey. (1976). A lithostratigraphic classification of the Ventersdorp succession. *Transactions of the Geological Society of South Africa*, **79**, 31-48.
- Winter, H. de la Rey. (1987). A cratonic foreland model for Witwatersrand Basin development in a continental back-arc, plate-tectonic setting. *South African Journal of Geology*, **90** (4), 409-427.

ACKNOWLEDGEMENTS

I gratefully acknowledge the continued support and advice given to me by my supervisor Mr. L. Nel. I thank Mr. Nel and Professor Van der Westhuizen for the many hours spent reading the various drafts of this dissertation.

I am indebted to Harmony Ltd., for their financial support throughout the duration of this study and in particular to Dawid Pretorius. Grateful thanks are also extended to the members of the Geology Department at Masimong 5 Shaft (P. Smit and P. Olivier) for their assistance and helpful suggestions.

Finally, I wish to thank my loving wife, Marianne, for her moral support.

APPENDIX I

Site 1: **1750 E13 X/Cut Drive S2**
Co-ords: **X – 3096288**
 Y – 11660.2
 Z – -2148.2

Grid Counting											
Mid Cycle											
Q	SQ	SQ	Q	Q	Q	M	Q	Q	Q	Code	
M	M	M	M	M	M	M	M	Q	SQ	M - Matrix	SQ - Smokey Quartz
M	M	M	YS	M	M	Q	M	M	M	C - Chert	YS - Yellow Shale
Q	Q	SQ	Q	Q	Q	M	M	M	M	Q - Quartz	BS - Black Shale
SQ	M	M	M	M	Q	M	Q	M	M	S - Shale	
M	Q	M	M	M	M	SQ	Q	M	M		
M	Q	Q	Q	M	Q	Q	M	SQ	M		
Q	M	SQ	M	SQ	YS	M	YS	Q	SQ		
M	M	M	M	M	M	M	M	M	M	Varieties and relative abundances	
M	M	M	Q	M	M	M	M	M	Q	Matrix	61%
M	M	Q	M	M	M	M	M	M	SQ	Durable Pebbles	
Q	M	Q	M	M	M	M	Q	SQ	M	Quartz	30%
Q	YS	M	Q	M	M	Q	M	M	M	SQ	6%
M	M	M	Q	YS	Q	M	M	M	M	BQ	0%
M	M	Q	M	M	M	Q	Q	M	Q	C	0%
M	Q	M	M	M	M	M	M	M	M	TOTAL	36%
Q	M	M	M	Q	Q	M	M	Q	M	Non-Durable Pebbles	
M	M	Q	Q	Q	S	Q	Q	M	M	YS	3%
M	M	M	M	M	Q	M	Q	Q	Q	BS	1%
Q	Q	Q	Q	Q	M	M	M	Q	M	TOT. S	4%

Grid Counting											
Bottom Cycle											
M	M	M	M	SQ	M	SQ	M	M	M	Code	
M	C	M	Q	M	M	M	M	M	M	M - Matrix	SQ - Smokey Quartz
M	M	Q	M	M	C	Q	Q	SQ	M	C - Chert	YS - Yellow Shale
YS	M	M	M	M	M	M	M	Q	YS	Q - Quartz	BS - Black Shale
M	M	M	Q	YS	M	Q	M	Q	M	S - Shale	
Q	M	Q	M	BS	YS	M	YS	M	M		
Q	M	M	Q	Q	Q	M	M	Q	Q		
M	SQ	M	Q	Q	Q	Q	M	M	Q		
Q	Q	SQ	M	M	M	Q	Q	M	SQ	Varieties and relative abundances	
Q	Q	M	Q	M	M	M	M	Q	M	Matrix	60%
M	M	M	M	M	Q	M	M	M	M	Durable Pebbles	
M	M	M	M	M	M	M	Q	Q	M	Quartz	27%
Q	Q	YS	YS	M	YS	M	M	M	Q	SQ	7%
M	SQ	M	M	YS	M	Q	M	M	M	BQ	0%
M	Q	M	M	M	M	M	M	SQ	M	C	1%
M	M	M	Q	M	Q	SQ	SQ	M	Q	TOTAL	35%
M	M	M	M	Q	M	M	M	M	M	Non-Durable Pebbles	
Q	SQ	Q	M	M	Q	Q	Q	Q	M	YS	6%
M	Q	YS	Q	Q	M	Q	Q	M	YS	BS	1%
Q	M	M	M	SQ	M	M	M	SQ	M	TOT. S	7%

Site 2: 1750 E13 X/Cut Stope S5

Grid Counting											
Top Cycle											
Q	M	M	M	M	M	M	M	M	M	Code	
M	Q	M	M	M	Q	Q	M	M	M	M - Matrix	SQ - Smokey Quartz
M	Q	Q	Q	M	Q	M	Q	Q	Q	C - Chert	YS - Yellow Shale
Q	M	M	Q	M	M	Q	Q	Q	M	Q - Quartz	BS - Black Shale
Q	Q	M	M	Q	Q	M	Q	M	M	S - Shale	
M	M	M	Q	M	M	M	M	Q	Q		
M	M	M	Q	Q	M	Q	Q	Q	M		
Q	M	Q	M	M	M	M	Q	M	M		
Q	M	M	M	Q	Q	Q	M	Q	Q	Varieties and relative abundances	
M	M	M	M	Q	M	M	M	Q	Q	Matrix	62%
Q	M	M	M	M	YS	M	M	Q	M	Durable Pebbles	
M	M	M	M	M	M	Q	M	Q	M	Quartz	37%
M	M	M	Q	M	Q	M	M	M	Q	SQ	1%
Q	M	M	Q	M	M	M	Q	M	M	BQ	0%
Q	M	M	M	M	Q	Q	Q	Q	M	C	0%
M	M	M	M	Q	Q	Q	M	Q	M	TOTAL	38%
M	Q	M	Q	SQ	M	M	M	Q	Q	Non-Durable Pebbles	
M	M	Q	M	M	M	M	Q	Q	Q	YS	
Q	M	M	M	Q	M	Q	M	M	Q	BS	1%
M	M	M	Q	M	Q	M	M	M	M	TOT. S	1%

Grid Counting											
Middle Cycle											
M	M	M	M	Q	Q	Q	M	Q	M	Code	
Q	Q	M	Q	Q	Q	SQ	Q	Q	Q	M - Matrix	SQ - Smokey Quartz
M	Q	M	Q	M	M	Q	M	M	Q	C - Chert	YS - Yellow Shale
M	M	Q	M	M	Q	M	Q	Q	M	Q - Quartz	BS - Black Shale
M	Q	M	M	Q	Q	M	M	M	Q	S - Shale	
M	Q	Q	Q	Q	M	M	M	Q	M	Varieties and relative abundances	
Q	Q	Q	M	Q	Q	M	M	M	M	Matrix	48%
Q	Q	Q	M	Q	Q	Q	Q	Q	Q	Durable Pebbles	
BS	Q	M	Q	M	M	M	Q	Q	M	Quartz	50%
Q	M	M	Q	Q	M	Q	M	M	M	SQ	1%
M	M	Q	M	Q	Q	Q	M	M	Q	BQ	0%
M	M	Q	M	M	Q	M	M	Q	Q	C	0%
										TOTAL	51%
										Non-Durable Pebbles	
										YS	
										BS	1%
										TOT. S	1%

Site 3: 1750 E14 X/Cut Drive S
 Co-ords: X – 3096492.2
 Y – 11433.5
 Z – -2172.3

Grid Counting												
Top Cycle												
M	Q	M	YS	M	M	Q	M	YS	M		Code	
Q	M	M	M	M	M	Q	SQ	Q	M		M - Matrix	SQ - Smokey Quartz
M	M	M	M	M	YS	M	Q	M	M		C - Chert	YS - Yellow Shale
M	M	M	Q	Q	Q	M	M	Q	Q		Q - Quartz	BS - Black Shale
YS	M	Q	M	M	M	M	M	M	M		S - Shale	
M	Q	M	M	M	M	Q	Q	M	M			
M	M	M	Q	Q	M	M	M	M	M			
M	M	M	M	M	Q	Q	M	M	M			
M	M	M	M	M	Q	M	Q	M	Q		Varieties and relative abundances	
M	Q	M	M	Q	M	Q	M	Q	Q		Matrix	68%
M	M	M	M	Q	Q	YS	M	M	M		Durable Pebbles	
M	M	M	M	M	Q	M	M	M	M		Quartz	26%
Q	M	M	M	M	Q	M	M	M	Q		SQ	1%
M	M	Q	Q	Q	M	M	M	M	M		BQ	0%
Q	C	M	Q	M	M	Q	M	Q	BS		C	0%
M	Q	M	Q	M	M	M	Q	M	M		TOTAL	27%
M	Q	M	M	M	SQ	Q	M	M	Q		Non-Durable Pebbles	
M	M	Q	M	Q	M	M	M	Q	Q		YS	3%
M	M	Q	BS	M	M	M	Q	M	M		BS	1%
M	M	M	M	M	M	M	M	M	M		TOT. S	4%

Grid Counting												
Middle Cycle												
M	M	YS	M	M	Q	YS	M	SQ	M		Code	
M	M	M	M	M	Q	M	M	M	M		M - Matrix	SQ - Smokey Quartz
M	Q	M	Q	BS	M	M	Q	Q	M		C - Chert	YS - Yellow Shale
Q	Q	Q	M	M	BS	Q	Q	Q	SQ		Q - Quartz	BS - Black Shale
M	M	Q	M	M	M	M	M	M	M		S - Shale	
M	SQ	M	M	M	M	Q	M	M	M		Varieties and relative abundances	
Q	M	M	M	M	Q	M	M	YS	SQ		Matrix	70%
M	M	Q	M	Q	Q	M	Q	M	M		Durable Pebbles	
M	M	M	Q	M	M	M	Q	M	M		Quartz	22%
M	M	M	M	M	M	M	M	M	Q		SQ	3%
Q	M	M	M	M	M	M	M	M	M		BQ	0%
											C	0%
											TOTAL	25%
											Non-Durable Pebbles	
											YS	3%
											BS	2%
											TOT. S	5%

Grid Counting											
Bottom Cycle										Code	
M	M	M	M	Q	Q	M	M	M	Q	M - Matrix	SQ - Smokey Quartz
Q	M	M	Q	Q	M	M	M	M	M	C - Chert	YS - Yellow Shale
Q	Q	Q	Q	M	Q	SQ	M	SQ	M	Q - Quartz	BS - Black Shale
M	M	M	M	SQ	M	M	M	M	M	S - Shale	
M	Q	M	Q	M	M	M	SQ	M	Q		
Q	Q	Q	Q	M	SQ	Q	M	Q	M		
M	Q	M	M	Q	M	M	M	M	M		
Q	Q	Q	Q	M	Q	M	Q	YS	Q		
M	M	M	Q	Q	M	M	Q	M	M	Varieties and relative abundances	
M	Q	M	M	M	M	M	M	M	M	Matrix	61%
Q	Q	M	M	M	M	M	M	M	M	Durable Pebbles	
M	Q	Q	Q	M	M	M	M	Q	Q	Quartz	34%
M	M	M	M	Q	M	Q	Q	M	M	SQ	2%
Q	M	M	Q	Q	M	M	M	BS	M	BQ	0%
M	M	Q	M	M	Q	M	M	M	Q	C	0%
M	Q	Q	M	M	M	M	M	M	Q	TOTAL	36%
Q	Q	YS	Q	Q	Q	Q	YS	M	M	Non-Durable Pebbles	
M	M	M	Q	Q	M	M	M	Q	Q	YS	2%
M	M	Q	M	M	M	M	M	M	M	BS	1%
M	Q	M	Q	Q	M	Q	M	Q	Q	TOT. S	3%

Site 4: 1750 E14 X/Cut Drive W
Co-ords: X – 3096443.3
Y – 11446.5
Z – -2171.1

Grid Counting											
Top Cycle										Code	
M	Q	M	M	M	Q	M	M	M	M	M - Matrix	SQ - Smokey Quartz
Q	Q	M	M	M	Q	M	M	M	M	C - Chert	YS - Yellow Shale
Q	M	M	M	M	Q	M	Q	Q	SQ	Q - Quartz	BS - Black Shale
M	SQ	Q	M	Q	M	M	M	M	M	S - Shale	
Q	M	M	Q	SQ	Q	M	M	M	M		
M	M	Q	Q	Q	M	Q	Q	Q	Q		
M	Q	M	M	M	M	Q	Q	M	Q		
M	Q	M	M	M	Q	M	M	Q	M		
Q	M	Q	Q	Q	Q	M	M	M	Q	Varieties and relative abundances	
M	Q	M	Q	Q	M	Q	M	Q	SQ	Matrix	54%
Q	M	M	M	M	M	M	Q	Q	Q	Durable Pebbles	
Q	M	M	M	M	M	M	Q	Q	M	Quartz	41%
Q	M	Q	M	M	Q	M	M	M	M	SQ	3%
BS	M	M	Q	M	Q	M	Q	Q	Q	BQ	0%
M	Q	M	Q	Q	BS	BS	Q	Q	Q	C	0%
M	Q	Q	M	Q	Q	M	M	M	Q	TOTAL	44%
Q	M	M	Q	M	M	M	M	M	M	Non-Durable Pebbles	
Q	M	SQ	Q	M	Q	BS	Q	Q	M	YS	0%
M	BS	M	M	Q	Q	Q	Q	BS	M	BS	3%
M	M	Q	Q	M	M	Q	Q	Q	Q	TOT. S	3%

Grid Counting											
Midde Cycle											
Q	M	Q	SQ	M	Q	M	M	M	M	Code	
Q	M	M	M	Q	M	M	M	Q	M	M - Matrix	SQ - Smokey Quartz
M	Q	M	M	Q	M	Q	Q	M	Q	C - Chert	YS - Yellow Shale
M	M	Q	Q	M	M	Q	Q	Q	Q	Q - Quartz	BS - Black Shale
M	M	BS	Q	M	Q	M	M	Q	M	S - Shale	
M	Q	M	Q	Q	M	M	Q	M	M	Varieties and relative abundances	
Q	M	M	M	Q	Q	Q	M	Q	Q	Matrix	54%
Q	Q	YS	M	M	Q	M	M	M	M	Durable Pebbles	
M	M	M	M	M	M	M	M	M	M	Quartz	43%
M	M	M	M	M	Q	Q	Q	Q	Q	SQ	2%
M	M	M	SQ	Q	M	Q	M	M	Q	BQ	0%
SQ	Q	Q	M	Q	M	Q	M	M	M	C	0%
Q	Q	M	M	Q	Q	M	Q	Q	Q	TOTAL	45%
M	M	Q	M	M	Q	M	Q	M	Q	Non-Durable Pebbles	
M	M	Q	M	Q	Q	Q	Q	Q	M	YS	1%
Q	M	M	Q	Q	Q	Q	M	Q	M	BS	1%
										TOT. S	2%

Grid Counting											
Bottom Cycle											
M	Q	Q	M	M	Q	M	M	M	M	Code	
Q	M	Q	M	M	Q	M	SQ	M	Q	M - Matrix	SQ - Smokey Quartz
Q	M	M	BS	Q	M	Q	Q	M	Q	C - Chert	YS - Yellow Shale
M	Q	Q	Q	Q	Q	M	Q	SQ	M	Q - Quartz	BS - Black Shale
M	M	Q	Q	Q	M	M	M	Q	Q	S - Shale	
Q	Q	M	M	M	M	Q	Q	Q	Q		
Q	Q	SQ	M	M	Q	M	M	M	M		
M	Q	Q	Q	Q	M	M	Q	BS	Q	Relative abundances	
Q	Q	M	M	Q	Q	M	Q	Q	Q	Matrix	50%
M	Q	M	Q	M	M	M	M	M	M	Durable Pebbles	
Q	Q	Q	SQ	M	M	Q	M	M	M	Quartz	45%
M	M	M	Q	M	Q	Q	M	M	M	SQ	4%
M	M	Q	M	YS	M	M	M	M	M	BQ	0%
Q	M	Q	M	M	M	M	SQ	M	Q	C	0%
Q	Q	Q	Q	Q	M	M	M	Q	Q	TOTAL	49%
M	SQ	M	Q	Q	M	Q	Q	M	M	Non-Durable Pebbles	
Q	Q	M	M	M	M	M	Q	Q	M	YS	1%
Q	SQ	M	M	Q	Q	Q	M	Q	Q	BS	1%
Q	Q	Q	M	M	M	M	Q	Q	Q	TOT. S	2%

Site 5: 1810 E12 X/Cut Drive S
 Co-ords: X – 3096443.3
 Y – 11446.5
 Z – -2171.1

Grid Counting											
Top Cycle											
M	M	M	M	M	M	M	M	M	M	Code	
M	M	M	M	M	M	M	M	M	Q	M - Matrix	SQ - Smokey Quartz
M	M	M	M	M	M	Q	M	Q	Q	C - Chert	YS - Yellow Shale
Q	M	M	Q	Q	M	M	Q	M	M	Q - Quartz	BS - Black Shale
BS	Q	Q	M	BS	M	M	Q	M	M	S - Shale	
M	SQ	M	M	M	Q	M	M	Q	M		
Q	M	BS	Q	M	M	M	Q	Q	M		
M	M	Q	Q	Q	Q	Q	M	M	Q		
M	Q	M	M	M	M	M	M	M	M	Varieties and relative abundances	
M	M	M	M	BS	M	M	Q	Q	M	Matrix	68%
M	M	M	M	M	M	M	M	Q	M	Durable Pebbles	
M	M	M	Q	BS	M	M	M	M	Q	Quartz	25%
M	M	Q	Q	M	SQ	Q	SQ	M	M	SQ	3%
M	SQ	M	M	M	M	M	Q	BS	Q	BQ	0%
Q	M	M	M	M	Q	Q	M	M	M	C	0%
Q	M	Q	M	M	M	SQ	BS	M	M	TOTAL	28%
M	M	M	Q	Q	M	Q	Q	M	BS	Non-Durable Pebbles	
Q	M	M	M	Q	Q	M	Q	M	Q	YS	1%
M	M	M	Q	M	YS	M	M	Q	M	BS	4%
M	M	M	M	M	M	M	M	SQ	M	TOT. S	5%

Grid Counting											
Bottom Cycle											
M	Q	M	M	M	M	Q	M	Q	M	Code	
M	M	M	M	Q	M	M	Q	M	Q	M - Matrix	SQ - Smokey Quartz
M	Q	M	M	M	Q	M	M	M	Q	C - Chert	YS - Yellow Shale
M	M	M	Q	Q	M	M	M	SQ	Q	Q - Quartz	BS - Black Shale
M	M	M	M	M	Q	M	Q	Q	M	S - Shale	
M	Q	BS	M	M	M	Q	M	M	M	Varieties and relative abundances	
M	M	M	M	M	M	M	M	M	M	Matrix	68%
M	M	Q	M	M	SQ	M	M	Q	Q	Durable Pebbles	
M	M	M	M	M	Q	Q	M	M	M	Quartz	25%
M	M	M	Q	M	M	M	Q	M	M	SQ	3%
M	Q	M	M	M	M	M	Q	M	SQ	BQ	0%
M	M	Q	M	M	Q	Q	M	M	M	C	0%
Q	BS	M	M	M	Q	M	Q	Q	Q	TOTAL	28%
										Non-Durable Pebbles	
										YS	1%
										BS	4%
										TOT. S	5%

Site 6: 1810 E13 X/Cut Drive S

Grid Counting											
Top Cycle											
BS	M	Q	Q	BS	Q	Q	M	M	M	Code	
M	M	M	M	SQ	Q	Q	M	M	C	M - Matrix	SQ - Smokey Quartz
Q	BS	SQ	SQ	M	M	M	M	C	M	C - Chert	YS - Yellow Shale
Q	SQ	SQ	M	Q	BS	SQ	Q	Q	M	Q - Quartz	BS - Black Shale
Q	SQ	M	M	M	Q	M	M	M	M	S - Shale	
SQ	SQ	M	Q	M	M	Q	M	Q	Q		
GS	M	M	Q	M	M	M	Q	Q	M		
Q	M	M	M	Q	Q	SQ	Q	M	Q		
M	Q	M	M	Q	M	M	M	M	Q	Varieties and relative abundances	
M	M	Q	Q	M	Q	M	Q	M	Q	Matrix	49%
M	SQ	Q	M	Q	M	M	Q	M	BS	Durable Pebbles	
SQ	M	Q	Q	Q	Q	Q	Q	M	M	Quartz	37%
Q	Q	Q	Q	SQ	Q	C	M	M	Q	SQ	8%
Q	Q	Q	M	Q	M	M	BS	Q	Q	BQ	0%
Q	Q	M	Q	M	M	M	M	M	M	C	2%
M	SQ	M	M	Q	M	Q	M	M	Q	TOTAL	47%
M	M	Q	M	M	Q	Q	Q	Q	M	Non-Durable Pebbles	
Q	M	Q	Q	M	Q	M	BS	M	M	YS	1%
M	M	BS	BS	Q	M	SQ	M	Q	M	BS	4%
M	M	M	M	M	Q	Q	M	M	M	TOT. S	5%

Site 7: 1810 W1 W3 S6

Grid Counting											
Top Cycle											
M	M	M	Q	M	Q	M	M	M	M	Code	
M	M	Q	Q	M	Q	Q	M	M	M	M - Matrix	SQ - Smokey Quartz
M	M	Q	M	M	M	M	Q	Q	M	C - Chert	YS - Yellow Shale
M	M	M	YS	Q	M	M	M	Q	M	Q - Quartz	BS - Black Shale
M	SQ	M	M	Q	Q	M	SQ	M	M	S - Shale	
Q	M	Q	M	M	Q	M	M	SQ	M		
Q	M	Q	M	M	SQ	SQ	M	Q	M		
SQ	SQ	M	Q	Q	M	M	M	M	M		
Q	YS	M	M	M	M	M	Q	Q	M	Varieties and relative abundances	
M	Q	M	M	SQ	SQ	M	Q	M	Q	Matrix	61%
Q	M	M	Q	M	SQ	Q	Q	M	M	Durable Pebbles	
M	M	M	M	M	Q	Q	M	M	M	Quartz	30%
M	M	Q	Q	Q	M	M	M	Q	Q	SQ	8%
Q	M	SQ	M	M	Q	M	M	M	SQ	BQ	0%
Q	Q	M	SQ	Q	Q	M	Q	YS	M	C	0%
M	M	M	M	Q	M	YS	M	M	SQ	TOTAL	38%
Q	Q	M	Q	M	M	M	M	M	Q	Non-Durable Pebbles	
M	Q	Q	M	SQ	Q	M	M	Q	M	YS	2%
M	M	M	Q	M	M	M	M	Q	Q	BS	0%
M	M	M	M	M	M	Q	Q	M	Q	TOT. S	2%

Site 8: 1810 W3 S3 S1b

Grid Counting											
Top Cycle											
Q	Q	M	SQ	M	M	M	SQ	YS	YS	Code	
Q	Q	Q	M	M	M	Q	Q	SQ	M	M - Matrix	SQ - Smokey Quartz
M	Q	M	M	M	M	M	Q	YS	M	C - Chert	YS - Yellow Shale
M	Q	M	Q	Q	Q	SQ	Q	Q	M	Q - Quartz	BS - Black Shale
Q	Q	M	SQ	M	M	Q	Q	M	M	S - Shale	
Q	M	Q	M	M	M	M	Q	Q	Q		
M	M	M	Q	Q	M	M	Q	M	Q		
M	M	BS	M	M	M	Q	M	M	M		
BS	M	M	YS	M	Q	M	M	SQ	M	Varieties and relative abundances	
SQ	M	Q	M	M	M	M	Q	M	M	Matrix	55%
SQ	SQ	Q	Q	M	Q	YS	M	SQ	M	Durable Pebbles	
M	Q	M	Q	Q	M	M	YS	YS	M	Quartz	30%
M	YS	M	M	M	Q	M	M	SQ	Q	SQ	10%
M	M	M	M	M	SQ	M	M	M	SQ	BQ	0%
M	Q	M	Q	M	M	M	M	M	SQ	C	0%
M	Q	M	M	M	M	M	M	Q	M	TOTAL	40%
Q	M	M	Q	M	SQ	M	M	M	M	Non-Durable Pebbles	
M	M	M	M	Q	M	M	Q	Q	Q	YS	5%
YS	SQ	SQ	Q	Q	Q	M	Q	M	Q	BS	1%
SQ	SQ	Q	Q	M	Q	M	M	Q	Q	TOT. S	6%

Site 9: 1810 W1 W5A Drive W
Co-ords: X – 3095149
Y – 13011.1
Z – -2252.6

Grid Counting											
Top Cycle											
Q	Q	M	SQ	M	M	M	M	YS	YS	Code	
Q	Q	Q	M	SQ	SQ	Q	Q	M	M	M - Matrix	SQ - Smokey Quartz
M	M	M	M	M	M	M	M	M	Q	C - Chert	YS - Yellow Shale
M	Q	M	Q	Q	Q	SQ	Q	Q	M	Q - Quartz	BS - Black Shale
Q	Q	M	SQ	M	M	Q	Q	M	M	S - Shale	
Q	M	Q	M	SQ	SQ	M	M	Q	Q		
M	M	M	Q	Q	M	M	Q	M	Q		
M	SQ	M	M	M	SQ	Q	M	M	M		
M	M	M	YS	SQ	Q	M	M	SQ	M	Varieties and relative abundances	
SQ	M	Q	M	M	M	M	Q	M	Q	Matrix	50%
SQ	SQ	Q	Q	M	Q	YS	M	SQ	M	Durable Pebbles	
M	Q	M	Q	Q	M	M	YS	YS	M	Quartz	30%
YS	YS	M	M	SQ	Q	M	M	SQ	Q	SQ	12%
M	M	M	M	M	SQ	Q	M	M	SQ	BQ	0%
YS	Q	SQ	Q	SQ	M	M	Q	M	SQ	C	2%
M	Q	M	M	M	M	M	M	Q	M	TOTAL	44%
Q	M	M	Q	M	SQ	SQ	M	M	SQ	Non-Durable Pebbles	
M	M	M	M	Q	M	M	Q	Q	Q	YS	6%
YS	SQ	SQ	Q	Q	Q	SQ	Q	M	Q	BS	0%
SQ	SQ	Q	M	M	Q	M	M	Q	Q	TOT. S	6%

Site 10: 1810 W1 W3 W1c

Grid Counting											
Top Cycle											
Q	Q	M	SQ	M	M	M	M	YS	YS	Code	
Q	Q	Q	M	M	M	Q	Q	YS	M	M - Matrix	SQ - Smokey Quartz
M	M	M	M	M	M	M	M	YS	M	C - Chert	YS - Yellow Shale
M	Q	M	Q	Q	Q	SQ	Q	Q	Q	Q - Quartz	BS - Black Shale
Q	Q	M	SQ	M	M	Q	Q	M	M	S - Shale	
Q	M	Q	M	M	M	M	Q	M	Q		
M	M	M	Q	Q	M	M	Q	M	Q		
M	M	BS	M	M	M	Q	M	M	M		
BS	M	M	YS	M	Q	M	M	SQ	Q	Varieties and relative abundances	
SQ	M	Q	M	SQ	M	M	Q	M	Q	Matrix	58%
SQ	SQ	Q	Q	M	Q	YS	M	SQ	M	Durable Pebbles	
M	Q	M	Q	Q	M	M	YS	YS	M	Quartz	31%
M	YS	M	M	M	Q	M	M	SQ	Q	SQ	8%
M	M	M	M	M	SQ	M	M	M	SQ	BQ	0%
M	Q	SQ	Q	SQ	M	Q	SQ	M	SQ	C	0%
M	Q	M	M	M	M	M	M	Q	M	TOTAL	39%
Q	M	M	Q	SQ	SQ	Q	M	M	M	Non-Durable Pebbles	
M	M	M	M	Q	M	M	Q	Q	Q	YS	4%
YS	SQ	SQ	Q	Q	Q	Q	Q	M	Q	BS	0%
SQ	SQ	Q	M	M	Q	M	M	Q	Q	TOT. S	4%

APPENDIX II

Site 1: **1750 E13 X/Cut Drive S2**
Co-ords: **X – 3096288**
 Y – 11660.2
 Z – -2148.2

Pebble Sizes								
Durable Pebbles			Non-Durable Pebbles			Top 10 Pebbles		
a-axis (mm)	c-axis (mm)	Actual size (mm)	a-axis (mm)	c-axis (mm)	Actual size (mm)	a-axis (mm)	c-axis (mm)	Actual size (mm)
51	18	30	62	20	35	64	23	38
48	28	37	58	22	36	63	23	38
49	30	38	63	23	38	62	20	35
28	12	18	44	14	25	58	22	36
26	11	17	22	8	13	55	21	34
30	14	20	64	23	38	51	18	30
55	21	34	36	18	25	49	30	38
38	14	23	36	9	18	48	28	37
38	23	30	29	18	23	44	14	25
36	16	24	30	12	19	38	14	23
Mean Pebble Size (mm)	27		27			33		

Site 2: **1750 E13 X/Cut Stope S5**

Pebble Sizes								
Durable Pebbles			Non-Durable Pebbles			Top 10 Pebbles		
a-axis (mm)	c-axis (mm)	Actual size (mm)	a-axis (mm)	c-axis (mm)	Actual size (mm)	a-axis (mm)	c-axis (mm)	Actual size (mm)
59	17	32	52	19	31	59	17	32
43	21	30	47	31	38	54	19	32
39	26	32	44	14	25	52	19	31
47	24	34	54	19	32	48	22	32
48	22	32	39	19	27	47	31	38
36	23	29	44	26	34	47	24	34
39	21	29	39	16	25	46	21	31
41	18	27	41	21	29	44	26	34
46	21	31	42	24	32	44	14	25
38	14	23	39	21	29	43	21	30
Mean Pebble Size (mm)	30		30			32		

Site 3: **1750 E14 X/Cut Drive S**
Co-ords: **X – 3096492.2**
 Y – 11433.5
 Z – -2172.3

Pebble Sizes								
Durable Pebbles			Non-Durable Pebbles			Top 10 Pebbles		
a-axis (mm)	c-axis (mm)	Actual size (mm)	a-axis (mm)	c-axis (mm)	Actual size (mm)	a-axis (mm)	c-axis (mm)	Actual size (mm)
35	20	26	40	18	27	48	20	31
29	18	23	36	12	21	44	23	32
35	8	17	34	18	25	40	18	27
48	20	31	26	14	19	40	18	27
26	13	18	39	18	26	39	14	23
44	23	32	37	18	26	39	18	26
36	6	15	30	9	16	37	18	26
39	14	23	27	12	18	37	16	24
37	16	24	31	14	21	36	12	21
40	18	27	29	12	19	36	6	15
Mean Pebble Size (mm)	24		22			25		

Site 4: **1750 E14 X/Cut Drive W**
Co-ords: **X – 3096443.3**
 Y – 11446.5
 Z – -2171.1

Pebble Sizes								
Durable Pebbles			Non-Durable Pebbles			Top 10 Pebbles		
a-axis (mm)	c-axis (mm)	Actual size (mm)	a-axis (mm)	c-axis (mm)	Actual size (mm)	a-axis (mm)	c-axis (mm)	Actual size (mm)
42	30	35	21	12	16	57	26	38
38	22	29	34	23	28	52	28	38
39	23	30	36	18	25	51	16	29
52	28	38	38	20	28	53	16	29
42	28	34	39	21	29	47	20	31
46	21	31	32	22	27	46	21	31
47	20	31	41	19	28	42	30	35
32	15	22	32	17	23	42	28	34
57	26	38	51	16	29	41	19	28
36	15	23	53	16	29	39	23	30
Mean Pebble Size (mm)	31		26			32		

Site 5: **1810 E12 X/Cut Drive S**
Co-ords: **X – 3096443.3**
 Y – 11446.5
 Z – -2171.1

Pebble Sizes								
Durable Pebbles			Non-Durable Pebbles			Top 10 Pebbles		
a-axis (mm)	c-axis (mm)	Actual size (mm)	a-axis (mm)	c-axis (mm)	Actual size (mm)	a-axis (mm)	c-axis (mm)	Actual size (mm)
38	19	27	47	19	30	59	23	37
52	21	33	54	20	33	54	20	33
46	21	31	37	16	24	52	21	33
41	22	30	40	18	27	47	19	30
44	15	26	38	13	22	46	21	31
39	21	29	59	23	37	46	19	30
36	13	22	38	16	25	45	20	30
45	20	30	36	20	27	44	15	26
46	19	30	39	18	26	42	22	30
42	22	30	40	17	26	41	22	30
Mean Pebble Size (mm)	29		28			31		

Site 6: 1810 E13 X/Cut Drive S

Pebble Sizes								
Durable Pebbles			Non-Durable Pebbles			Top 10 Pebbles		
a-axis (mm)	c-axis (mm)	Actual size (mm)	a-axis (mm)	c-axis (mm)	Actual size (mm)	a-axis (mm)	c-axis (mm)	Actual size (mm)
46	22	32	41	24	31	76	33	50
49	26	36	46	32	38	68	24	40
34	32	33	62	32	45	62	32	45
76	33	50	40	24	31	58	24	37
58	24	37	44	16	27	52	16	29
24	3	8	43	22	31	50	28	37
52	16	29	39	16	25	49	31	39
49	31	39	68	24	40	49	26	36
50	28	37	39	22	29	48	28	37
42	26	33	48	28	37	46	32	38
Mean Pebble Size (mm)	33		33			39		

Site 7: 1810 W1 W3 S6

Pebble Sizes								
Durable Pebbles			Non-Durable Pebbles			Top 10 Pebbles		
a-axis (mm)	c-axis (mm)	Actual size (mm)	a-axis (mm)	c-axis (mm)	Actual size (mm)	a-axis (mm)	c-axis (mm)	Actual size (mm)
61	31	43	42	28	34	64	34	47
64	34	47	47	20	31	64	30	44
47	31	38	46	28	36	62	29	42
52	27	37	62	29	42	61	31	43
43	20	29	49	24	34	58	29	41
46	29	37	44	30	36	52	27	37
48	29	37	47	31	38	51	29	38
44	19	29	42	32	37	49	24	34
58	29	41	49	23	34	49	23	34
64	30	44	51	29	38	48	29	37
Mean Pebble Size (mm)	38		36			40		

Site 8: 1810 W3 S3 S1b

Pebble Sizes								
Durable Pebbles			Non-Durable Pebbles			Top 10 Pebbles		
a-axis (mm)	c-axis (mm)	Actual size (mm)	a-axis (mm)	c-axis (mm)	Actual size (mm)	a-axis (mm)	c-axis (mm)	Actual size (mm)
57	23	36	40	23	30	79	44	59
52	30	39	56	30	41	75	48	60
57	29	41	50	18	30	67	39	51
49	17	29	75	48	60	63	35	47
58	32	43	67	39	51	61	28	41
54	30	40	52	40	46	58	32	43
53	25	36	48	35	41	57	29	41
55	34	43	61	28	41	57	23	36
63	35	47	44	40	42	56	30	41
79	44	59	50	38	44	55	34	43
Mean Pebble Size (mm)	41		43			46		

Site 9: 1810 W1 W5A Drive W
Co-ords: X – 3095149
Y – 13011.1
Z – -2252.6

Pebble Sizes								
Durable Pebbles			Non-Durable Pebbles			Top 10 Pebbles		
a-axis (mm)	c-axis (mm)	Actual size (mm)	a-axis (mm)	c-axis (mm)	Actual size (mm)	a-axis (mm)	c-axis (mm)	Actual size (mm)
50	23	34	39	23	30	79	42	58
55	31	41	47	30	38	75	48	60
57	28	40	52	18	31	69	39	52
48	20	31	75	48	60	63	34	46
58	30	42	55	39	46	60	30	42
52	30	39	51	39	45	58	32	43
53	26	37	50	34	41	55	28	39
51	34	42	51	26	36	52	24	35
60	33	44	45	30	37	50	30	39
80	41	57	46	36	41	55	29	40
Mean Pebble Size (mm)	41		40			45		

Site 10: 1810 W1 W3 W1c

Pebble Sizes								
Durable Pebbles			Non-Durable Pebbles			Top 10 Pebbles		
a-axis (mm)	c-axis (mm)	Actual size (mm)	a-axis (mm)	c-axis (mm)	Actual size (mm)	a-axis (mm)	c-axis (mm)	Actual size (mm)
48	23	33	40	23	30	70	46	57
55	31	41	42	30	35	75	48	60
57	35	45	54	22	34	65	35	48
48	22	32	60	48	54	63	34	46
55	30	41	56	41	48	51	30	39
52	29	39	51	39	45	58	31	42
53	37	44	50	34	41	55	34	43
51	34	42	49	26	36	52	24	35
31	33	32	42	30	35	50	35	42
60	36	46	46	36	41	55	28	39
Mean Pebble Size (mm)	40		40			45		

APPENDIX III

Site 1: 1750 E13 X/Cut Drive S2
Co-ords: X – 3096288
Y – 11660.2
Z – -2148.2

Pebble Sorting					
a-axis (mm)	c-axis (mm)	Actual size (mm)	a-axis (mm)	c-axis (mm)	Actual size (mm)
42	22	30	11	5	7
30	15	21	32	23	27
48	30	38	9	3	5
9	3	5	6	4	5
23	11	16	33	18	24
18	10	13	22	11	16
33	16	23	22	14	18
34	20	26	16	8	11
14	7	10	18	7	11
26	12	18	18	9	13
18	6	10	14	6	9
34	20	26	12	5	8
17	6	10	14	8	11
11	5	7	9	5	7
29	15	21	16	9	12
9	3	5	18	12	15
11	3	6	24	15	19
14	4	7	28	14	20
6	2	3	22	10	15
8	3	5	28	14	20
8	5	6	18	8	12
6	4	5	26	12	18
20	12	15	8	4	6
6	2	3	4	3	3
8	3	5	16	9	12
11	5	7	22	15	18
18	10	13	18	13	15
5	4	4	9	6	7
4	2	3	11	5	7
14	7	10	11	8	9
19	10	14	30	18	23
18	11	14	15	8	11
23	15	19	20	15	17
18	9	13	15	9	12
32	23	27	3	2	2
42	33	37	4	2	3
26	18	22	2	2	2
32	18	24	6	5	5
38	22	29	4	4	4
6	2	3	12	5	8
9	6	7	6	6	6
11	4	7	8	4	6
14	5	8	19	14	16
8	6	7	32	22	27
28	18	22	9	6	7
18	11	14	22	15	18
9	6	7	22	14	18
11	6	8	8	5	6
10	5	7	20	8	13
18	8	12	12	8	10

Site 2: 1750 E13 X/Cut Slope S5

Pebble Sorting					
a-axis (mm)	c-axis (mm)	Actual size (mm)	a-axis (mm)	c-axis (mm)	Actual size (mm)
23	15	19	29	15	21
19	10	14	20	15	17
32	18	24	41	33	37
16	8	11	16	8	11
14	8	11	17	10	13
18	10	13	19	13	16
21	15	18	25	18	21
11	5	7	22	12	16
23	14	18	19	12	15
36	25	30	20	11	15
14	8	11	26	16	20
12	5	8	24	15	19
19	12	15	25	16	20
19	13	16	30	19	24
12	6	8	26	20	23
24	12	17	28	19	23
26	15	20	20	12	15
22	15	18	34	25	29
32	20	25	20	10	14
20	12	15	21	11	15
21	14	17	32	25	28
19	10	14	25	12	17
24	10	15	43	33	38
21	14	17	35	25	30
14	6	9	36	29	32
22	9	14	34	28	31
16	7	11	26	13	18
11	6	8	21	13	17
10	6	8	26	18	22
34	25	29	14	7	10
14	6	9	16	8	11
8	4	6	38	20	28
17	9	12	24	13	18
29	20	24	13	8	10
21	15	18	13	7	10
30	22	26	31	16	22
17	9	12	14	8	11
29	18	23	29	18	23
32	25	28	30	23	26
34	30	32	14	8	11
28	20	24	32	20	25
22	11	16	21	18	19
18	9	13	20	10	14
20	12	15	26	22	24
14	8	11	25	19	22
36	25	30	25	24	24
16	8	11	31	22	26
29	15	21	24	12	17
43	30	36	29	18	23
25	15	19	24	17	20

Site 3: 1750 E14 X/Cut Drive S
Co-ords: X – 3096492.2
Y – 11433.5
Z – -2172.3

Pebble Sorting					
a-axis (mm)	c-axis (mm)	Actual size (mm)	a-axis (mm)	c-axis (mm)	Actual size (mm)
11	4	7	22	13	17
13	7	10	18	7	11
13	8	10	4	2	3
11	5	7	11	6	8
16	8	11	13	10	11
15	8	11	15	9	12
14	9	11	3	2	2
20	12	15	4	2	3
11	5	7	7	3	5
19	12	15	8	4	6
13	6	9	13	10	11
14	9	11	12	6	8
8	4	6	13	8	10
14	6	9	11	7	9
22	13	17	11	5	7
16	9	12	14	8	11
11	5	7	17	9	12
19	12	15	19	10	14
23	15	19	13	10	11
19	15	17	11	9	10
27	20	23	11	5	7
13	7	10	22	12	16
18	8	12	15	9	12
23	14	18	11	5	7
18	9	13	15	5	9
14	7	10	3	2	2
20	12	15	15	8	11
23	15	19	9	5	7
24	18	21	6	4	5
15	9	12	5	3	4
18	13	15	10	5	7
19	15	17	15	8	11
26	18	22	18	12	15
12	6	8	13	10	11
18	10	13	11	11	11
23	13	17	23	15	19
21	9	14	13	9	11
24	15	19	18	16	17
23	14	18	10	4	6
11	5	7	12	6	8
14	8	11	22	14	18
19	10	14	20	12	15
10	6	8	20	10	14
4	3	3	18	10	13
6	4	5	15	8	11
18	10	13	16	10	13
22	13	17	11	5	7
14	6	9	8	3	5
4	2	3	18	10	13
16	9	12	7	4	5

Site 4: 1750 E14 X/Cut Drive W
Co-ords: X – 3096443.3
Y – 11446.5
Z – -2171.1

Pebble Sorting					
a-axis (mm)	c-axis (mm)	Actual size (mm)	a-axis (mm)	c-axis (mm)	Actual size (mm)
34	25	29	28	15	20
30	22	26	20	15	17
40	33	36	28	16	21
21	15	18	27	17	21
28	14	20	28	14	20
22	14	18	34	25	29
19	9	13	47	35	41
20	12	15	30	25	27
34	23	28	20	10	14
29	22	25	23	13	17
36	29	32	18	9	13
20	10	14	18	10	13
26	15	20	7	5	6
9	5	7	11	7	9
20	12	15	19	14	16
46	33	39	17	9	12
18	10	13	31	25	28
22	11	16	20	15	17
24	14	18	12	6	8
11	4	7	20	12	15
12	5	8	20	12	15
8	5	6	20	10	14
7	3	5	12	8	10
8	4	6	13	6	9
21	12	16	21	12	16
28	15	20	18	9	13
22	12	16	14	8	11
33	20	26	30	28	29
29	24	26	24	18	21
20	15	17	19	9	13
14	7	10	17	8	12
20	10	14	12	8	10
30	19	24	8	6	7
29	19	23	28	20	24
22	18	20	26	18	22
20	10	14	19	15	17
22	13	17	23	14	18
26	15	20	17	9	12
29	19	23	8	4	6
20	15	17	13	7	10
9	4	6	24	13	18
24	14	18	20	12	15
19	9	13	36	26	31
20	9	13	29	23	26
9	5	7	28	20	24
11	6	8	19	11	14
23	15	19	17	14	15
25	20	22	38	30	34
19	12	15	44	32	38
29	20	24	33	27	30

Site 5: 1810 E12 X/Cut Drive S
Co-ords: X – 3096443.3
Y – 11446.5
Z – -2171.1

Pebble Sorting					
a-axis (mm)	c-axis (mm)	Actual size (mm)	a-axis (mm)	c-axis (mm)	Actual size (mm)
38	25	31	41	35	38
20	12	15	30	26	28
19	12	15	14	8	11
29	22	25	7	3	5
20	10	14	12	7	9
26	14	19	12	8	10
42	35	38	16	8	11
20	12	15	19	10	14
40	36	38	21	11	15
23	15	19	11	5	7
21	14	17	16	9	12
25	12	17	34	22	27
28	15	20	17	10	13
34	22	27	11	8	9
19	14	16	21	12	16
52	40	46	8	5	6
36	25	30	12	8	10
36	29	32	14	10	12
20	10	14	20	15	17
29	18	23	39	30	34
26	15	20	18	12	15
20	11	15	17	16	16
36	23	29	34	30	32
36	25	30	19	13	16
18	14	16	14	8	11
19	9	13	28	15	20
19	8	12	18	15	16
30	21	25	35	23	28
9	4	6	19	10	14
25	14	19	15	7	10
44	28	35	17	10	13
28	16	21	24	15	19
20	12	15	28	18	22
16	8	11	14	8	11
31	18	24	26	20	23
32	15	22	18	12	15
30	19	24	26	13	18
14	8	11	28	19	23
19	10	14	16	11	13
31	19	24	34	29	31
32	24	28	41	36	38
19	12	15	23	22	22
30	20	24	16	10	13
14	7	10	32	28	30
31	25	28	25	21	23
18	15	16	22	11	16
29	23	26	23	18	20
24	15	19	29	22	25
20	12	15	22	15	18
20	13	16	38	30	34

Site 6: 1810 E13 X/Cut Drive S

Pebble Sorting					
a-axis (mm)	c-axis (mm)	Actual size (mm)	a-axis (mm)	c-axis (mm)	Actual size (mm)
18	12	15	40	32	36
20	13	16	18	10	13
24	14	18	24	14	18
35	28	31	28	15	20
20	11	15	17	10	13
11	5	7	29	21	25
24	16	20	22	14	18
20	13	16	27	20	23
18	13	15	34	22	27
30	24	27	9	3	5
28	25	26	23	13	17
20	14	17	46	34	40
30	25	27	20	16	18
16	9	12	21	15	18
30	23	26	29	19	23
22	19	20	23	15	19
14	10	12	11	6	8
30	21	25	24	16	20
19	10	14	24	15	19
8	5	6	28	21	24
30	26	28	15	5	9
30	22	26	18	7	11
18	11	14	26	14	19
15	11	13	19	10	14
30	19	24	19	12	15
32	25	28	20	10	14
34	27	30	16	10	13
8	4	6	40	37	38
40	34	37	16	9	12
32	26	29	24	14	18
23	12	17	34	23	28
15	9	12	22	18	20
54	42	48	31	26	28
28	15	20	28	23	25
43	36	39	28	27	27
48	38	43	30	20	24
20	12	15	17	13	15
20	14	17	31	19	24
28	14	20	20	13	16
33	22	27	20	15	17
28	20	24	24	17	20
37	36	36	26	17	21
19	10	14	29	20	24
28	13	19	28	21	24
24	16	20	32	28	30
40	30	35	20	13	16
23	14	18	38	28	33
28	17	22	20	13	16
40	36	38	23	11	16
32	23	27	31	23	27

Site 7: 1810 W1 W3 S6

Pebble Sorting					
a-axis (mm)	c-axis (mm)	Actual size (mm)	a-axis (mm)	c-axis (mm)	Actual size (mm)
28	17	22	41	35	38
15	9	12	34	29	31
20	15	17	43	39	41
17	8	12	30	23	26
30	22	26	33	27	30
34	27	30	28	20	24
29	23	26	31	28	29
23	16	19	12	6	8
32	26	29	13	7	10
30	23	26	29	20	24
17	9	12	24	20	22
19	13	16	24	17	20
20	12	15	16	15	15
28	18	22	8	4	6
28	19	23	10	5	7
32	23	27	12	6	8
35	26	30	24	16	20
30	19	24	19	15	17
36	27	31	21	14	17
30	27	28	26	17	21
19	10	14	26	19	22
38	30	34	33	26	29
27	21	24	21	20	20
17	10	13	34	30	32
26	19	22	16	9	12
38	37	37	32	25	28
28	23	25	21	17	19
30	26	28	24	15	19
18	10	13	34	26	30
31	27	29	14	9	11
34	25	29	22	15	18
29	21	25	26	18	22
34	25	29	18	4	8
26	17	21	24	17	20
33	23	28	29	24	26
14	7	10	23	16	19
26	20	23	17	5	9
39	31	35	26	20	23
17	10	13	32	28	30
23	22	22	47	40	43
31	30	30	34	31	32
31	28	29	29	28	28
19	13	16	32	25	28
40	35	37	32	29	30
23	16	19	28	23	25
22	14	18	37	29	33
26	19	22	31	26	28
18	9	13	30	22	26
28	14	20	20	15	17
21	14	17	18	10	13

Site 8: 1810 W3 S3 S1b

Pebble Sorting					
a-axis (mm)	c-axis (mm)	Actual size (mm)	a-axis (mm)	c-axis (mm)	Actual size (mm)
22	12	16	11	5	7
9	5	7	24	20	22
18	12	15	14	8	11
16	11	13	16	10	13
21	15	18	11	4	7
24	17	20	17	13	15
18	12	15	4	4	4
23	17	20	5	4	4
5	3	4	5	3	4
11	5	7	9	7	8
20	13	16	17	12	14
9	4	6	16	10	13
2	2	2	14	13	13
14	9	11	13	13	13
6	4	5	12	10	11
5	4	4	10	3	5
12	7	9	14	9	11
10	6	8	16	9	12
28	23	25	5	3	4
11	9	10	7	5	6
14	10	12	12	8	10
15	12	13	12	9	10
8	4	6	13	9	11
10	6	8	24	17	20
11	9	10	14	9	11
5	2	3	15	12	13
16	8	11	15	12	13
12	8	10	18	14	16
15	9	12	17	16	16
13	7	10	3	2	2
12	9	10	9	5	7
14	6	9	12	6	8
21	18	19	7	3	5
19	15	17	6	2	3
13	10	11	6	4	5
11	7	9	7	5	6
9	6	7	9	7	8
9	7	8	11	9	10
12	9	10	13	11	12
13	9	11	18	15	16
17	12	14	23	20	21
11	10	10	18	15	16
11	9	10	15	7	10
14	9	11	17	9	12
9	7	8	16	9	12
14	10	12	4	2	3
10	6	8	20	16	18
15	10	12	11	9	10
15	11	13	11	6	8
9	4	6	14	10	12

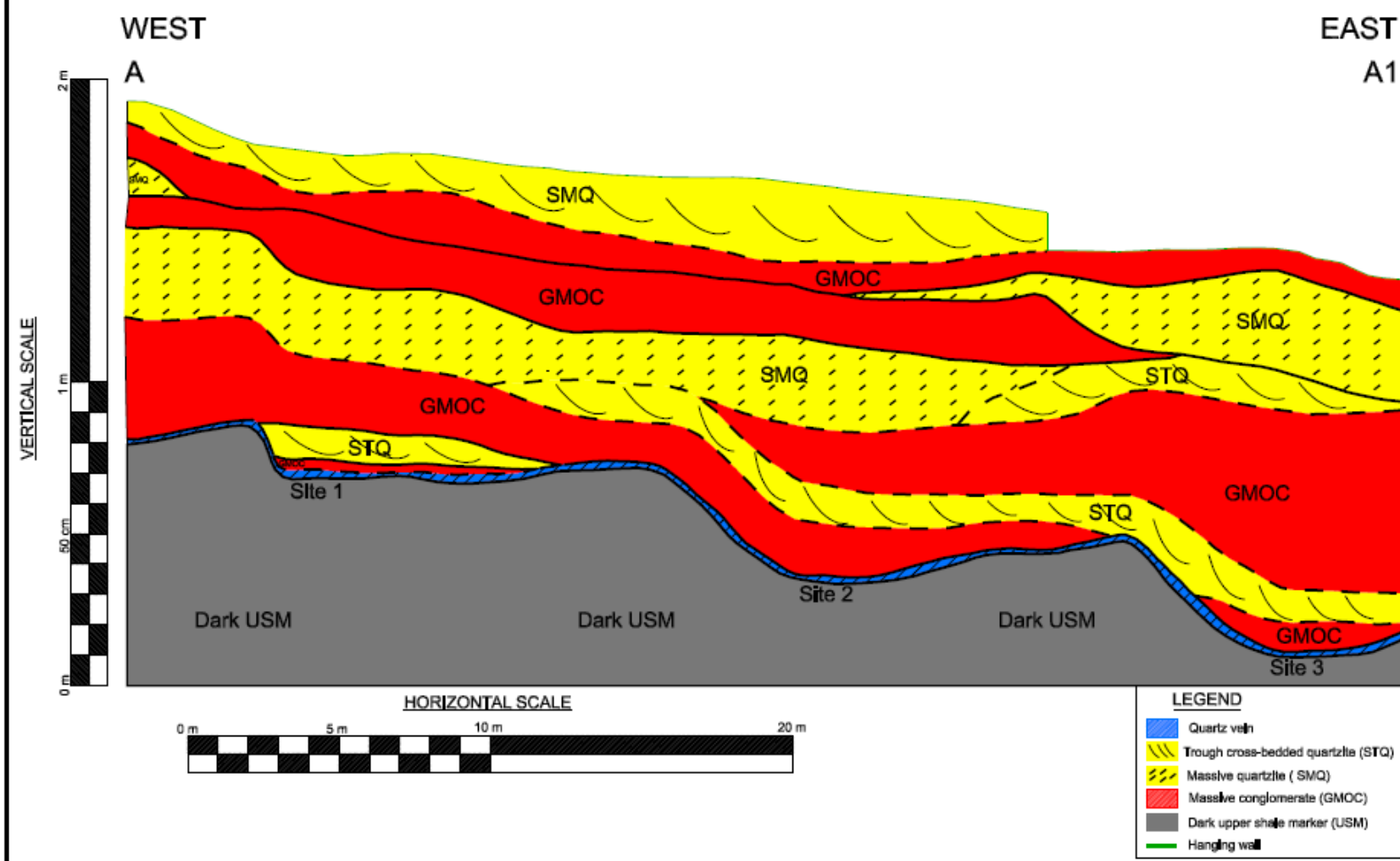
Site 9: 1810 W1 W5A Drive W
Co-ords: X – 3095149
Y – 13011.1
Z – -2252.6

Pebble Sorting					
a-axis (mm)	c-axis (mm)	Actual size (mm)	a-axis (mm)	c-axis (mm)	Actual size (mm)
45	30	37	29	18	23
31	26	28	26	13	18
29	15	21	50	30	39
20	20	20	18	14	16
40	18	27	17	3	7
30	20	24	26	12	18
25	20	22	20	14	17
24	14	18	15	10	12
15	10	12	14	9	11
20	18	19	26	14	19
18	8	12	25	12	17
20	12	15	28	20	24
18	12	15	23	14	18
10	6	8	26	16	20
14	4	7	26	14	19
42	24	32	23	20	21
40	20	28	14	9	11
33	25	29	15	8	11
34	30	32	18	12	15
36	29	32	20	8	13
22	12	16	17	14	15
18	12	15	10	7	8
21	9	14	19	8	12
33	16	23	24	16	20
20	18	19	15	8	11
37	20	27	36	30	33
25	17	21	28	19	23
42	20	29	35	15	23
20	11	15	38	23	30
25	12	17	20	4	9
47	40	43	20	12	15
30	30	30	24	22	23
19	17	18	18	16	17
15	8	11	30	20	24
20	7	12	30	18	23
20	15	17	30	28	29
24	20	22	42	15	25
22	15	18	37	26	31
24	14	18	15	5	9
24	16	20	20	10	14
25	23	24	22	10	15
40	27	33	25	14	19
33	20	26	32	22	27
50	22	33	22	13	17
48	42	45	18	14	16
30	29	29	40	29	34
28	8	15	22	14	18
24	18	21	20	10	14
38	15	24	29	14	20
40	34	37	45	29	36

Site 10: 1810 W1 W3 W1c

Pebble Sorting					
a-axis (mm)	c-axis (mm)	Actual size (mm)	a-axis (mm)	c-axis (mm)	Actual size (mm)
23	16	19	20	15	17
28	17	22	20	10	14
23	14	18	25	15	19
29	17	22	17	15	16
23	18	20	20	18	19
20	15	17	15	12	13
24	19	21	35	17	24
20	15	17	20	6	11
30	15	21	20	13	16
11	2	5	33	11	19
19	6	11	23	16	19
17	12	14	25	15	19
15	10	12	32	30	31
19	18	18	13	3	6
7	3	5	20	13	16
43	18	28	9	3	5
15	10	12	30	20	24
22	18	20	35	15	23
22	13	17	4	2	3
17	15	16	10	7	8
17	13	15	18	12	15
22	18	20	19	12	15
17	10	13	25	16	20
23	12	17	24	18	21
30	20	24	30	24	27
15	10	12	5	2	3
40	23	30	20	13	16
6	5	5	40	18	27
25	12	17	20	13	16
16	13	14	10	10	10
32	25	28	55	27	39
30	19	24	20	10	14
20	11	15	30	14	20
11	14	12	10	6	8
18	8	12	18	10	13
26	15	20	22	22	22
15	12	13	30	20	24
20	12	15	10	5	7
29	19	23	16	10	13
20	15	17	22	13	17
11	7	9	8	3	5
7	5	6	18	16	17
8	6	7	25	18	21
4	2	3	35	23	28
9	4	6	15	12	13
18	9	13	23	13	17
17	15	16	9	8	8
15	11	13	17	11	14
10	5	7	20	10	14
22	15	18	22	12	16

B1 CONGLOMERATE GEOLOGICAL SECTION A (1750 X/CUT 14 STOPE)



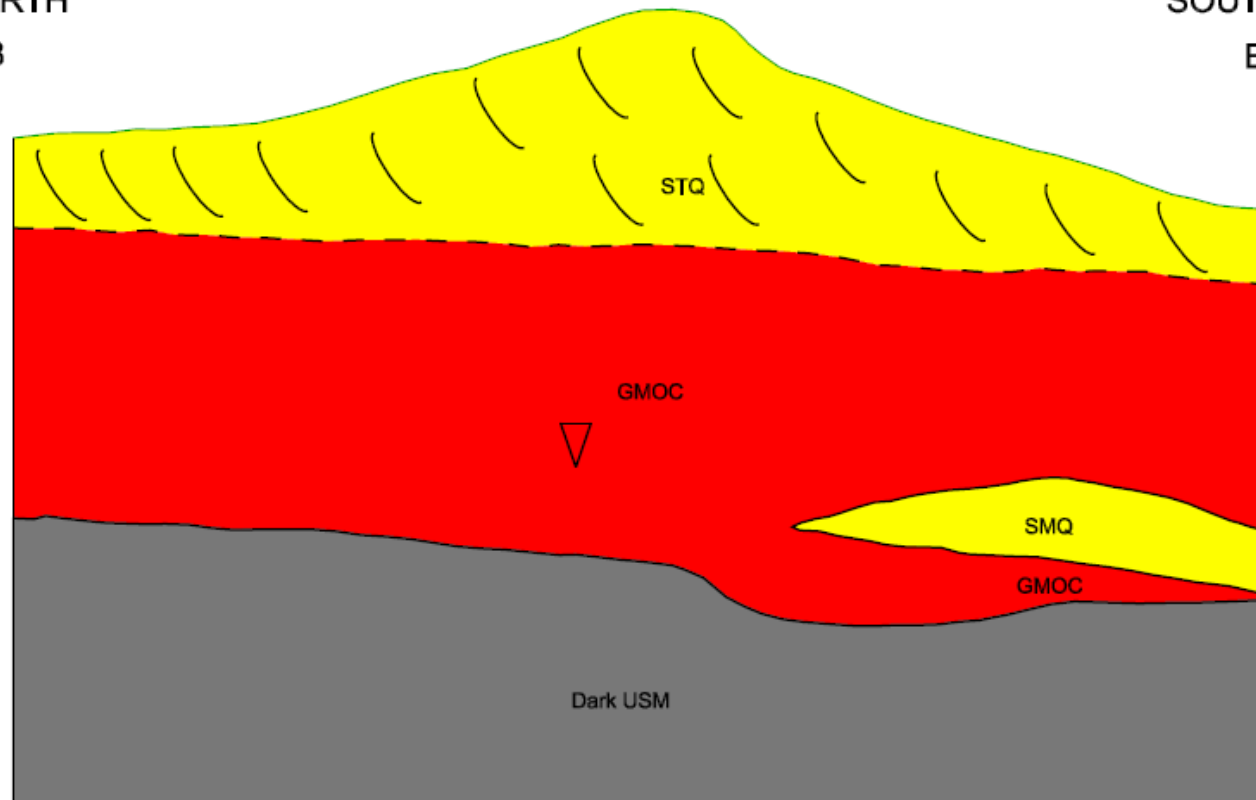
B1 CONGLOMERATE GEOLOGICAL SECTION B (PEG 9634)

NORTH
B

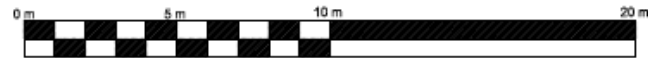
SOUTH
B1



SCALE 1:10



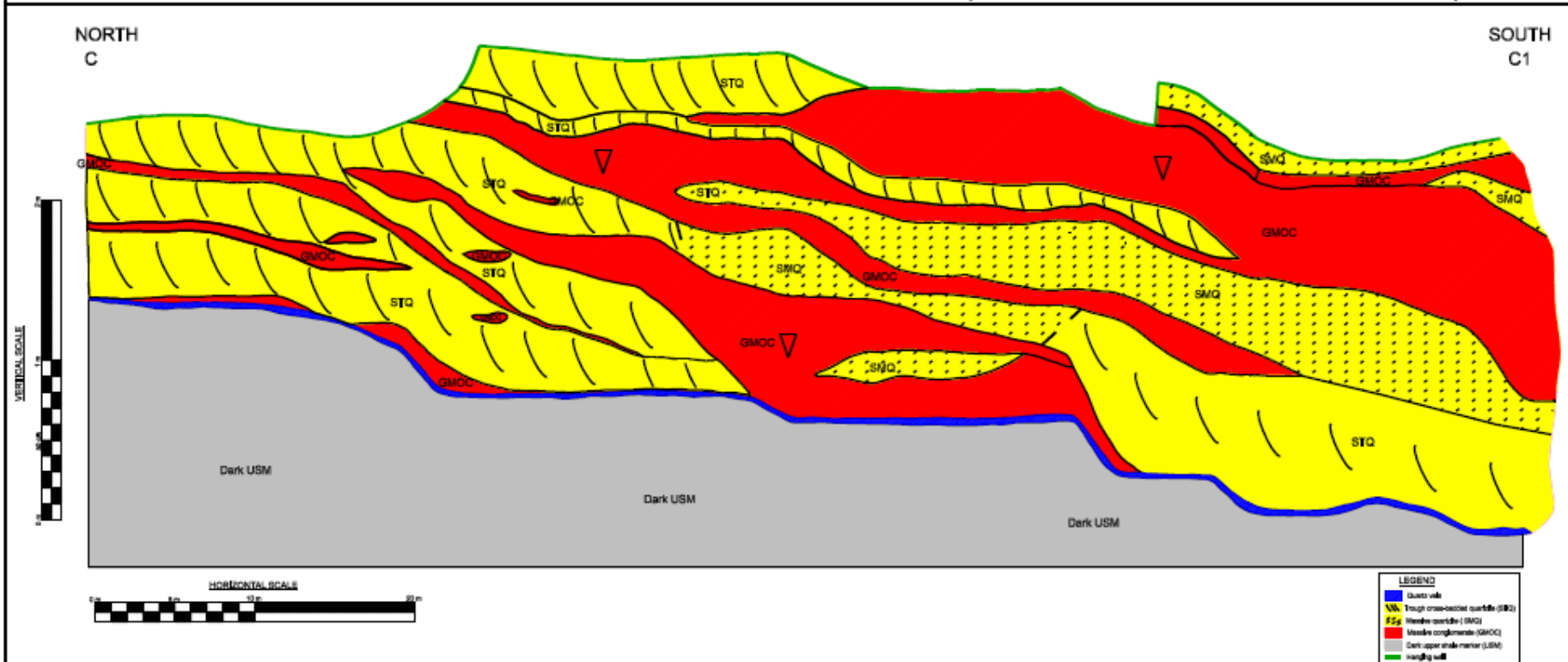
HORIZONTAL SCALE



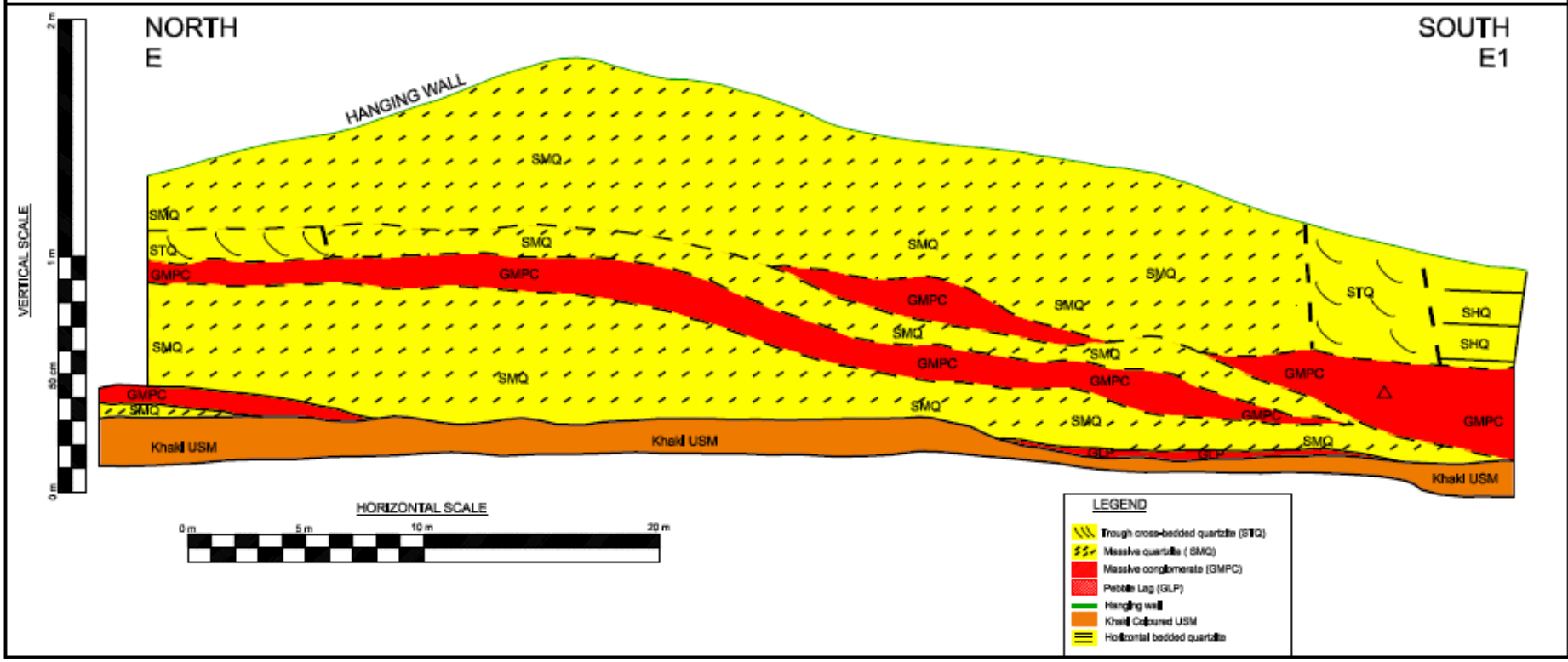
LEGEND

- Trough cross-bedded quartzite (STQ)
- Massive quartzite (SMQ)
- Massive conglomerate (GMOC)
- Dark upper shale marker (USM)
- Hanging wall

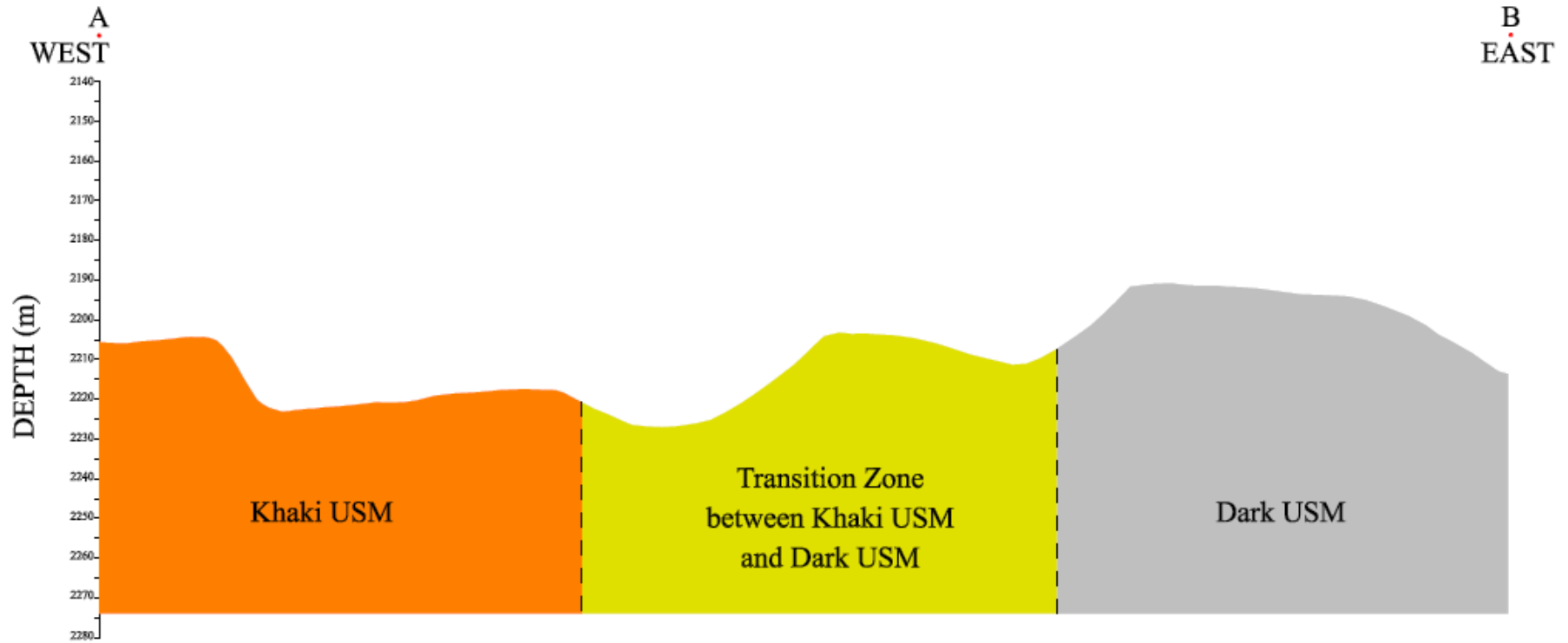
B1 CONGLOMERATE GEOLOGICAL SECTION C (1750 EAST X/CUT14 DRIVE S2)



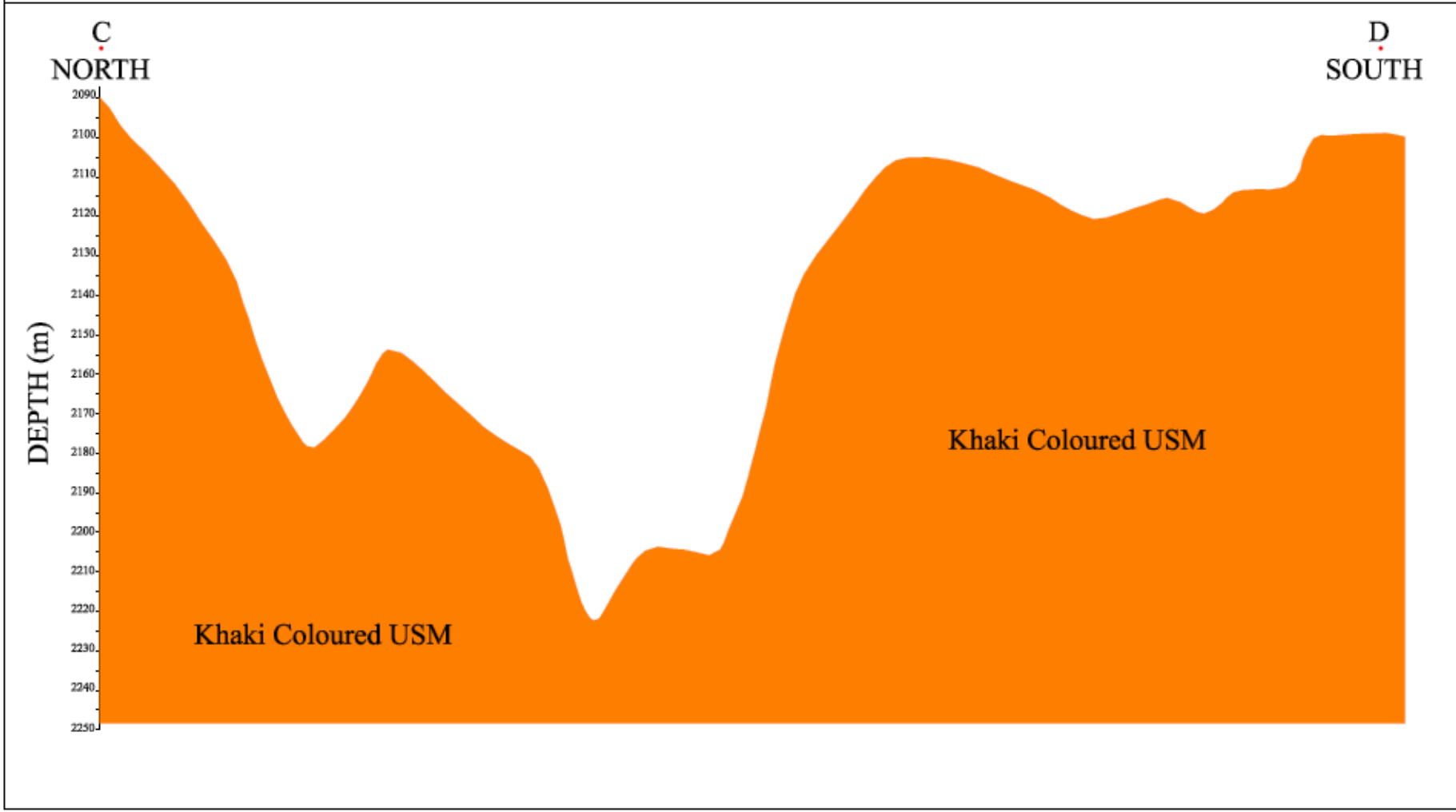
B3 CONGLOMERATE GEOLOGICAL SECTION E



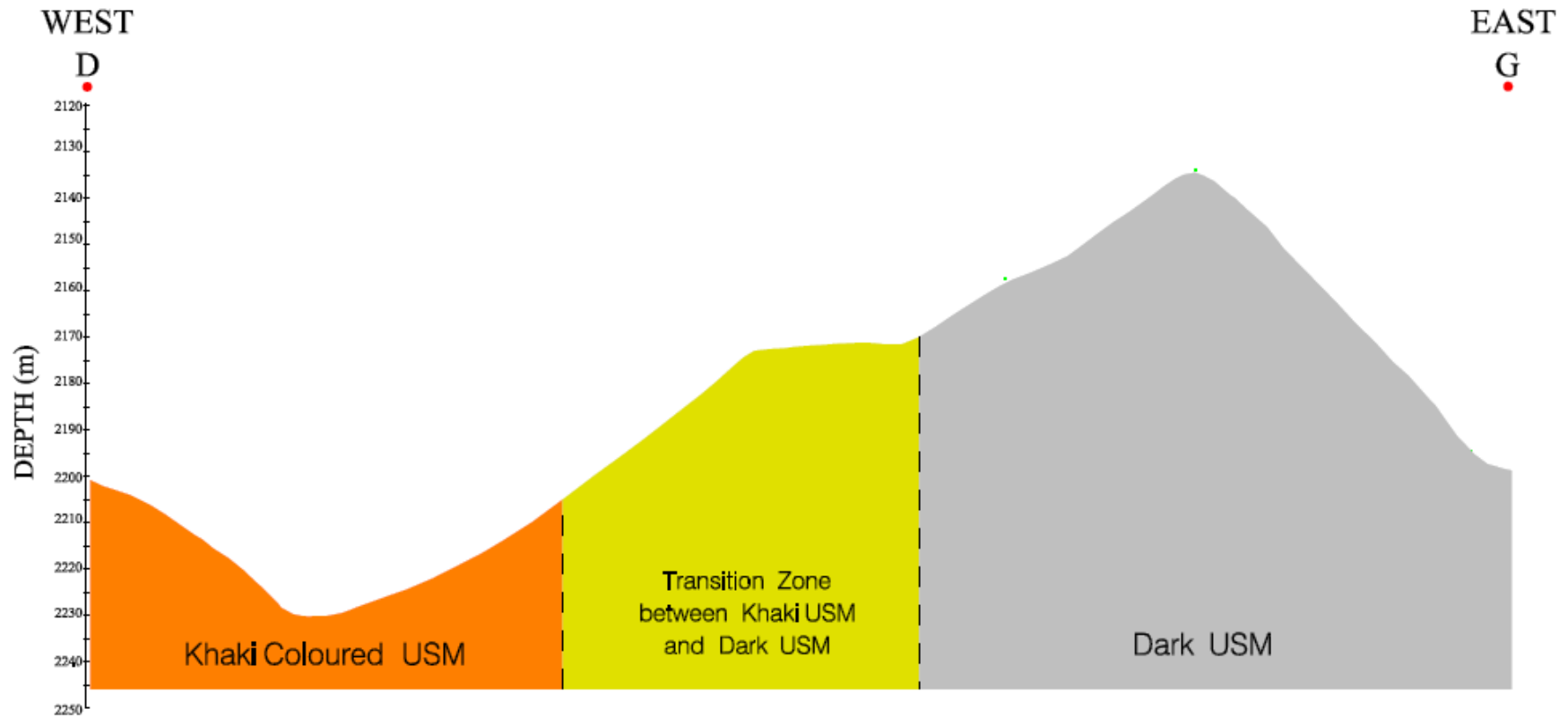
B PLACER PALAEO - FLOOR RECONSTRUCTION (SECTION A-B)



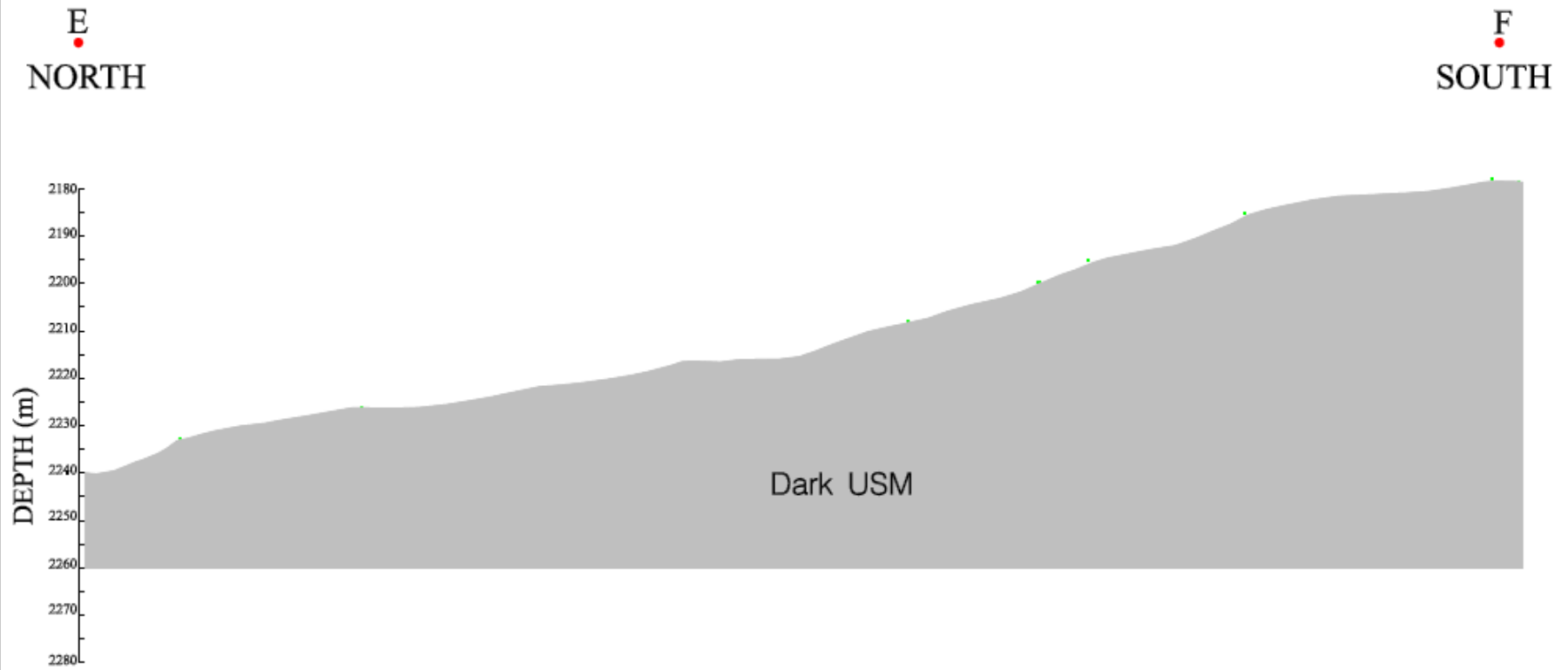
B PLACER PALAEO - FLOOR RECONSTRUCTION (SECTION C-D)



B PLACER PALAEO - FLOOR RECONSTRUCTION (SECTION D-G)



B PLACER PALAEO - FLOOR RECONSTRUCTION (SECTION E-F)



B PLACER PALAEO - FLOOR RECONSTRUCTION (SECTION D-G)

